STUDIES ON CATALYSTS FOR PREFERENTIAL OXIDATION OF CO IN H_2-RICH GAS MIXTURE

BY

Musead Salem Al-Ghamdi

A Thesis Presented to the
DEANSHIP OF GRADUATE STUDIES

KING FAHD UNIVERSITY OF PETROLEUM & MINERALS

DHAHRAN, SAUDI ARABIA

In Partial Fulfillment of the
Requirements for the Degree of

MASTER OF SCIENCE

In

CHEMICAL ENGINEERING

June, 2006

KING FAHD UNIVERSITY OF PETROLEUM & MINERALS

DHAHRAN, SAUDI ARABIA

DEANSHIP OF GRADUATE STUDIES

This thesis, written by

MUSAED SALEM MUSAED AL-GHAMDI

Under the direction of his thesis advisor and approved by his thesis committee, has been presented to and accepted by the Dean of Graduate Studies, in partial fulfillment of the requirement for the degree of

MASTER OF SCIENCE IN CHEMICAL ENGINEERING

Thesis Committee

Dr. Tomoyuki Inui (Chairman)

Dr. Mazen A. Al-Shalabi (Member)

Dr. Shakeel Ahmed (Member)

Dr. Mohamed B. Amin
(Department Chairman)

Dr. Mohammad A. Al-Ohali
(Dean of Graduate Studies)

June 12, 2006
Date

ACKNOWLEDGMENT

I sincerely acknowledge the support provided by King Fahd University of Petroleum & Minerals (KFUPM). My deep gratitude is extended to the Center of Refining and Petroleum (CRP), KFUPM-RI for their support to complete my research.

With deep sense of gratitude and appreciation, I would like to express my sincere thanks to my thesis advisor, Prof. Tomoyuki Inui for his inspiring guidance and excellent cooperation in supervising this research work. I am also very grateful to Prof. Mazen A. Al- Shalabi, and Dr. Shakeel Ahmed, for facilitating this research, continuous encouragement and several discussions.

I owe thanks to Prof. Muhammad A. Al-Saleh, manager of CRP, and Prof. Halim Hamid, manager of refining section, for their support. I would like to thank the laboratory researchers at CRP, RI, KFUPM, specially Mr. M. Bari, Mr. Owais, Mr. K. Alam, and Mr. K. Nawad for their help and assistance during the experimental work.

Finally, I offer my thanks to my parents and family members for their encouragement, support, and prayers.

CONTENTS

LEST OF TABLES

LEST OF FIGURES

Figure

ABSTRACT

Name: Musaed salem Musaed Al-Ghamdi
Thesis Titel: Studies on Catalysts for Preferential Oxidation of CO in H_2-Rich Gas Mixture
Major Field : Chemical Engineering
Date of Degree: June 2006

Preferential oxidation is one of the most effective methods for CO clean-up from the reformate stream prior to its introduction in the PEM fuel cell. In this work, Cu–Ce/γ-Al_2O_3 as a base catalyst promoted with Pt and Rh was prepared for the low temperature selective oxidation of CO in hydrogen rich syn gas mixture. Seven catalysts with atomic ratio of 100: 20: 3: 1 for Cu: Ce_2O_3: Pt: Rh were prepared with Cu loading in the range of 0.5 to 6%. Also, four catalysts were prepared to investigate the role of Pt and Rh in the catalyst activity. The effects of stoichiometric ratio of O_2/CO and water vapor on the selective oxidation of CO as a function of temperature were investigated. The prepared catalysts were characterized by ICP, Gas Sorption Analyzer, and Temperature Programmed Reduction (TPR). Slight decrease in surface area and pore volume were observed with increasing metal loadings. The TPR results indicate shift towards higher temperature when Pt and Rh were added to Cu–Ce/γ-Al_2O_3 catalyst. Moreover, TPR result showed that there is correlation between reduction temperature and the activity and selectivity of the catalyst. The loading of Cu, Ce, Pt, Rh metals for maximum activity and selectivity were 2.0, 0.657, 0.183, 0.0324 wt % respectively which decreased CO concentration in the product to 4ppm (99.96%). A synergistic effect addition of Pt or/and Rh was observed as an enhancement of the activity and selectivity of the base catalyst (Cu–Ce/γ-Al_2O_3). The CO conversion was increased from 24.7 to 96.77% with addition of 0.183 wt% Pt to the base catalyst. Whereas the addition of 0.0324 wt% Rh to the base catalyst increased the CO conversion from 24.7 to 44.1%. Addition 10 vol% of water vapor to the feed resulted in higher conversion at lower temperature. The CO conversion was increased whereas the temperature of maximum conversion was decreased by 20ºC. Both CO conversion and temperature were reduced when water vapor content in the feed was increased to 20 vol%.

Master of Science Degree
King Fahd University of Petroleum& Minerals
Dhahran, Saudi Arabia
June, 2006

خـــلاصـــة الـــرســـــالـــة

إســم الطالب : مساعد سالم مساعد الغامدي

عنوان الرسالة :دراسة حفازات الأكسدة الإنتقائية لأول أكسيد الكربون في مزيج غني بغاز الهيدروجين

التـخـصـص: الهندسة الكيميائية

تاريخ الرسـالة: يونيو 2006م

تعتبر الأكسدة الانتقائية من أفضل الطرق فعالية لإزالة أول أكسيد الكربون من ناتج عملية تصنيع الهيدروجين، وذلك لاستخدامه في خلايا الوقود التي تعمل بالهيدروجين (PEMFC). تم تحضير حفازات تحتوي على النحاس والسيريوم على الألومينا (CuCe/γ-Alumina) كما تم زيادة نشاطها الحفزي بإضافة البلاتين (Pt) والروديوم (Rh) بكميات ضئيلة، وذلك لقياس نشاطها الحفزي في الأكسدة الانتقائية لأول أكسيد الكربون في مزيج غني بغاز الهيدروجين. لقد تم تحديد نسبة العناصر المضافة باستخدام مطيافية الكتلة (ICP)، كما تم قياس المساحة السطحية للحفاز وحجم المسامات الكلى ومتوسط قطرها. كما تم قياس النشاط الحفزي للاختزال باستخدام الاختزال الحراري (TPR)، وأظهرت النتائج أن المساحة السطحية للحفاز والحجم الكلي للمسامات تناقصت بصورة بسيطة مع الإضاف من المعادن أما متوسط قطر المسامات فقد زاد وذلك لتأثير المعادن المضافة على المسامات ذلك القطر الصغير. كما أظهرت اختبارات (TPR) أن درجة اختزال أكاسيد النحاس والسيريوم ازدادت بإضافة عنصري أ للبلاتين أو الروديوم مما أدى إلى زيادة الانتقائية للحفاز لأكسدة أول أكسيد الكربون. لقد أظهرة نتائج اختبار نشاط الحفازات أن نسبة الوزن المضاف من النحاس وأكسيد السيريوم والبلاتين والروديوم التي أعطت أعلى نتائج للأكسدة الانتقائية لأول أكسيد الكربون كانت (2.0) (0.657) (0.183) (0.0324) على التوالي، حيث وصلت نسبة التحويل أول أكسيد الكربون (99.96)% باستخدام (O_2/CO =2) مع اللقيم، ولقد ازدادت نسبة تحويل أول أكسيد الكربون من (24.7%) إلى (44.1)% بإضافة (0.0324) % من الروديوم وإلى (96.8%) بإضافة 0.183 من البلاتين. ولقد أظهرة النتائج أن إضافة 10% من بخار الماء إلى اللقيم أدت إلى خفض درجة حرارة التفاعل أما إضافة 20% من بخار الماء فقد أدت إلى خفض نشاط الحفاز.

درجة الماجستير في علوم الهندسة الكيميائية

جامعة الملك فهد للبترول والمعادن

الظهران- المملكة العربية السعودية

يونيو 2006

CHAPTER 1

INTRODUCTION

1.1 Introduction

Research for alternative fuels has increased dramatically in the last decade because of growing interest in energy-efficiency and environmental compatibility. Among the various ranges of fuels demand, hydrogen is considered as one of the most important promising fuel for future demand. In several H_2 production processes such as steam reforming, partial oxidation reforming, or autothermal reforming the reformate gas contains about 10 vol% CO in rich H_2 gas. It is well known that CO is very harmful compound for human as will as for the proton-exchange membrane fuel cell (PEMFC). Because it is adsorbed on the surface of the Pt-Ru anode catalyst, blocking its access to H_2 and decreases the electrochemical performance of fuel cell [1-3]. Therefore, it is essential to convert CO in reformate gas to a friendly product. One option is to use water gas shift reaction to convert CO to CO_2 in two series steps. High temperature water gas shift reaction (first step) reduces CO concentration in H_2-rich gas mixture from 10 to 3%. Whereas low temperature gas shift reaction (second step) reduces CO concentration from 3 to 0.5 vol%. Therefore, the product of water gas shift reaction still contains about 5000ppm CO. This amount of CO still extremely high and above human limitation which is 35 ppm. Also, it is extremely

above limitation of PEMFC which 10 ppm. Consequently, the deep removal of CO from the H_2 stream after hydrocarbon fuel reforming and water-gas-shift reactions is an essential requirement for the PEMFC which is viewed as most promising technology to replace the ordinary energy generators.

The preferential oxidation reaction (PROX) process is one of the most effective methods for the removal of CO trace from the reformate stream. PROX of CO is a reaction to convert CO in a H_2-rich gas mixture to CO_2 with minimal H_2 consumption. Therefore, preferential oxidation process is an indispensable step to reduce the concentration of CO to 10 ppm level in a H_2 generation process. The preferential oxidation step includes contacting a fuel stream comprising H_2 and CO in the presence of O_2 at a preferential oxidation temperature as low as 150~180°C on a preferential oxidation catalyst.

The PROX of CO is a catalytic reaction where the catalyst plays a significant role in enhancing the CO oxidation and suppressing H_2 oxidation. The key factors to achieve very low CO concentration fuel is synthesizing a high active, stable, and selective catalyst for PROX reaction in H_2-rich gas mixture at the lower temperature range mentioned above. Purification of H_2 by selective oxidation of CO to reduce 10 ppm level using noble metal catalysts have been widely investigated. PROX of CO catalyst was first proposed in 1963 by Engelhard Company as an effective catalyst for cleaning H_2-rich gas from CO [4]. After the fuel cell research and development started to accelerate, researchers attempted to find a new catalyst with higher activity for CO removal and with small hydrogen consumption.

Due to the high exothermicity of PROX reaction, catalyst stability can be a major drawback for any newly developed catalyst. Thus any attempt to synthesize a new catalyst should take the thermal stability to in consideration. Alumina is one of the most promising supports due to its high thermal stability. Mutimetallic catalyst gained an important role to be suitable catalyst for PROX of CO reaction.

Oxidation reaction

$CO + 1/2O_2 \rightarrow CO_2$ ΔH^o_{298}= - 283.6 kJ/mol (1)

$1/2O_2 + H_2 \rightarrow H_2O$ ΔH^o_{298}= - 243.5 kJ/mol (2)

Water-gas shift reaction

$CO + H_2O \rightarrow CO_2 + H_2$ ΔH^o_{298}= - 41.2 kJ/mol (3)

Steam reforming reaction

$C_nH_m + nH_2O \rightarrow nCO + (n+m/2)H_2$ $\Delta H^o_{298} > 0$ kJ/mol (4)

1.2 Objective

The overall objective is to prepare an effective catalyst for CO cleanup from reformate gas for fuel sell application.

The specific objectives are as follows:

1. Preparation of multicomponent high activity catalysts.
2. Characterization of the prepared catalysts by BET surface area, temperature programmed reduction (TPR), and chemical analysis.
3. Evaluation of catalyst activity and selectivity in a fixed bed reactor.

CHAPTER 2

LITERATURE REVIEW

2.1 Catalysts for Preferential Oxidation

Studies in PROX reaction of CO have generally focused on different catalysis systems.

Many researchers investigated different supports, combination of active metals, and methods of preparation in order to prepare highly active and selective catalyst for PROX reaction in H_2-rich gas mixture with minimal H_2 consumption. Al_2O_3 was used as the catalyst support extensively, however; zeolite and other metal oxides were also adopted. -

2.1.1 Catalysts Supported on Alumina

Recently, many studies were conducted to prepare promising PROX catalyst. A brief overview of the studies related to this system is provided. Researchers attempted to find a new catalyst that is cheap, stable, and highly active for CO removal with minimal consumption of H_2. Al_2O_3 is a promising support since it is cheap, stable. Different combinations (monometallic and Bimetallic) of active metals were loaded on Al_2O_3 to prepare high activity PROX catalyst.

Alumina is extensively adopted as the support for PROX catalyst. The PROX reaction has been extensively investigated on Pt/Al_2O_3 catalysts [5–10].

Pt/Al_2O_3 was proposed by Los Alamos National Laboratory in1963 as an effective catalyst for preferential oxidation of CO in the H_2-rich gas mixture [2]. Ru/Al_2O_3 was proposed in 1993 by Oh and Sinkeivity [8] as a more efficient catalyst than Pt/Al_2O_3 catalyst. They observed a maximum in CO conversion with temperature on 0.5% Pt/Al_2O_3 at 200ºC in the presence of excess H_2 in the feed stream. In contrast, a constant conversion of 100% above 200 ºC was achieved in absence of H_2. They compared the efficiency of several noble metals for the PROX reaction; the CO conversion was found to decrease in the following order: Ru/Al_2O_3 > Rh/Al_2O_3 > Pt/Al_2O_3 > Pd/Al_2O_3 (metal loading 0.5 wt% for all catalysts). While Pd showed a similar CO oxidation activity to Ru and Rh at lower temperatures, it showed significantly inferior activity at higher temperatures. This effect was attributed to the change in oxidation state (highly active reduced form to less active oxidized form) of Pd with increasing reaction temperature. Although this study clearly shows the high efficacy of Ru and Rh, these catalysts, surprisingly, have not been explored subsequently in greater details.

A similar trend has been observed by Kahlich et al [9] on a 0.5% $Pt/\gamma\text{-}Al_2O_3$ catalyst. The decrease in CO conversion (in presence of H_2) with increasing temperature was attributed to a greater contribution from the competitive H_2 oxidation at higher reaction temperatures. It is noteworthy that the presence of H_2 caused a decrease in the ignition temperature for the CO oxidation reaction [8, 9]. The Pt/Al_2O_3 catalyst showed no significant CO methanation activity in the temperature range between 150 and 250ºC.

Chan et al [11] tested two catalyst types of Pt loaded on alumina aerogel prepared by single step and stepwise impregnation. These two catalysts reduced the CO to less than 10 ppm from a feed mixture contained 10,000 ppm H_2, 1000 ppm CO, 1000 ppm O_2, and nitrogen balance at a range of space velocity from 6,600 to 44,000 h^{-1} on a fixed bed reactor at 200°C. These catalysts show high selectivity for PROX reaction as shown in Figure 2.1. The oxidation reaction of both CO and H_2 with O_2 started above 100°C. At above 150°C, both reactions slowed down. In the range of temperature of 100 to 150°C, H_2 reduced from 10,000 to 9,000 ppm while CO reduced 1,000 to less than 10 ppm.

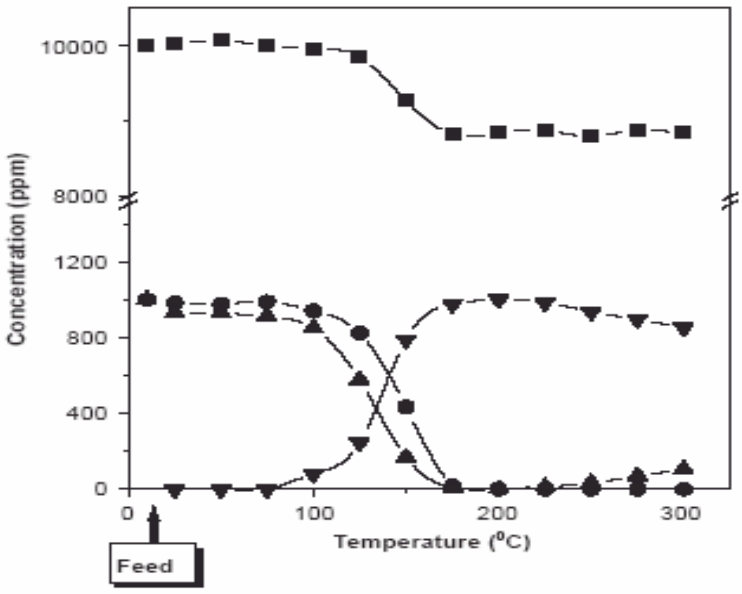

Figure 2.1 Activity and selectivity of Pt/xero catalyst for PROX of CO. [Changes in concentrations of H_2(■), CO(▲), CO_2(▼), and O_2(●) as a function of temperature over Pt/xero. The feed contained 10,000 ppm of H_2, 1000 ppm of, CO, 1000 ppm of O_2, and N_2 balance. The GHSV was 23,100 h^{-1}]. [12].

In 2005, Cécile Rossignol et al [13] investigated the PROX activity of Au/Al_2O_3, Au/ZrO_2, and Au/TiO_2 catalysts. These catalysts were prepared by low-energy

cluster beam deposition. Then the samples are air transferred, characterized, and tested for catalytic reactions [14].

These tests were carried out at atmospheric pressure in a continuous-flow fixed-bed reactor. 750 mg of the as-obtained gold-based powders was loaded into the quartz reactor. The reactant flow rate was 50 Nml h^{-1} consisting of a mixture of 2% CO + 2% O_2 + 48% H_2 + 48% He. Au/γAl_2O_3 prepared by laser vaporization gave about 65% conversion of CO in H_2-rich mixture at 115°C. The alumina support activity and selectivity was the best among all the other support used in the same study.

Dond and et al [15] investigated the conversion efficiencies of CO (in a mixture gas containing 10,100 ppm H_2, 1,100 ppm CO, 990 ppm O_2, and N_2 balance) over Ru/Al_2O_3, Au/Fe_2O_3, Pt/Al_2O_3, Rh/Al_2O_3, and Pd/Al_2O_3 catalysts in 2004. The space velocity was varied in the range of 7,500 ~ 36,000 h^{-1}. The mixed gas was supplied into the reactor at a total flow rate of 100 cm^3 min^{-1}. The amount of catalyst used was kept at 0.20 g. The test shows that the CO conversion was decreased in the order of Ru/Al_2O_3 > Pt/Al_2O_3 > Rh/Al_2O_3 > Pd/Al_2O_3 as shown in Figure 2.2. Ru/Al_2O_3 exhibited higher activity of CO removal than Pt/Al_2O_3 at the temperature rang of 25 ~175°C and above 250°C. The activity of Pd/Al_2O_3 catalyst for CO removal was very poor compared with other three catalysts. The hydrogen loss was in the order of Pt/Al_2O_3 < Ru/Al_2O_3 =Rh/Al_2O_3 < Pd/Al_2O_3. Ru/Al_2O_3 and Rh/Al_2O_3 consumed large amounts of H_2 above 250ºC–because methanation occurs in this temperature region. On Pd/Al_2O_3, the H_2-O_2 reaction

occurred to a great extent at relatively low temperature (75ºC) resulting in large loss of H_2.

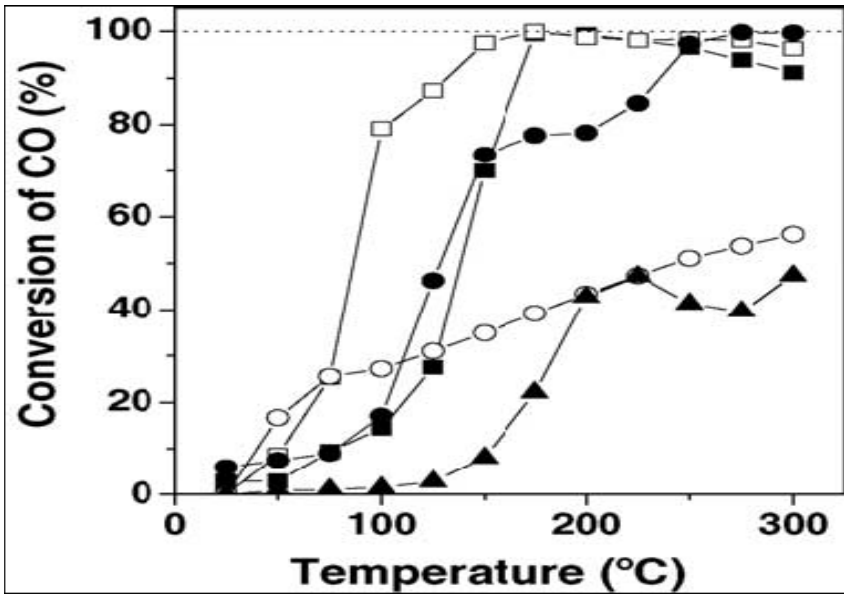

Figure 2.2 Conversion of CO over various noble metal catalysts.
[Data are shown for Pt/Al_2O_3 (■), Ru/Al_2O_3 (□), Rh/Al_2O_3 (●), Pd/Al_2O_3 (○), and Au/Fe_2O_3] [15]

In recent years, there has been great interest in investigating the CO oxidation reaction over gold-based catalysts [16–23]. Although bulk gold is highly inefficient for CO oxidation, supported nano-gold clusters have incredible CO oxidation activity; these catalysts show high activity even at sub-ambient temperatures. The nano-gold catalysts are also extremely promising from the point of view of the PROX reaction; while bulk gold and larger Au particles show higher oxidation activity for H_2 as compared to CO, the situation is entirely reversed for supported nano-gold catalysts.

Haruta et al [20] observed a greater than 95% conversion for CO (1% CO, 1% O_2, balance H_2) in a temperature range between 50 and 80ºC. This clearly is very promising, as the normal operation temperature of a PEMFC is ca. 80ºC.

Alumina-supported nano-gold catalysts have also been effectively employed as PROX catalysts [24, 25].

The promoted catalysts showed selectivities greater than 90% for the PROX reaction at temperatures ≤ 100°C. Catalyst comparison studies by Kahlich et al. [26] for the Au/Fe_2O_3 and Pt/Al_2O_3 [9] systems for the PROX reaction has revealed the former to be a better catalyst. However, Pt catalysts have an advantage over Au catalysts in terms of stability. In general, nano-Au catalysts are known to undergo rapid deactivation during CO oxidation [22, 27–29].

In 2004, Suh et. Al. [15] applied $PtCo/Al_2O_3$ catalyst prepared by various methods for the PROX reaction where highly active catalyst are needed to reduce (1- 2% CO) to less than 20 ppm at low temperature with limited O_2. Chan et. al., [12] alumina supports were prepared by the sol–gel processing of aluminum in ethanol and subsequent drying and calcination. The fires supports are alumina xerogels obtained by drying in a conventional oven at 110ºC for 12 h. Alumina aerogels were dried supercritically with CO_2 at 60 ºC for 24 h. The dried support was subjected to a standard calcination procedure, which consisted of heating in helium at 300 ºC for 2 h and in O_2 at 500 ºC for 2 h [30].

Pt and Co were deposited on calcined alumina surface by successive impregnation with an aqueous solution of chloroplatinic acid and cobalt nitrate.

After each impregnation step, the catalysts were dried at 110 ºC for 12 h and calcined at 500 ºC for 4 h. The second was composite gels prepared by the single step sol–gel processing of a Pt precursor, Co nitrate, and ASB in ethanol. The gels were dried by different methods (viz., oven drying, supercritical drying, and vacuum drying) for 12, 4, and 12 h, respectively. The dried gel was calcined by the standard calcination procedure described above. For example, PtCo/xero designates the catalyst prepared by impregnation of platinumand cobalt precursors to xerogel alumina support and PtCo-xero represents the Pt–Co–alumina composite xerogel catalyst. The catalysts were reduced with a H_2 stream at 400ºC for 2 h. A feed stream (10,000 ppm H_2, 1000 ppm CO, 1000 ppm O_2, and nitrogen balance) was introduced to a fixed-bed microreactor system consisting of a 0.75 cm i.d. x 40 cm long quartz tube under atmospheric pressure at a space velocity of 6,600 ~ 44, 000 h^{-1}.

The Co-added Pt catalyst, prepared by the single step sol–gel method (composite gels), exhibits higher activity than the impregnated catalyst. The Pt-Co composite aerogel catalyst activity for CO removal was improved by supercritical drying wet gel treatment. The PROX reactions over the catalysts prepared reduced CO concentration below 10 ppm but the temperature decrease shifts to lower or higher regions depending on the catalysts.

All catalyst prepared shows similar selectivity of PROX reaction over Pt/Al_2O_3 catalyst as shown in Figure 2.3 and 2.4. First, CO reacted then followed by H_2 consumptions. In the presence of CO, the H_2-O_2 reaction cannot occur at low

temperatures until CO disappears. Hydrogen reduces the onset temperature of CO oxidation but inhibits the CO removal at higher temperatures.

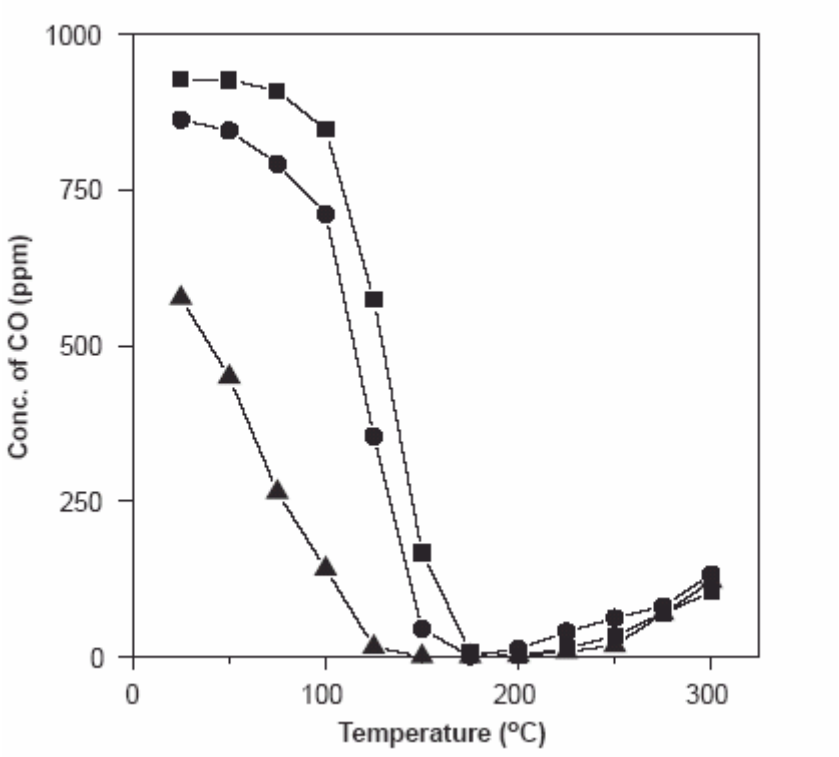

Figure 2.3 Conversion of CO over Pt/xero, PtCo/xero and PtCo/xero catalyst. [Pt/xero *(■)*, PtCo/xero *(●)*, and PtCo-xero *(▲)*. The feed contained 10,000 ppm of H_2 , 1000 ppm of CO , 1000 ppm of O_2 , and N_2 balance. The GHSVs were 23,100, 23,400, and 24*,* 000 h^{-1}, respectively]. [15]

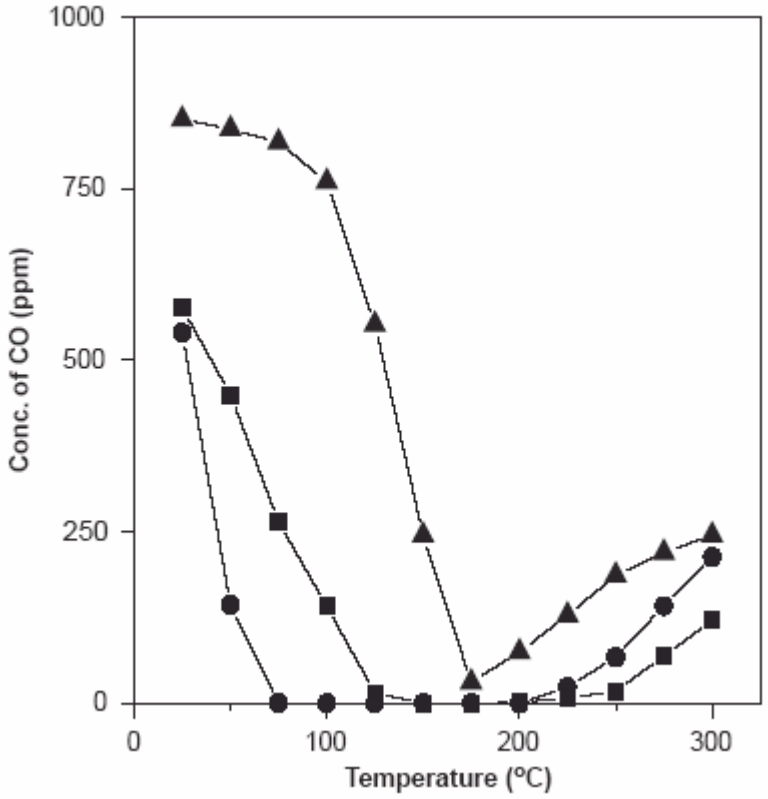

Figure 2.4 Conversion of CO over PtCo-xero, PtCo-aero, and PtCo/aero catalyst [PtCo-xero *(■)*, PtCo-aero *(●)*, and PtCo/aero *(▲)*. The feed contained 10,000 ppm of H_2, 1000 ppm of CO, 1,000 ppm of O_2, and N_2 balance. The GHSVs were 24,000, 6,600, and 7,500h^{-1}, respectively]. [15]

Preferential oxidation performance of Pt/Al_2O_3 catalyst was improved after addition of Co, Ni, and manganese [15]. All these catalysts exhibit excellent performance for preferential oxidation reaction of CO in a reaction feed mixture of – 1.01% H_2, 0.11% CO, 0.099% O_2, and N_2 balance (10,100 ppm H_2, 1,100 ppm CO, 990 ppm O_2, N_2 balance). For all of them, 90% CO conversion was achieved at below 175°C as shown in Figure 2.5. $PtCo/Al_2O_3$ reduces the outlet CO

concentration to below 10 ppm in the temperature range of 25 to 175ºC. $PtNi/Al_2O_3$ shows lower conversion than that of $PtCo/Al_2O_3$ at room temperature, but Ni-catalyst is more efficient than Co catalyst at temperature range of 200 to 300°C.

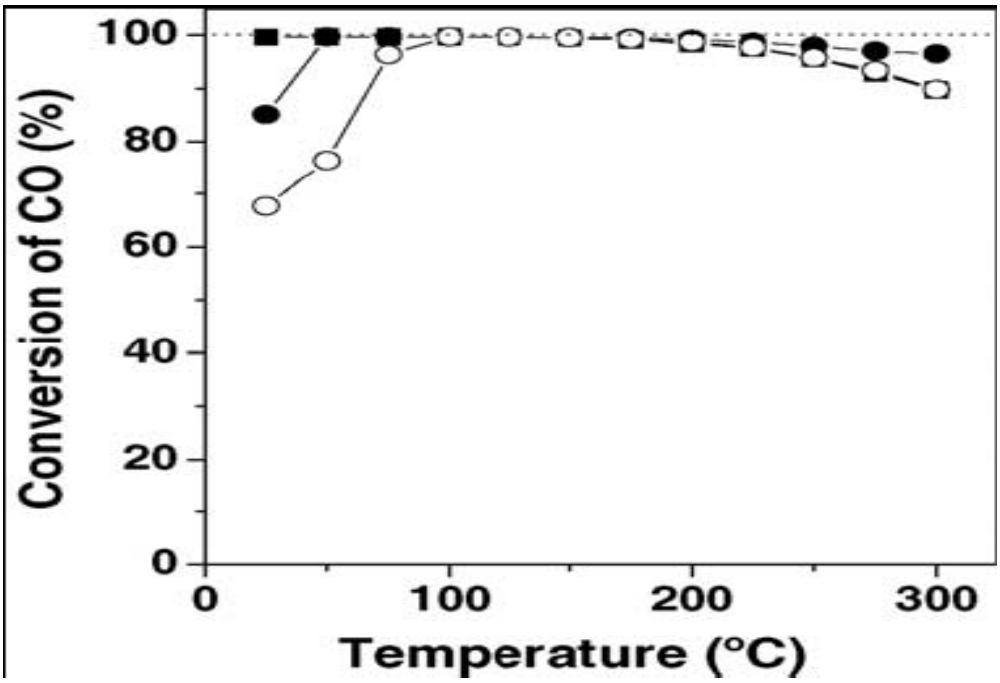

Figure 2.5 Conversion of CO over $PtCo/Al_2O_3$, $PtNi/Al_2O_3$ and $PtMn/Al_2O_3$ [Data are shown for $PtCo/Al_2O_3$ (♦), $PtNi/Al_2O_3$ (•), and $PtMn/Al_2O_3$ (O)][15]

2.1.2 Catalyst Supported on Zeolite

Although alumina is the most common support for noble metal-based catalysts, recent studies [15] have indicated that the use of zeolites as supports for active metal catalysts for PROX reaction is promising to improve the catalyst selectivity, probably due to the molecular sieve effects.

Since zeolite A has low cost and high thermal stability, zeolite A-supported Pd, Ru, Pt were developed for preferential CO oxidation. The catalytic activity and selectivity in H_2, CO_2, H_2O rich stream was investigated as a function of temperature, in order to find a catalyst able to completely remove CO at a temperature similar to that of the outlet gas from low-temperature water gas shift reaction (LTWGS), as this would enable elimination of the intermediate cooler. In particular, Pt/A catalysts resulted as the most selective among those tested (Pt/mordenite, Pt/X, Pt/A and Pt/Al_2O_3) [31]. The result showed that the Pt/modernite catalyst required the least amount of excess oxygen for the complete conversion of CO (1%) in presence of excess of H_2 Mashiro et. al. [32] proposed that the Pt catalysts supported on A-type zeolite for removal of 1% CO from H_2-rich gas by the PROX, taking advantage of its "chemical and/or physical molecular sieve effect" to make CO react with O_2 [16]. The selectivity was found to be much superior to the conventional Pt/Al_2O_3 and be affected by the types of supports used, in the order, A-type zeolite > mordenite > X-type zeolite > Al_2O_3. Pt/mordenite showed the highest conversion from CO to CO_2 with almost similar selectivity to that of Pt/A-type zeolite among the catalysts examined [17].

Ilaria Rosso et. al., [33] investigated three different type of A-zeolite loaded with Pd, Ru, and Pt were tested at various temperatures for feed stream flow rate ($100Ncm^3\ min^{-1}$) containing 37 vol.% H_2, 18 vol.% CO_2, 0.5 vol.% CO, 5 vol.% H_2O, 1 vol.% O_2, 39.5 vol.% He. The result analysis of the effluent gas is shown in Figures 2.6 - 2.8. The Pd and Ru-supported catalysts did not reach a

complete CO-conversion, whereas the Pt-catalysts showed the highest CO-conversion and selectivity.

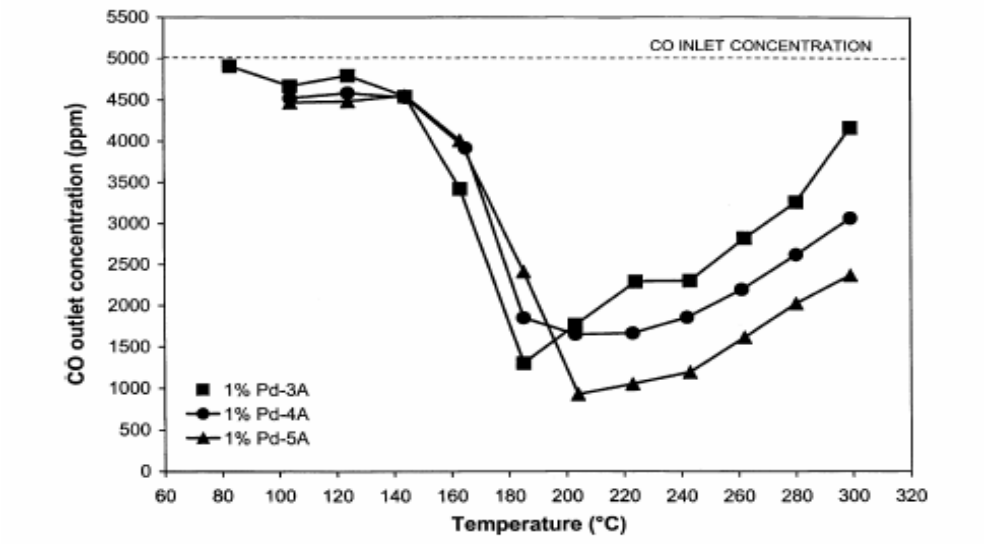

Figure 2.6 Conversion of CO over 1% Pd-3A, 1% Pd/4A and 1% Pd/5A catalysts [with standard feed gas composition (5,000 ppm CO, 1% O_2, 18% CO_2, 5% H_2O, 37% H_2 and He as balance). Hourly space velocity was 67,000 h^{-1}.] [33]

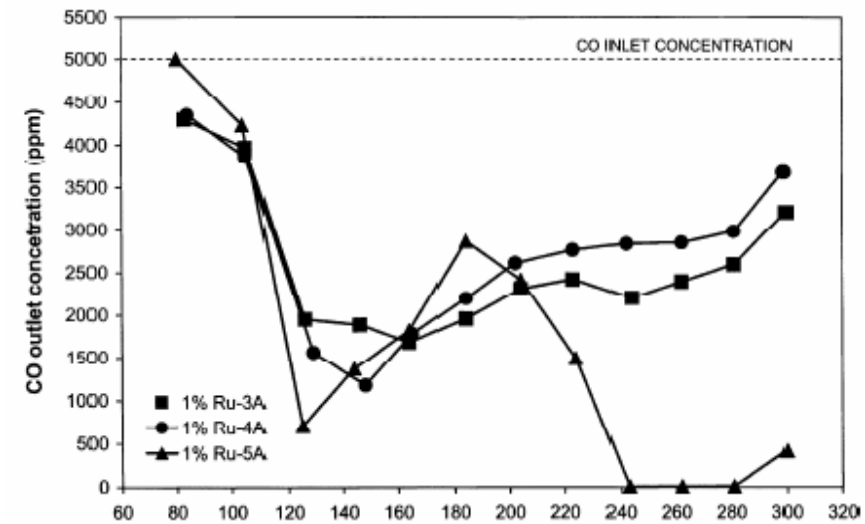

Temperature ºC

Figure 2.7 Conversion of CO over 1% Ru/3A, 1% Ru/4A and 1% Ru/5A catalysts [with standard feed gas composition. Hourly space velocity was 67,000 h^{-1}.] [33]

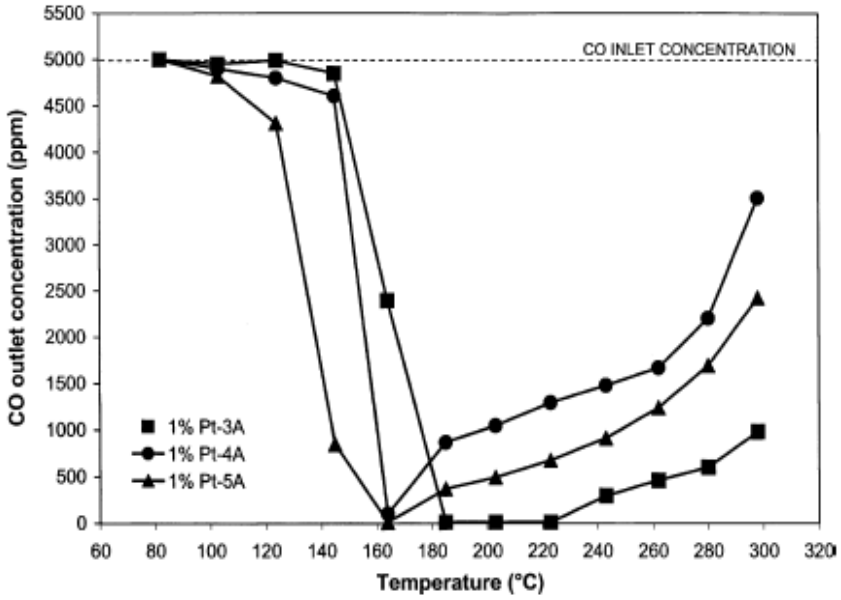

Figure 2.8 Conversion of CO over1% Pt/3A, 1% Pt/4A and 1% Pt/5A catalysts [with standard feed gas composition. Hourly space velocity was 67,000 h^{-1}.] [33]

Activity of Pt/zeolite catalysts was the best of all catalyst tested in this study. Also, they were reported to have much more selectivity in large excess of H_2 with the addition of a low concentrated of O_2 than a conventional Pt/Al_2O_3 catalyst [35]. Among various metals (Pt, Ru, Pd, Co, Pt–Ru) loaded on mordenite, Pt–Ru/mordenite exhibited fairly high conversion with a high selectivity of ca. 90% over a wide fuel-flow rate condition even at relatively low temperature of 150 ºC - [34, 35].

2.1.3 Catalyst Supported on Other Carriers

Dong et. al. [15] tested Au/Fe_2O_3, Pt/C, and Pt/aerogel-SiO_2 for PROX reaction in a fixed bed reactor with a feed stream (10,100 ppm H_2, 1100 ppm CO, 990 ppm O_2, and N_2 balance). The Au/Fe_2O_3 catalyst shows very low activity for PROX reaction than Au/Al_2O_3 catalyst. The CO conversion was only 50 % at 300ºC as shown in Figure 2.1. The consumption of hydrogen was high at high temperature over the Au/Fe_2O_3 catalyst because of methanation side reaction. The Pt/C and Pt/aerogel-SiO_2 catalyst shows very high activity and selectivity for PROX reaction. The activities of these catalysts compared to Pt/Al_2O_3 catalyst. The C support was the best among of the two other supports.

In 2004, Cecile et. al., [13] studied the effect of Au supported on Al_2O_3, ZrO_2, and TiO4 on catalyst activity and selectivity for PROX reaction. The three catalysts used in this study (Au/Al_2O_3, Au/ZrO_2, and Au/TiO_2) were prepared by low-energy cluster beam deposition. The reactant flow consisted of a mixture of 2% CO + 2% O_2 + 48% H_2 + 48% He for the preferential oxidation of CO (PROX). The prepared catalyst showed very low activity and selectivity for PROX of CO.

Fernando et al, [36] studded fluorite-type oxides (CeO_2, CeO_2–ZrO_2) were shown to be some very interesting supports for the total oxidation reactions. In fact, in the case of CeO_2 and CeO_2-based supports the redox cycle Ce(III)–Ce(IV) is easy and the oxygen mobility in the crystallographic structure is very much facilitated. As a result, such oxides are able to reversibly ‘‘absorb’’ oxygen [37, 38]. The high activity of the above-mentioned CuO–CeO_2 catalyst,

comparable with or even superior to the performances of the costly precious metal catalysts, was attributed to the strong interaction between the Cu nanoparticles and the ceria support [39–41].

In 2004, several ceria and ceria–zirconia supported base metal (Co, Cr, Cu, Ni, Zn) catalysts were explored by Marino et al [42] for the catalytic performances of PROX in presence of high concentration of H_2. In addition, the effect of acidic and basic properties of SiO_2–Al_2O_3, La_2O_3, MgO supports was examined for the Cu catalysts. Catalytic tests were carried out in an atmospheric glass fixed-bed reactor placed in an electrical oven. In a typical run, the mass of catalyst used was fixed at 100 mg. Because of the small size of the catalyst bed (8 mm in diameter and 4 mm in height), it was assumed that there was no significant temperature profile in the bed. In general, the reaction mixture consisted of 70 vol.% H_2, 2 vol.% CO, 1–4 vol.% O_2 (oxygen excess, l ¼ 2pO_2=pCO, varies from 1 to 4) and N_2 as a balance. In some experiments, up to 15 vol.% of CO_2 were also added to the feed. The total inlet gas flow rate was fixed at 100 N ml min^{-1}. The evolutions as a function of temperature of the CO conversion and selectivity over 1 wt.% metal M–Ce0.63Zr0.37O_2 catalysts (M = Co, Cr, Cu, Ni, Zn). The catalyst showed poor CO conversion. The maximum CO conversion was about 70% at temperatures around 150ºC over Cu catalyst. Figure 2.9 shows that less than 80% of CO conversion was achieved with SiO_2-Al_2O_3 and CeO_2 at 135°C.

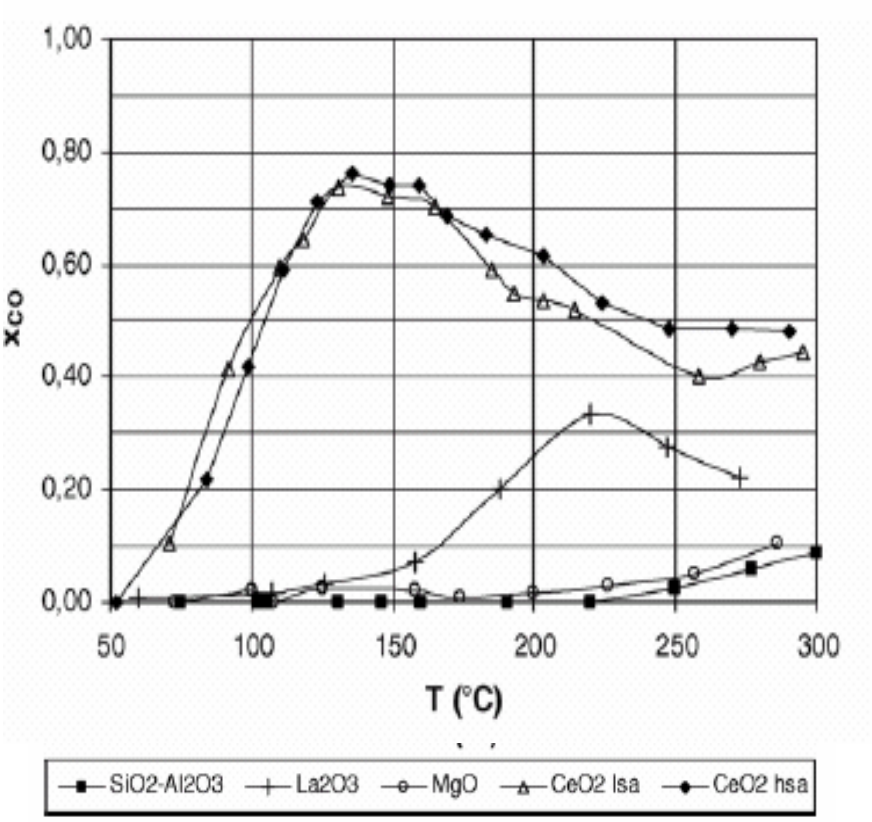

Figure 2.9 Preferential oxidation of CO over Si, La, Ce supported catalysts.

The effect of the copper content is shown in Figure 2.10. The maximum CO conversion is only 80%.

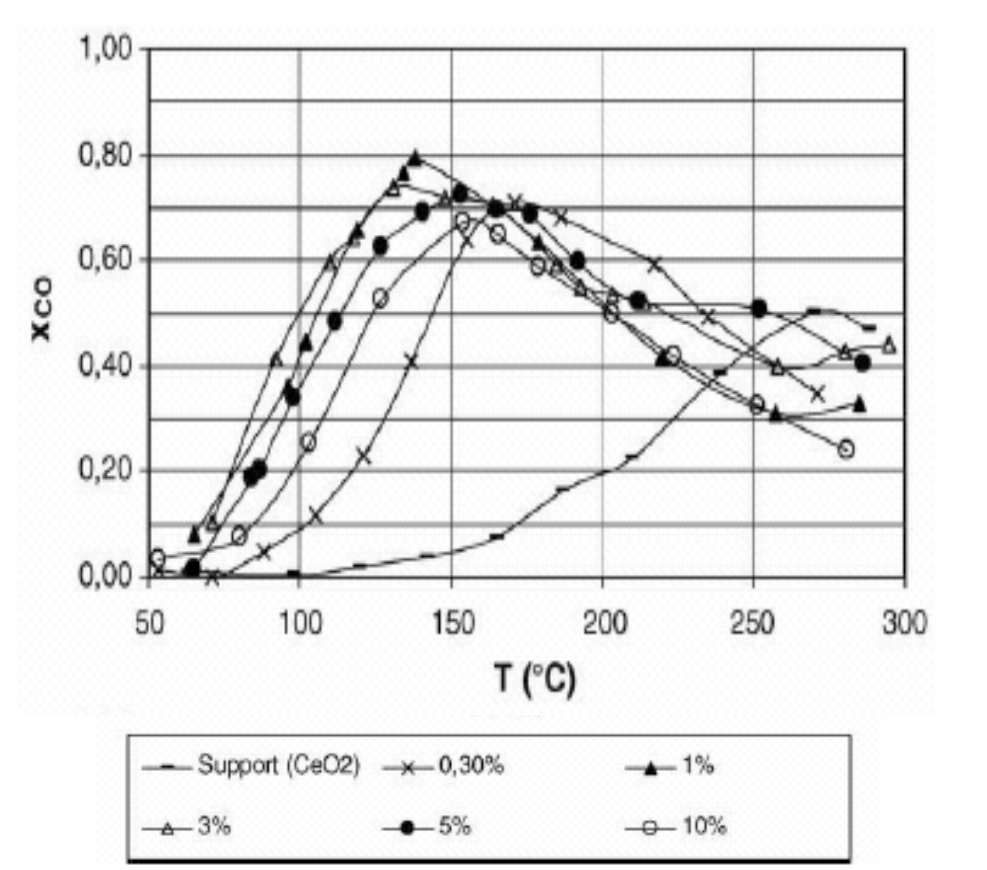

Figure 2.10 Preferential oxidation of CO over a series of Cu–CeO_2 catalysts [nominal Cu loading ranking between 0.3 and 10 wt.%) and over the bare ceria support. Evolution of the CO conversion, the O_2 conversion and the CO_2 selectivity as a function of the reaction temperature. (Mass of catalyst = 100 mg; total flow = 100 N ml/min^{-1}; feed composition: 70% H_2, 27% N_2, 2% CO, 1% O_2 (l = 1)).]

Other systems, which have been investigated for the PROX reaction of CO include metal oxides [43] and bimetallic [44] catalysts. PROX studies over catalysts consisting of 3d transition metal oxides have revealed CoO to be an interesting candidate for the desired reaction [43]. It showed a near 100% CO conversion (feed: 1% CO; 1.86% O_2; 90% H_2 and balance N_2) and selectivity of 60% for CO_2 formation at 130ºC; the catalyst activity was maintained for >20 h in this study. NiO and CuO were found to catalyze the CO methanation reactions at

temperatures above 200ºC and 300ºC, respectively. These temperatures corresponded to the reductive transformation of the metal oxide catalysts. Schubert et al. have recently reported a superior CO oxidation activity and selectivity (than Pt/Al_2O_3) for a bimetallic carbon-supported PtSn system at low temperatures (0~80ºC) [45]. Unlike in case of Pt/Al_2O_3, the CO oxidation reaction was not limited by CO desorption for the carbon-supported PtSn catalysts. Based on their spectroscopic studies, the authors proposed amechanistic model involving competitive adsorption of CO and H_2 on Pt sites, and O_2 adsorption mainly on Sn sites and SnO*x* islands present in the vicinity of the active PtSn particles.

Inui [46-53] investigated the fundamental and practical issues of supported Cu catalysts for partial oxidation of hydrocarbons, combustion of CO, and decomposition of NOx in diesel exhaust. He concluded that the basic performance of Cu catalysts and intrinsic functions are follows:

- Preoxidized supported Cu catalysts can be reduced to metallic Cu by CO faster than by H_2 [46].
- Oxidation activity of Cu catalyst is enhanced with small concentrations of precious metals such as Ag, Pt, and Rh. Among those, in case of Rh, even at very low concentration, oxidation activity of Cu is enhanced very much [47].
- A correlation was found between the catalytic activity of Cu catalyst and reduction rate of the pre-oxidized Cu catalyst by comparing catalytic activity of propylene oxidation and redox properties of Cu catalyst [47, 48].

- Cu catalyst modified with a low concentration of Rh by ion-exchanged method exhibited extraordinary high activity to CO oxidation at lower temperatures range even just above 100°C [49].
- Cu catalyst prepared by intrinsic NH_3-H_2O vapor treatment before eliminate NO_3 from the source of impregnation, has very high active for oxidation [50].

Components to Enhance Hydrogen- and Oxygen- Spillover

At low temperatures such as below 200°C, Cu opts to change copper basic carbonate in existence of H_2O and CO_2. In such state of Cu, catalyst is deactivated fast and often changed to irreversible deterioration. The key point here is how to protect it from this change.

For this purpose, Inui [51 - 53] conducted several studies to establish the basic catalyst characteristic controlling the catalyst function and methods. The typical one has been realized using the composition of thermo-neutral reaction (TNR) catalyst.

Most of the researchers on this subject investigated platinum group metals such as Pt, Ru, Ir, or Pd, especially Pt. Some researchers investigated Au catalyst [13]. However, in general platinum group metals are very expensive, and sensitively suffer from catalytic poisons by sulfur compounds even at lower concentrations. Ru has higher methanation activity. Au has, in general very low activity, irrespective of academic interest.

2.2 Catalysts Preparation Methods

Many preparation methods were attempted in order to achieve very high activity and selectivity for PROX reaction. Some of these methods involve support improvement and the others concerned with the active metal loading processor. Some of these methods were simple and the other was complicated. Both support property and method of active metal loading are very important in catalyst preparation. The support properties depend on the support type, modification, and pretreatment. The activity of metal on support depends on the status of the metal on the support and also on the interaction between the metal and the support.

Most catalysts for PROX of CO were generally prepared via standard methods, namely coprecipitation, deposition-precipitation or impregnation, which were optimized for the respective systems by varying the preparation parameters. The procedures are briefly summarized below. The following are examples for preparation of Au supported catalyst by each method mentioned above [47].

2.2.1 Coprecipitation (Au/γ-Fe_2O_3, Au/Ni_2O_3, Au/$Mg(OH)_2$, and Au/MgO):

These catalysts (CP catalysts) were prepared in close accordance to the procedure described in reference [26]: Aqueous solutions (each 1 M) of the respective metal nitrates ($Fe(NO_3)_2$*$9H_2O$, $Ni(NO_3)_2$*$6H_2O$, $Mg(NO_3)_2$*$6H_2O$; all Fluka, p.a.) containing $HAuCl_4$*$3H_2O$ (Merck, p.a.) and of Na_2CO_3 (Fluka, p.a.) or NaOH (Merck, p.a.) for the Mg-containing supports, respectively, were added

over 30 min. to ca. 300 ml water at 60°C and at a constant pH value. Stirring was continued for 30 min. before the suspension was cooled to room temperature. The resulting precipitate was filtered and then washed and redispersed in water (at 40°C) several times in order to eliminate chlorine and sodium residuals. Finally, the samples were dried in air at 80°C and pulverized in an electric mill (only Au/γ-Fe_2O_3).

2.2.2 Deposition-precipitation (Au/γ-Fe_2O_3, Au/CeO_2, and Au/MnO_2)

For Au/a-Fe_2O_3, the support component was first precipitated in the same way as for the CP catalysts, but without addition of $HAuCl_4$, similar to the route described in reference [27]. Then Au-containing solution (0.15 M) was added, together with a Na_2CO_3 buffer solution. For Au/CeO_2, the (Ce3+- free) support precursor was prepared by precipitation of CeO_2 from a 1 M aqueous solution of $Ce(NH_3)_2(NO_3)6$ (Fluka, p.a.) with 1 M Na_2CO_3. Before adding the Au-containing solution (see above), residual NH_3 was removed by repeated filtration, redispersion and heating to 80°C. For the preparation of Au/MnO_2, first $NaMnO_4$*H_2O (Fluka, purum) was reduced to MnO_2 by conc. HCl [25]. Subsequent treatment with 1 M HNO_3 yielded the Hx MnO_2-y precursor, which was impregnated with a solution of $HAuCl_4$ (0.1 M) at 60°C and a pH value of 2 (buffered by LiOH). All three samples were further stirred for 30 min., filtered, and dried, as described above.

2.2.3 Impregnation (Au/Co_3O_4, Au/TiO_2, $Au/g\text{-}Al_2O_3$, and Au/SnO_2):

For Au/Co_3O_4, the oxidic support was prepared by thermal treatment of CoOOH in air at 400 °C. Previously, CoOOH was obtained by oxidation of $Co(OH)_2$ at 90°C with air, according to reference [29], $Co(OH)_2$ by precipitation from an aqueous solution of $Co(NO_3)_2*6H_2O$ (Fluka, p.a.) with NaOH.

For the Au/SnO_2 catalyst, SnO_2 was prepared by oxidation of Sn (Heraeus, 99.999%) with concentrated HNO_3 and subsequent calcination of the resulting oxide at 910 °C (2 h). Finally, for Au/TiO_2 and Au/Al_2O_3 commercially available support materials (Degussa P25 and Degussa 213, resp.) were employed. The pulverized oxides were suspended in 200 ml water (60 °C) and a solution of $HAuCl_4$ was added (within ca. 5 min.), together with a Na_2CO_3 buffer solution. The further processing of all samples (stirring, filtering, washing) was identical to that described above. After preparation, the samples were stored in closed glasses at ambient conditions. All bright colored catalyst samples (e.g., Au/Al_2O_3 or Au/TiO_2) were stored in darkness in order to prevent light. The catalysts were calcined for 30 min. in synthetic air for gravimetric measurements (110 Nml/min) or in 10 kPa O2 in N_2 (20 Nml/min) at 400°C for conversion measurements. This pretreatment, which reduces the Au to its metallic state, was found to produce the most active and selective gold catalysts for PROX [43]. Only for the $Au/Mg(OH)_2$ sample a lower calcination temperature of 300 °C had to be used, since pretreatment at 400 °C yielded the corresponding Au/MgO sample.

2.3 Kinetic literature Review

Several kinetic studies were done in the past to investigate Kinetics of the selective low-temperature oxidation of CO in H_2-rich gas over supported metal catalyst [13,54-56]. Y-F. Han et al [57] studied kinetic of the selective CO oxidation in H_2-Rich gas on a Ru/ϑ-Al_2O_3 catalyst and compared it to Pt/ϑ-Al_2O_3. The preferential oxidation reaction of CO (PROX) over Ru/ ϑ-Al_2O_3 in simulated reformer gas (1.0 kPa CO, 75 kPa H_2 , rest N_2) was investigated over a wide range of CO concentrations (0.02-1.5 kPa) and O_2 excess (/pCO = 0.5-5.0). With respect to side reactions it was shown that despite of the well known methanation activity of Ru catalysts CO methanation and, more important, CO_2 methanation are negligible below 200 °C. Likewise, no CO formation via the RWGS was observed up to 250 °C under present conditions. Within the parameter range investigated the kinetic of the selective CO oxidation over Ru/ϑ-Al_2O_3 can be expressed by a simple power-law rate equation, with reaction orders of α = - 0.5 for CO and α = 0.85 for O_2, at 150 °C. The apparent activation energy, Ea*, was found to be from 90 to 95 kJ/mol at temperatures up to 200 °C, increasing at higher temperatures and CO partial pressures. These results are consistent with a Langmuir-Hinshelwood reaction mechanism, in the low-rate branch. Similar to the reaction on a Pt catalyst the presence of an inhibiting CO adlayer is held responsible for the high selectivity. Accordingly, the loss of selectivity at 200 and 250 °C at low CO concentrations (e.g., S~30% at 200 °C and S~10% at 250 °C at 0.02 kPa CO) is ascribed to a reduced steady-state CO coverage, due to reduced CO re-adsorption, and an increasing H_2 oxidation rate

at high temperature. Model calculation of the oxygen excess and noble metal mass required for the complete removal of 2000 ppm CO in simulated reformer gas showed that the amount of active noble metal is by more than an order of magnitude (at l = 2) lower for Ru/ϑ-Al_2O_3 than for Pt/ϑ- Al_2O_3. More important, only the Ru/ϑ-Al_2O_3 catalyst achieves CO levels below the tolerance limit of 50 ppm at variable loads from 1-100 %, while the Pt/ϑ-Al_2O_3 catalyst remains far above these levels, restricted by the RWGS reaction. In total, the Ru/ϑ-Al_2O_3 catalyst was demonstrated to be clearly superior to the conventionally used Pt/ϑ-Al_2O_3 system for the selective oxidation of CO in H_2-rich gas mixtures.

In 1999, M J Kahlich et al [58] studied Kinetics of the selective low-temperature oxidation of CO in H_2-rich gas over Au/a-Fe_2O_3 catalyst in simulated reformer gas (low concentrations of CO and O2, 75 kPa H_2; balance N_2) at atmospheric pressure. It was investigated over almost two orders of magnitude in CO partial pressure (0.0251.5 kPa) and over a large range of /pCO-ratios (0.25-10). The orders of reaction rate for CO and O_2 at 80 °C found to be 0.55 and 0.27, respectively. The apparent activation energy for this reaction evaluated in the temperature range of 40-100 °C is 31 kJ/mol.

M. Schubert et al [59] conducted a Kinetics study in 2000 to Correlation between CO surface coverage and selectivity/kinetics for the preferential CO oxidation over Pt/Al_2O_3 and Au/α-Fe_2O_3. The optimum operating temperatures on Pt/Al_2O_3 and Au/a-Fe_2O_3 catalysts was found to be 200 and 80 °C, respectively. Kinetic data show that the underlying reason for the very different PROX reaction

kinetics on these two catalysts is the difference in steady-state CO coverage. Reaction order on platinum catalyst was found to be (-0.4) because it always near saturation under reaction conditions. Whereas the CO adsorbed on Au/aFe_2O_3 on the Au surface is shown to be significantly below saturation.

2.4 Catalyst Deactivation

Approximately 5000 h life-time are commonly assumed for mobile applications. This is an important key feature. Most of the catalysts in literature used as a preferential oxidation of CO hydrogen-rich gas have short life. They loose their activities fast. On the other hand, some of PROX catalysts show a long-term stability. Markus [60] investigated long-term stability of different metal oxide supported gold catalysts for the preferential CO oxidation in H_2-rich Gas.

Extensive efforts have been undertaken in their laboratory to study the deactivation mechanism [13,27–29]; STM/STS studies on model Au catalyst studies have shown that the deactivation is induced by oxygen. In order to employ Au as PROX catalysts, it is essential to synthesize nano-Au catalysts with high stability towards CO oxidation. Recently, they obtained highly active and fairly stable catalysts by a temperature programmed reduction–oxidation treatment of an Au–phosphine complex on TiO_2 [28]. Time on stream CO oxidation studies revealed a slow initial deactivation followed by stable activity for several hours as shown in Figure 2.11. Moreover, the catalyst could be completely regenerated by a reduction–oxidation treatment.

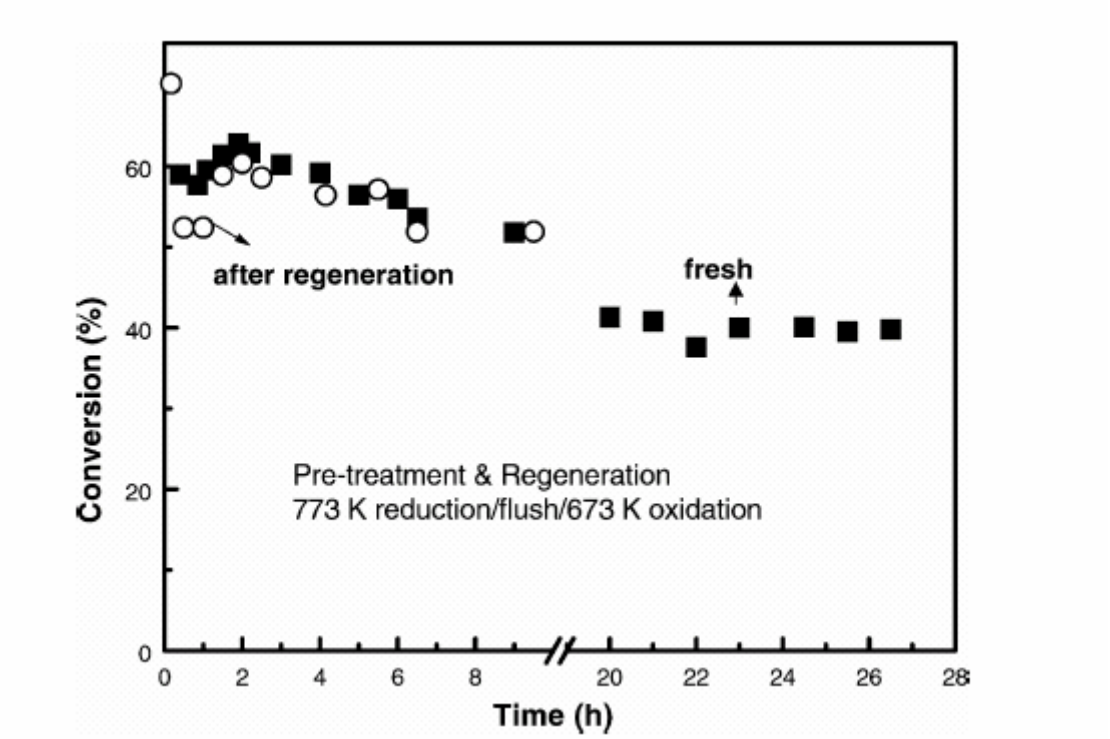

Figure 2.11 Catalyst stability/regeneration after CO oxidation on Au/TiO_2 [at 40 °C (GHSV = 20,000 cc/g/h; *P*CO = 27.5 Torr and PO_2 = 55 Torr).]

2.5 Catalyst Characterization

There are many test techniques available for chemical, physical, and mechanical catalyst characterization of catalyst. A chemical catalyst characterization includes infrared spectroscopy, x-ray diffraction, Temperature program desorption of ammonia (TPD), Temperature programmed reduction (TPR). The physical characterization includes scanning electron microscopy (SEM), Surface area unit (BET). Mechanical characterization includes crushing strength, attrition loss. In literature, the characterization conducted usually for PROX catalyst mainly surface area, TPR, and chemisorptions of O_2, CO, and

H_2O. The following is a summary of some PROX catalyst characterization result of BET surface area, XRD, XPS and TPR reported in literature.

2.5.1 Gas Sorption Analysis

BET surface areas, pore volumes, and pore size distributions were measured for many catalysis used for preferential oxidation using different setup measurement. However, all procedures involve outgassing, adsorption and desorption. The surface area, pore volume, and pore size result show that the catalyst used for PROX reaction has very large range. The effect of sodium addition on surface areas, pore volumes, and pore size distributions of Al_2O_3 are shown in Table 2.1. Alumina has surface area 244 m^2/g. The surface area and pore volume of Al_2O_3 decreases with increases of sodium content as shown in Table 2.1.

TABLE 2.1 BET surface area of Na-Al_2O_3 [12]

Sample	S_{BET} (m^2/g	V_P cm^3	D_P (nm)
Al_2O_3	224	0.58	10.4
Na(0.5)	221	0.58	10.4
Na(1.0)	214	0.55	10.3
Na(2.0)	206	0.56	10.8
Na(3.0)	171	0.48	10.9

Ceria-based supports have very low surface area as shown in Table 2.2. The surface area of MgO is also low but higher than Ce, Ze, and CeZe oxides. The SiO_2–Al_2O_3 support has very high surface area compared to other support where La_2O_3 surface area is the least of all support [54].

TABLE 2.2 BET surface area of various metal oxides [54]

Support	*S*BET ($m^2\ g^{-1}$)
$Ce0.15Zr0.85O_2$	27
$Ce0.5Zr0.5O_2$	45
$Ce0.63Zr0.37O_2$	43
CeO_2	25
MgO	66
La_2O_3	2
SiO_2	175
SiO_2–Al_2O_3	215
Al_2O_3	525

2.5.2 Temperature Programmed Reduction (TPR)

Temperature programmed reduction (TPR) has been widely used in studying the reduction behavior of supported and unsupported catalyst system. TPR is a convenient and rapid technique providing qualitative information of the oxidation state of reducible species. Studying and analysis TPR peak profiles can aid the selection of pretreatment condition of oxidic catalyst precursors. Understanding reducibility behavior is essential for catalyst development.

The TPR profiles of sodium-added aluminas are depicted in Figure 2.12. One major reduction peak of sodium oxide appears at 450–490 °C.

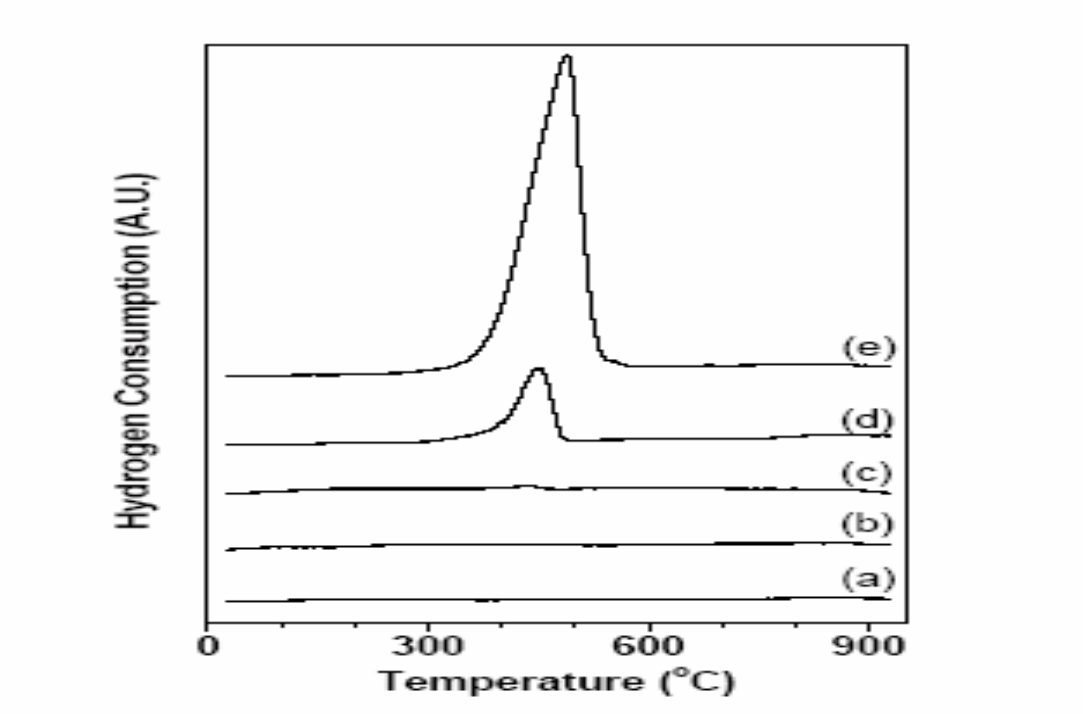

Figure 2.12 TPR patterns of Al_2O_3 and Na [(a) Al_2O_3; (b) Na(0.5); (c) Na(1.0); (d) Na(2.0); and (e) Na(3.0).] [12]

The hydrogen consumption does not appear up to the sodium content of Na(1.0) and then increases suddenly at higher sodium content. The peaks of Na(2.0) and Na(3.0) resemble those reported by Chen et al [12] and are assigned to the reduction of Na_2O. The TPR pattern of Co (1.8), curve (a) in Figure 2.15, shows one peak above 850 °C, which is strong even at 927 °C. This peak is assigned to the reduction of diluted Co2+–Al3+ spinel structures or $CoAl_2O_4$ [13]. The TPR pattern of Pt(1.0), curve (b), shows one peak at 230 °C (region I). It is assigned to the reduction of PtOxCly [14] or PtO_2 [15]. When cobalt is added to Pt(1.0), two changes are observed in the TPR pattern, curve (c). One is the shift of the cobalt reduction peak from above 850 °C to lower temperatures, 550–927 °C (region III), and the other is the appearance of a new

peak at 320 °C (region II). The peak at 550–927 °C is assigned to the reduction of the surface spinal cobalt species [13]. It was reported that platinum decreased the reduction temperature of the cobalt species [61]. With increasing sodium content, complicated changes are observed in the TPR pattern of platinum-cobalt catalysts, as shown in Figure 2.13.

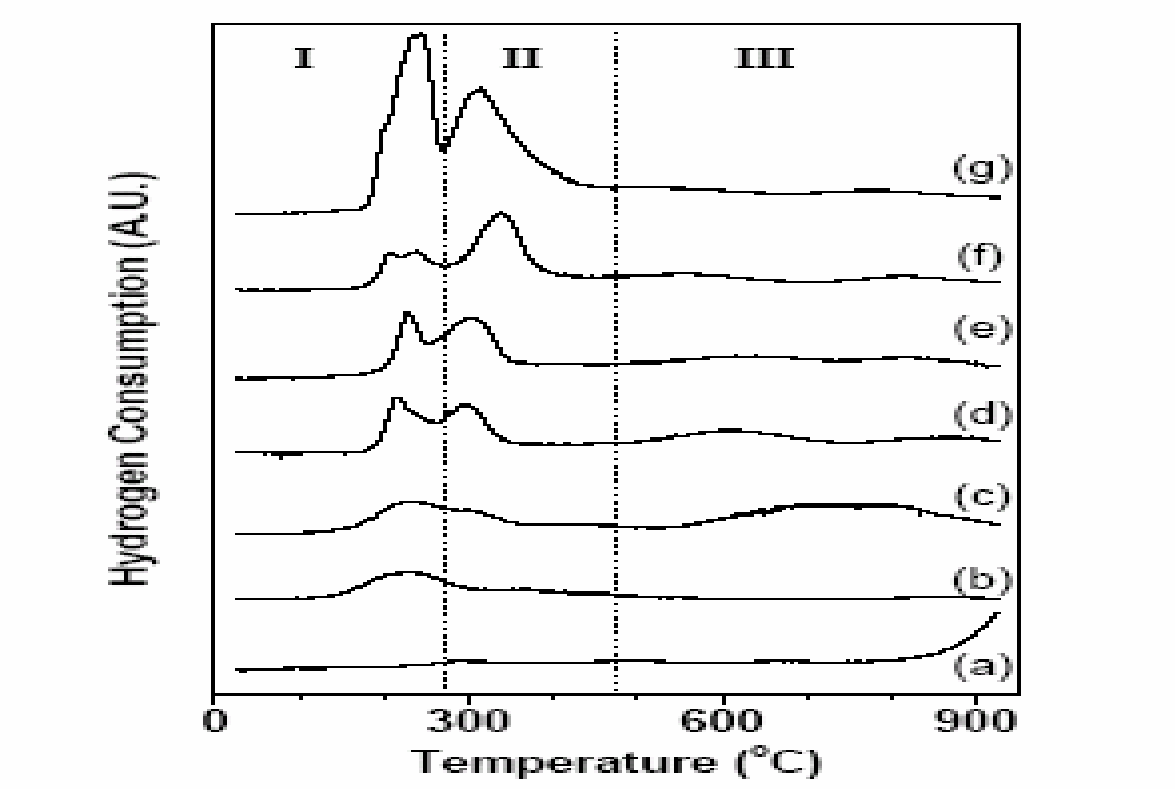

Figure 2.13 TPR patterns of Co, Pt, and Na. [(a) Co(1.8); (b) Pt(1.0); (c) Pt(1.0)Co(1.8);(d) Na(0.5)Pt(1.0)Co(1.8); (e) Na(1.0)Pt(1.0)Co(1.8); (f) Na(2.0)Pt(1.0)Co(1.8); and (g) Na(3.0)Pt(1.0)Co(1.8).] [61]

The main change is the increase of the peaks at region II, accompanied by the decreases of the peak at regions I and III. The reductions of Na(2.0)Pt(1.0)Co(1.8) and Na(3.0)Pt(1.0)Co(1.8), curve (f and g) show two peaks in region I, but in the case of Na(3.0)Pt(1.0)Co(1.8) the former peak at 200 °C is in the form of a shoulder. Based on the area of the peak and a separate TPR experiment with Na(X)Pt(1.0), the low-temperature peak at 200 °C is attributed to the reduction of platinum, while the other peak is attributed to the reduction of sodium. In the previous report [12], reduction of platinum alone in a sodium-added platinum catalyst could not be distinguished because the reduction peak is much smaller than that of sodium [62].

Figure 2.14 shows the TPR profiles of the 50 ppi foam-based PtFe catalyst compared to that of the powdered PtFe catalyst. As also found for the foam-based Pt catalysts [63], multiple peaks were detected for the foam-based PtFe catalyst whereas only two peaks were evident for the powdered one.

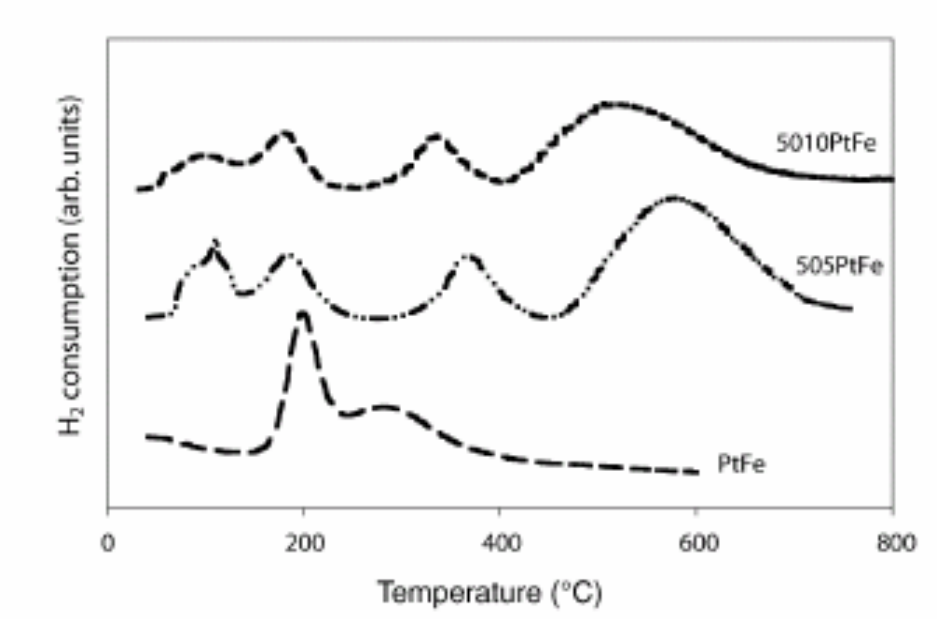

Figure 2.14. TPR profiles of the powdered and foam-based PtFe catalysts. [metal foam supported PtFe (5 wt.% Pt, 0.5 wt.% Fe based on the loading of alumina washcoat) catalysts. Foam-based PtFe catalysts with different numbers of pores-per-inch (30–50) and percentage relative metal densities were characterized].[62]

In order to get rid of residual impurities from preparation that might be leading to confusing TPR results, additional pre-treatments were performed before TPR. They were:

1. Washing with 908 °C water and drying overnight at1108 °C.
2. Reducing at 550 8C for 1 h in a stream of H_2.
3. Recalcining at 500 8C for 2 h in a stream of air.

The effect of pre-treatment on TPR for the foam-based PtFe catalysts was the same as that for the foam-based Pt catalysts [64]. Four reduction peaks of the

foam-based catalyst became three main peaks after pre-reduction and recalcination. Washing the catalyst in hot water before reduction and calcination resulted in a slight increase in the magnitude of the low temperature peak. The low temperature peaks (100–220 °C) were located at the same place as the low temperature peaks of the original catalyst and can be assigned to the reduction of Pt and possibly neighboring Fe. The higher temperature peak which was not observed for the powdered catalyst, is assigned to the reduction of Fe highly dispersed on the γ-Al_2O_3 and possibly accessible metal foam surfaces by hydrogen spill-over. The reduction peak for Fe/g-Al_2O_3 in the absence of Pt has been shown in previous work [65] to be around 400 °C. No TPR peaks were detectable for the metal foam alone [66].

Ojeda et al [67] investigated H_2-TPR profile for Rh/Al_2O_3 catalysts as illustrated in Figure 2.15.

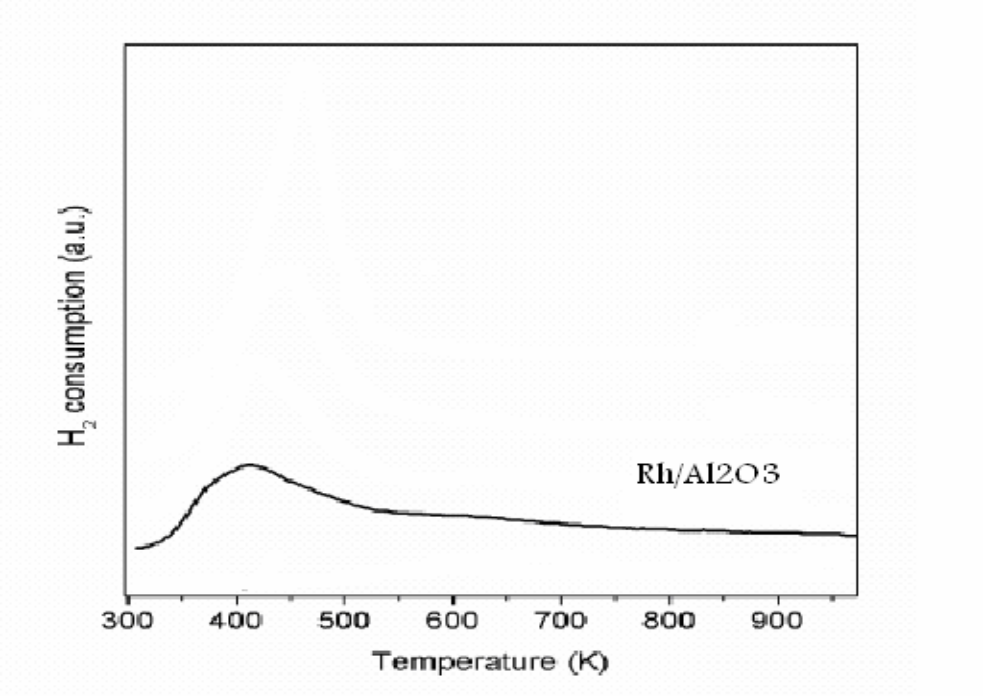

Figure 2.15 TPR profile for Rh/Al_2O_3 [67]

The Rh/Al_2O_3 catalyst gave a broad reduction peak centered at 138°C (415K), which corresponds to the reduction of Rh_2O_3 to give metallic Rh. It should be noted that the amount of H_2 was consumed in the reduction process was lower than expected according to the reaction stoichiometric. The fraction of reducible rhodium oxide was about 60–70%. A very similar observation was reported by Burch et. al. [68], suggesting that when calcining at 500 ºC, some rhodium oxide on the Al_2O_3 may spread over the support and diffuse into defect sites in the alumina, becoming strongly bound and non-reducible. In fact, X-ray photoelectron spectroscopy (XPS) confirmed the above suggestion. Identification of Rh chemical states was in agreement with the literature [69]. During reduction, Rh_2O_3 was transformed into metallic Rh, and a new Rh 3d5/2 peak appeared at 307.0 eV, which corresponded to RhO species (spectrum B). It can be seen that not all Rh^{3+} species are reduced after treatment with H_2 at 500 ºC for 1 h. By integration of the different Rh 3d5/2 peak areas, it may be concluded that the fraction of Rh atoms remaining as Rh^{3+} species after reduction is about 0.40, thus confirming in the previous TPR results, which show that some rhodium oxide can interact with the alumina support and cannot be reduced.

Carvalho et. al. [70] showed that Pt/Al_2O_3 has a large H_2 consumption peak centered at 250°C as illustrated in Figure 2.16.

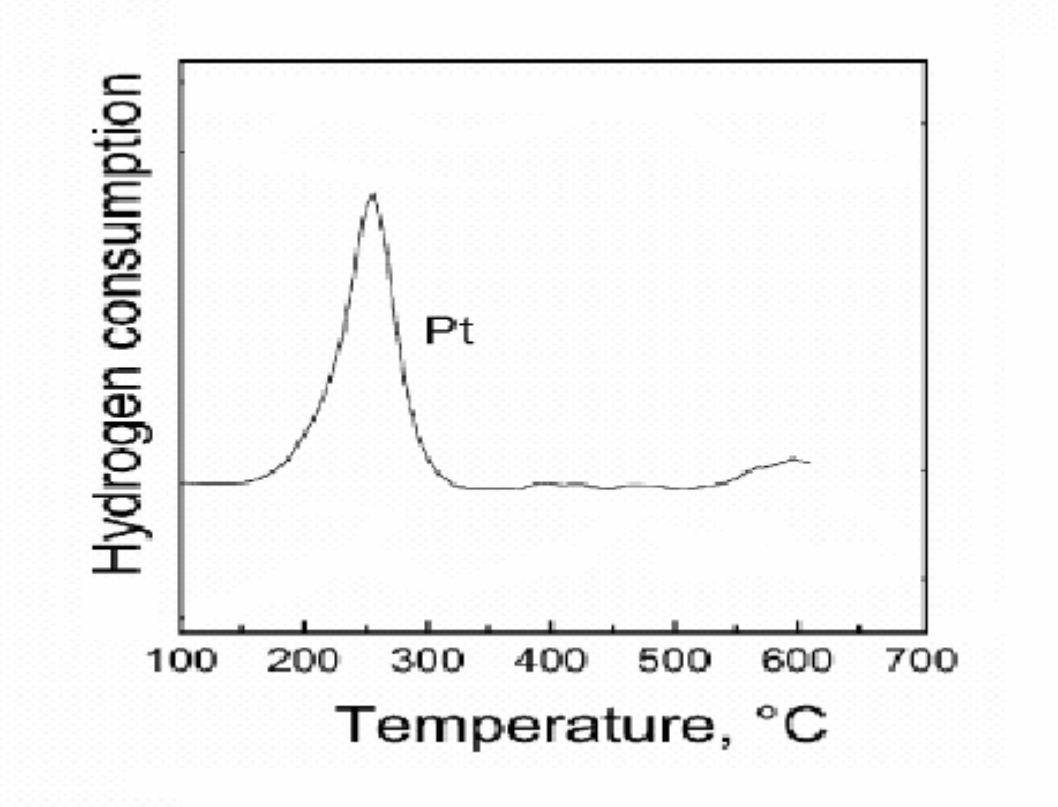

Figure 2.16 TPR profile for Pt/Al_2O_3 [70]

This peak can be divided into three peaks; the first peak (228 ºC) corresponds to the reduction of big crystals of Pt oxide weakly interacting with the support. The second peak (257 ºC) would correspond to the reduction of most of the Pt oxide, which is distributed among smaller crystals and with mild interaction with the support. The third peak (293 ºC) would correspond to the reduction of highly dispersed oxychloride species (PtClxOy) in strong interaction with the alumina support. The total H_2 consumption (TPR area in 2.18) corresponds to the total reduction of Pt(IV) to Pt(0).

Chena et. al. [71] investigated the reduction behavior of $Cu\text{-}CeO_2/\gamma\text{-}Al_2O_3$ by H_2-TPR. They found that the H_2 consumption increased with Ce content up to 25

wt.%, but declined when Ce content was raised to 30 wt.% as shown in Figure 2.17.

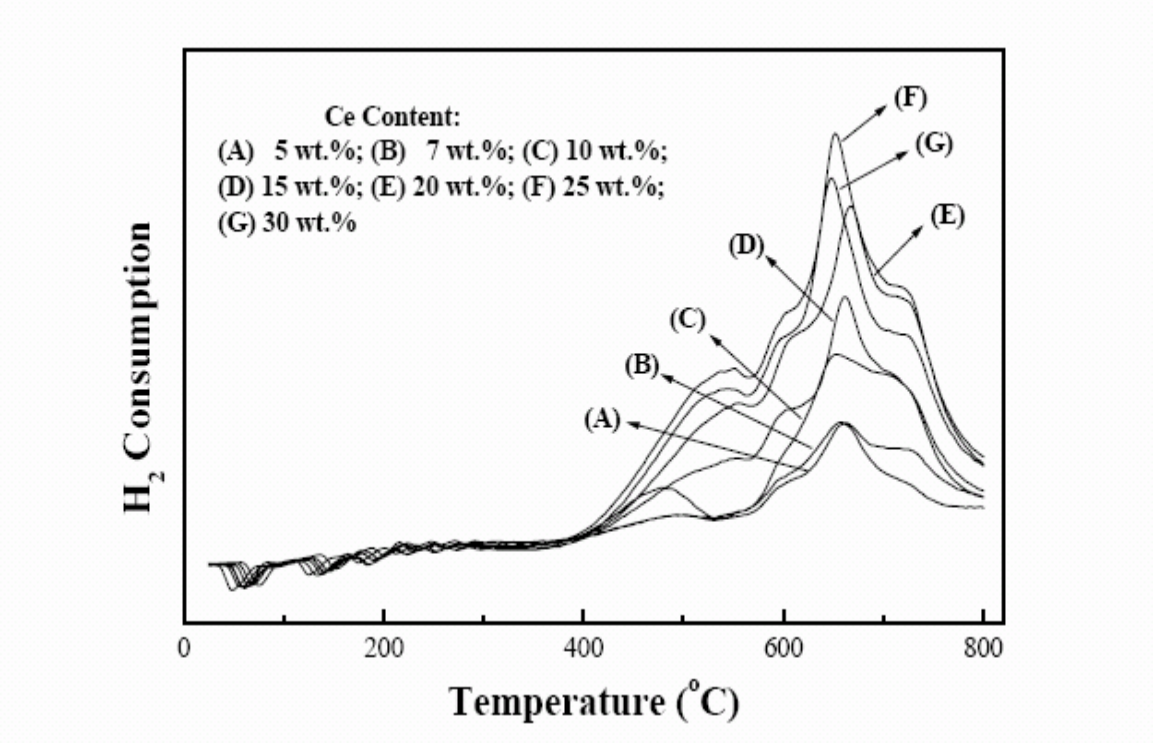

Figure 2.17 H_2-TPR profiles of CeO2/γ-alumina. [71]

As known that H_2 consumption equates to the amount of reducible Ce species in $CeO_2/\gamma\text{-}Al_2O_3$ means H_2 consumption increases with the Ce content. The decline at 30 wt.% is caused by the large increase in crystal size leading to more internal Ce species of CeO_2 being non-attainable by H_2 molecules. They additionally found that H_2 consumption at 20 wt.% Ce content was less than at 25 and 30 wt.% Ce content.

Parka et. al. [72] investigated the reduction behavior of $Cu\text{-}CeO_2/\gamma\text{-}Al_2O_3$ by H_2-TPR. They found that no peak was observed until the reduction temperature

reached 500ºC for ceria. In the system containing only copper, only one peak was observed with temperature 210ºC as shown in Figure 2.18

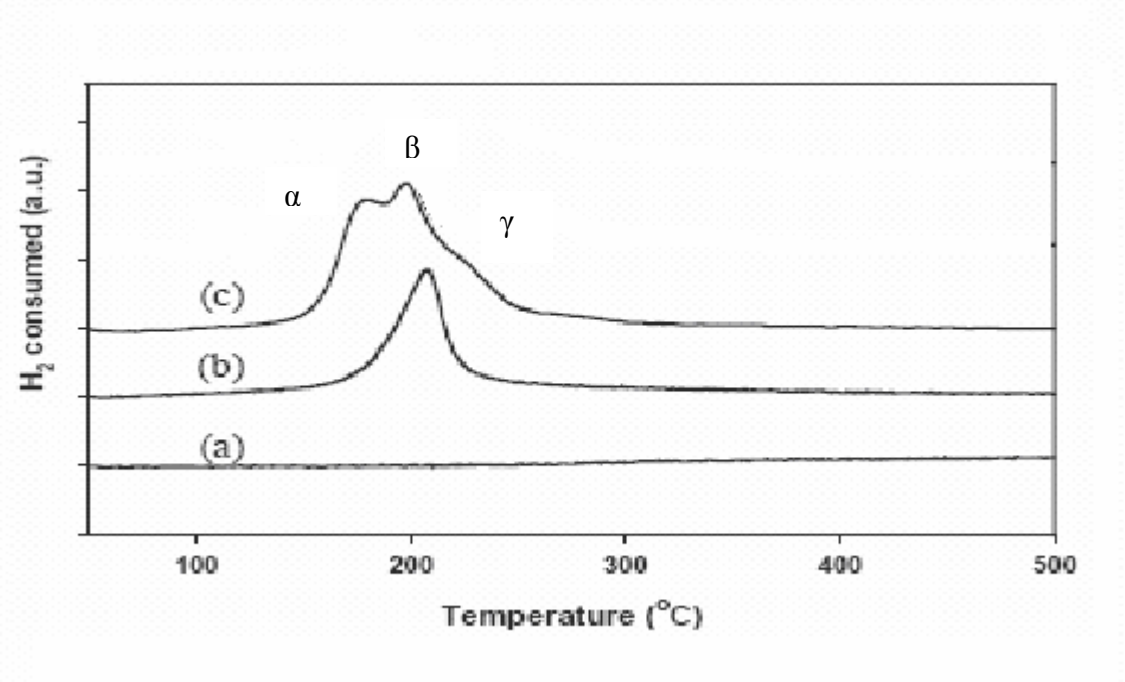

Figure 2.18 H_2-TPR profiles Ce, Cu, and Cu–Ce over γ-Al_2O_3. [[(a) Ce [10 wt%], (b) Cu [5 wt%], (c) Cu–Ce [4 : 16 wt%].] [72]

. Reduction reaction was started at 180ºC and terminated at 250ºC. All cupper oxide was reduced at temperature lower than 250ºC. In the system containing both Cu and CeO_2, the formation of (α, β, and γ)-peaks overlapped at about temperature maxima of 178, 298, and 230ºC respectively were remarkable. The reduction reaction started at 150ºC and finish at 270ºC. It is obvious that the α peak formation and β peak shift to lower temperature suggest the existence of metal oxide–metal oxide interaction induced by the establishment of intimate contact between the two components. This means when the reaction temperature of 150–200ºC is reached, both H_2 and CO can react with O_2 competitively resulting in progressive decline of selectivity as evidenced.

TABLE 2.3 Temperature of TPR peak profiles for Cu, Ce, Pt, and Rh on γ-Alumina

Catalyst	T_{Peak1}	T_{Peak2}	T_{Peak3}
Cu/γ-Alumina	210	-	-
Ce/γ-Alumina	600	660	730
Pt/γ-Alumina	250	-	-
Rh/γ-Alumina	138	-	-
CuCe/γ-Alumina	178	298	230

2.6 Effect of H_2O on the Selective CO Oxidation

Parka et al [72] investigated the effect of water vapor on the activity and electivity of CO oxidation over CuCe/A catalyst and CuCeCo0.2/A catalyst with or without 10 vol% H_2O in the reactant feed. Addition of H_2O to the hydrogen rich feed stream decreases the catalytic activity for the selective CO oxidation and the temperature at which 50% conversion of CO was obtained, T50, shifted to a higher temperature by 15ºC and 40ºC for both CuCe/A and CuCeCo0.2/A, respectively as illustrated in Figure 3.19. The decrease of CO conversion at selective oxidation of CO over the Cu–Ce based catalysts in the presence of water vapor may be attributed to the blockage of catalytic active sites by adsorbed water as well as to the formation of CO-H_2O surface complexes which are less active than adsorbed

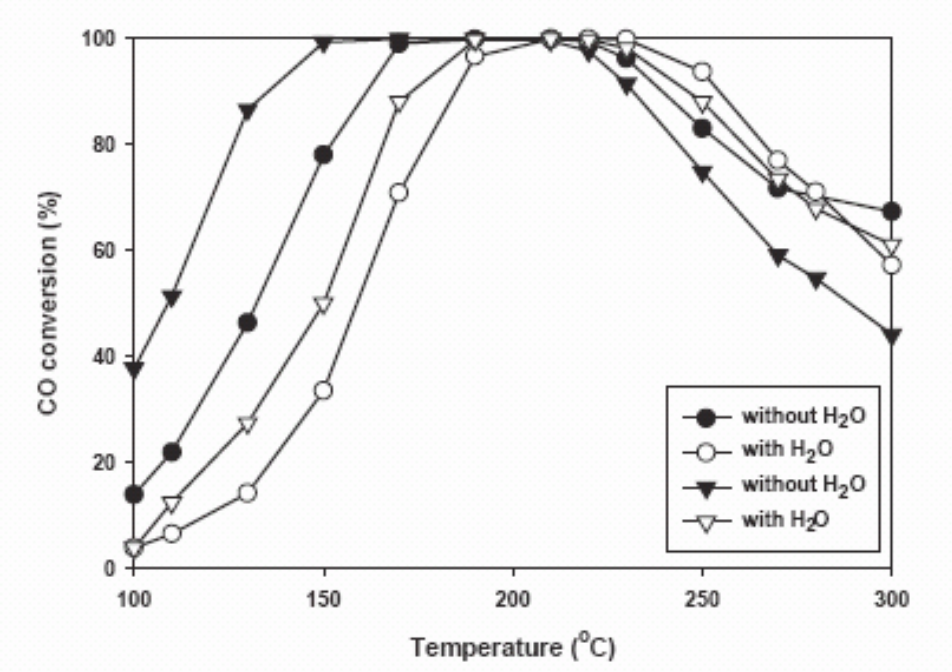

Figure 2.19 Effect of water vapor on CO conversion of CuCe/A and CuCeCo/A catalyst, [CuCe/A (circle) and CuCeCo/A (triangle down)] [72]

Avgouropoulos [73] studied the effect of ware addition on the Au/α-Fe_2O_3, CuO–CeO_2, and Pt/γ-Al_2O_3 activity and selectivity. He found that the effect of H_2O on the Pt/γ-Al_2O_3 catalyst was markedly different than Au/α-Fe_2O_3, CuO–CeO_2 As shown in Figure 2.20. Fro Pt/γ-Al_2O_3 catalyst, the CO conversion achieved at a given temperature is significantly higher in the presence of H_2O than in its absence below 140ºC. For the other two catalysts, the CO conversion achieved at a given temperature is significantly lower in the presence of H_2O than in its absence.

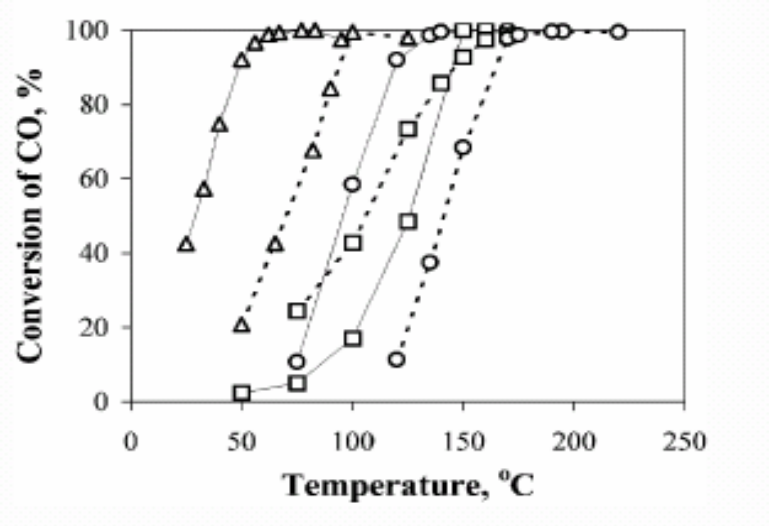

Figure 2.20 Effect of water vapor on CO conversion on Au/α-Fe_2O_3, CuO–CeO_2, and Pt/γ-Al_2O_3 catalyst, [Au/α-Fe_2O_3 (Δ), CuO–CeO_2 (O), and Pt/γ-Al_2O_3 (□) catalysts in the presence of 15 vol.% CO_2 (solid lines) and in the presence of both 15 vol.% CO_2 and 10 vol.% H_2O in the reactant feed (dotted lines). [73]

CHAPTER 3

EXPERIMENTALS

3.1 Experimental Design

For successful completion of this research work, experiment was planed as follows:

a- Preparation of multicomponent catalyst with atomic ration of 100:20:3:1 for Cu:Ce_2O_3:Pt:Rh respectively based on Inui [46,53] research work.

b- Using Commercial γ-Al_2O_3 as a support.

c- Characterize the prepared catalyst.

d- Evaluation of these catalysts in a fixed bed reactor for selective oxidation using gas mixture consisting of CO and high H_2 concentration as a feed.

f- Study the effect of Pt and Rh addition on CuCe/γ-Al_2O_3 as a base catalyst by preparing catalyst with and without Pt and Rh and test their activity and selectivity.

g- Investigate the effect of water vapor in the feed on activity of the catalyst.

3.2 Catalyst Preparation

Catalyst Composition

The designed composition for the preferential oxidation catalyst is Cu-Ce_2O_3-Pt-Rh/γ-Al_2O_3 having atomic ratio of 100: 20: 3: 1.

The roles of these metals are

- Cu is main active metal
- Ce_2O_3 is to enhance oxygen- spillover
- Pt and Rh is to enhance hydrogen-spillover

The Weight % of Cu was ranged between 0.5 and 6 and the other components were calculated with respect to the atomic ratios mentioned above.

Thirteen catalysts were prepared with different percentages of four metals loading as shown in Table 3.1. Cat-0.5 to Cat-6 catalysts were prepared to find optimum metal loading for maximum CO conversion. Cat-2A, Cat-2B, Cat-2C, and Cat-5A catalyst were prepared to study the effect of Pt and Rh addition on the activity and selectivity of CuCe/γ-Al_2O_3 as a base catalyst. The letters A, B, and C signify the catalyst without Pt and Rh, with out Pt, and without Rh long with CuCe/γ-Al_2O_3 base catalyst. Cat-2R1 and Cat-2R2 were prepared to test for reproducibility.

TABLE 3.1 composition of prepared catalysts

Catalyst Code	Components (wt %)			
	Cu	Ce_2O_3	Pt	Rh
Cat-0.5	0.5	0.52	0.046	0.0080
Cat-1	1.0	1.03	0.092	0.016
Cat-2	2.0	2.1	0.18	0.032
Cat-3	3.0	3.1	0.28	0.048
Cat-4	4.0	4.1	0.37	0.064
Cat-5	5.0	5.2	0.46	0.080
Cat-6	6.0	6.2	0.55	0.096
Cat-2A	2.0	2.1	0	0
Cat-2B	2.0	2.1	0.18	0
Cat-2C	2.0	2.1	0	0.032
Cat-5A	5.0	5.2	0	0
Cat-2R1	2.0	2.1	0.18	0.032
Cat-2R2	2.0	2.1	0.18	0.032

Catalyst Preparation Procedure

Commercial γ-alumina was selected to be the catalyst support. It was dried at 210°C for 2 h then transferred to a dessicator to cool to room temperature. The active metal was loaded on the dried alumina in the following sequence.

I- Loading Rh by incipient impregnation on γ-alumina

The Rh solution was prepared by disolving rhodium chloride ($RhCl_3$) in distilled water. The weight of $RhCl_3$ was calculated as shown in Appendix C. For each gram of the support, 1.15g of water was used to prepare the metal salt solution. Alumina was dipped into the solution at once then mixed by glass rode for a minute. The catalyst was then transferred immediately into an appropriate size of filter paper and the excess impregnated solution was swiped off.

II- Drying

After swiping the excess water out, the support was heated from room temperature at 0.3°C per minute to 60°C to provide a nice moisture-drying process. If the support is dried at high heating rate, large crystals of the salt will be formed and will be difficult to react with ammonia in next step of procedure.

III- NH_3-H_2O vapor treatment

In order to convert the metal-salt anion to ammonium salt, the 85% dried material was exposed to vapor mixture of 10 wt% of NH_4OH in aqueous solution at 60°C for 5 min. Excess exposure of the catalyst to ammonia vapor enhances crystallization of ammonium complex and decreases the dispersion.

IV- Thermal decomposition of nitrate salt-anion by sublimation

After ammonia treatment, the material was heated from 60 to120°C in 1h, and then temperature was elevated up to 250°C in 1.5 h. In this step, the ammonium salt was moved by sublimation. High heating rate can caused sintering of the metal.

V- Hydrogen reduction and thermal treatment

The salt-removed material was shifted to hydrogen reduction setup and heated from room temperature up to 430°C in 2 h, in a stream of 10 vole% H_2 diluted with N_2 with a rate of 6 liter /h.

VI- Procedure to support Pt by incipient impregnation

The procedure above was repeated from step I to V but using [Pt $(NH_3)Cl_2 \cdot nH_2O$] instead of rhodium chloride.

VII- Procedures to support Ce-Ce by incipient impregnation

The procedures was repeated from step I to V but using $Cu(NO_3)_2 \cdot 6H_2O$ $+Ce(NO_3)_3 \cdot 6H_2O$ in stead of $RhCl_3$.

VIII- High-temperature treatment

The salt-removed material was transferred to the pipe-type electric furnace, and heated from room temperature up to 650°C in 2 h, in a stream of 10 vol% H_2 was diluted with N_2 with a rate of 6 liter /h.

3.3 Characterization of Prepared Catalysts

Chemical analysis, BET surface area, total pore volume, average pore radius, and TPR measurements were conducted to characterize the prepared catalysts. The characterization results were used to explain the differences in the activity of prepared catalysts.

3.3.1 Chemical Analysis

The catalysts prepared were analyzed for the metals loaded by inductive coupled plasma technique (ICP) using Spectro- Ciros instrument.

Sample solution preparation procedures:

The catalyst sample was grinded to a very fine powder. A sample of 0.10 g of a fine powder catalyst was transferred to 100 ml glass beaker, then 10 ml of a solution consisting of a 50% of HCl and 50 % of HNO_3 was added. The solution mixture was heated at boiling temperature with refluxing for 1 h then cooled at room temperature. The solution was transferred to a 100 volumetric flask then filled with 5% of HNO_3. This volumetric flask was stirred for 5 min. After that, the mixture was filtered. The filtrate was analyzed by ICP.

ICP Analysis

Standard solutions containing all four metals and sample solution matrixes were prepared in ppm concentrations. After the calibration curve was established, the solutions were measured in ppm concentration. The weight

percentages of all four metals in each catalyst were calculated. The results were compared with the calculated weight percent.

3.3.2 Gas Sorption Analysis

BET surface area, total pore volume, and average pore radius of the catalysts were measured by NOVA-1200 system (*Quanta Chrome Corporation)*. A schematic flow diagram of apparatus is shown in Figure 3.1.

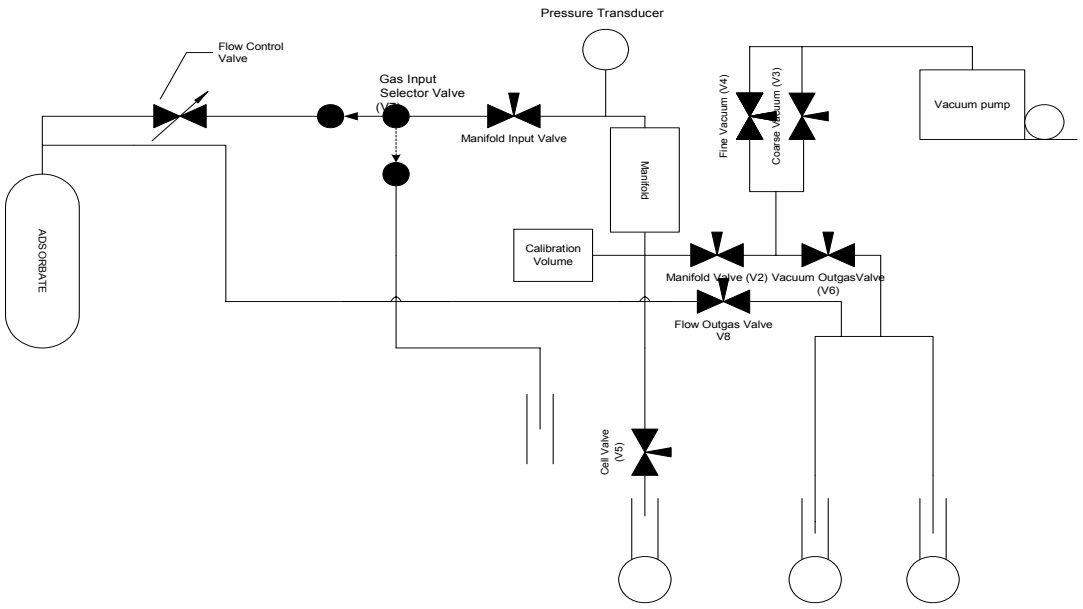

Figure 3.1 Schematic Flow Diagram of Nova Sorption Analyzer

Operational procedure

A weight of 0.25 gram of catalyst sample was placed in a sample cell and then heated to 90 ^{o}C in 10 min and maintained for 1 h at that temperature. The temperature was increased to 350 ^{o}C and maintained for 2 h. The adsorbate used was nitrogen. The measurement was fully automatically programmed.

The pore size was calculated assuming cylindrical pore geometry using Kelvin Equation by machine.

$$r_k = \frac{-2\gamma V_m}{RT \ln(P/P_0)}$$

Where

γ is the surface tension of nitrogen at its boiling point (8.85 ergs/cm^2 at 77K).

V_m is molar volume of liquid nitrogen (34.65cm^3/mol).

R is gas constant (8.314x10^{7}ergs/deg mol).

T is boiling point of nitrogen.

P/P_0 is nitrogen relative pressure.

r_k is Kelvin radius of the pore.

Kelvin radius r_K is the radius of pore in which condensation occurs at a relative pressure of P/P_o. But Actual pore radius is given by

$r_p = r_K + t$

t is adsorbed thickness layer which is given by:

$$t(A^0) = 3.54 \left[\frac{5}{2.303 \log(P_0/P)} \right]^{1/3}$$

Total pore volume was calculated from the amount of vapor adsorbed at a relative pressure by assuming that pores are filled with liquid adsorbate. Most common method for determining the total surface area of the catalyst is BET method developed by Braunner, Emmet and Teller.

BET equation is given by

$$\frac{P}{V_a\left(P_o - P\right)} = \frac{1}{V_m C} + \frac{c-1}{V_m C}\left(\frac{P}{P_o}\right)$$

V_a is the amount of gas adsorbed at a relative pressure P/P_0.

V_m is the amount of adsorbate constituting a monolayer of surface coverage.

C is BET constant related to energy of adsorption.

The amount of nitrogen adsorbed at equilibrium and its normal boiling point of nitrogen was measured over a range of atmospheric partial pressure less than 1. The total pore volume is equal to volume of the gas adsorbed calculated from pressure variation that is calculated from adsorption of known volume of N_2 gas by test sample.

3.3.3 Temperature Programmed Reduction (TPR)

TPR was used to characterize metal-support and supported metal-metal interactions. TPR provides useful information on the temperatures needed for the complete reduction of a catalyst. Reduction behavior is important information in the preparation of metallic catalysts. The reduction of metal oxide MO_n by H_2 can be described by the following equation.

$MO_n + nH_2 \longrightarrow M + n\,H_2O$

The amount of hydrogen consumed for the reaction can be found using TPR. Also, the TPR profile provides information at what temperature the reaction occurs. By using the amount of hydrogen consumed in the reaction with the metal concentration on the catalyst, the state of metal oxide can be found.

TPR Measurement Procedure

TPR measurements were carried out in a system supplied by *Ohkura Riken Co. Ltd.*, (model TP-200). A schematic flow diagram of apparatus is given in Figures 3.2. The equipment was developed for obtaining data related to reduction characteristics of metal oxides or metal supported catalysts.

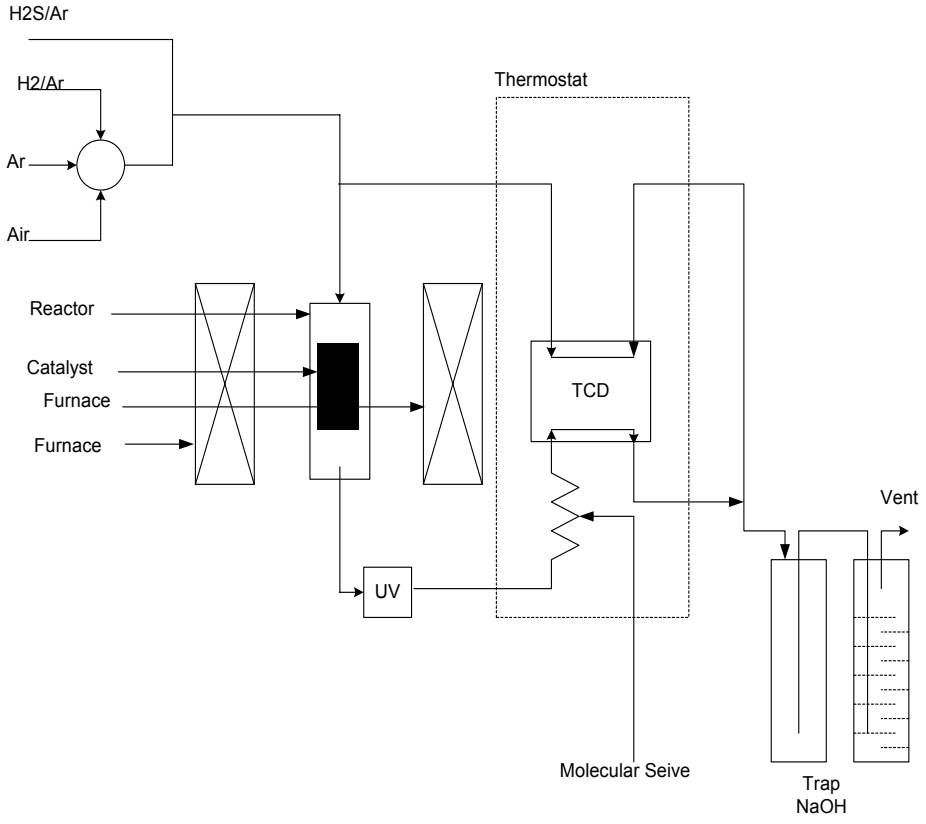

Figure 3.2 Temperature Programmed Reduction Apparatus

The operational procedure was carried out into two steps as follows

I. Pretreatment

150 mg of powder sample was placed in a quartz tube (8 mm O.D.) reactor. Temperature was raised to 400^{o}C at a rate of 10^{o}C per min and kept for 2 h, then cooled to ambient temperature. Air was purged by flowing Argon (22 cm^{3}/min) for 30 min at ambient temperature.

II. Reduction

The gas used for reduction contained 5 % H_2 in Argon. The flow rate was 30 cm^{3}/min. Temperature of the reactor was raised from 30 to 1,030^{o}C at a heating rate of 10^{o}C/min and then kept for 15 min. Thermal conductivity detector (TCD) was used determine H_2 concentration. The temperature of the catalyst and H_2 consumption were monitored and recorded.

3.4 Reaction Set-up for Activity Test

The prepared catalysts were tested in a fixed bed stain less steel reactor with 1cm inside diameter at temperature range from 25 to 300ºC with following feed composition. The gas containing CO and H_2 was mixed and with air in different amounts to achieve the desired concentrations as shown in Appendix B and the result of these calculations is shown in Table 3.2.

TABLE 3.2 Feed compositions with out steam

O_2/CO Ratio	Flow rate			Feed Composition				
	Gas ml/min	Air ml/min	Feed ml/min	y_{H2}	y_{CO2}	y_{CO}	y_{O2}	y_{N2}
1.0	143	6.8	150	0.802	0.143	0.00954	0.00954	0.0359
1.5	140	10.0	150	0.784	0.14	0.00933	0.014	0.0527
2.0	137	13.0	150	0.767	0.137	0.00913	0.0182	0.0685

CO in the feed gas should be preferentially and selectively oxidized to CO_2 at lower temperatures around 120–150°C while avoiding both H_2 combustion and methanation reactions. Target of unreacted CO concentration is less than 10 ppm, considering the usage for PEFC at fairly lower temperature of about 80°C. Because, at these lower temperatures CO strongly adsorbed on the surface of Pt catalyst in the fuel cell anode, and inhibits the activity.

3.4.1 Reaction System

The reaction system consisted of three main parts as shown in Figure 3.3. The first part is a teed section consisting of gas mixer. The second part is heating system that consists of three temperatures controllers and high temperature furnace, and temperature monitor. The last part is the reactor. These three parts will be described in detail with experimental procedure.

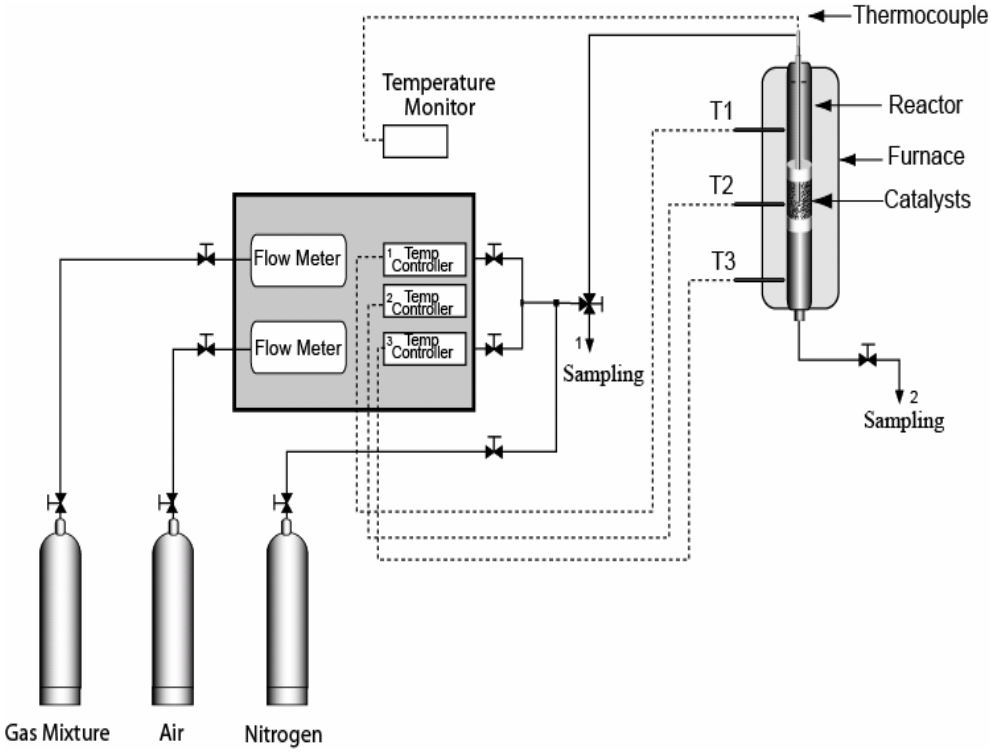

Figure 3.3 Reaction System used for PROX reaction

The reactant gases were mixed using two precise mass flow meters. These mass flow meters were connected to the gas cylinder as shown in Figure 3.3. The outlet tubes were connected togather. Three valves were placed in each line to control the flow. After connections were done, leak test was performed to make shore there is no leak. The flow meters were calibrated with the same gas using soap bubble-meter. The calibrations were checked in the beginning and the end of each experiment to make sure no change in calibrations.

The schematic of the reactor is shown in Figure 3.4. It is meter stainless steel tube with a centimeter ID diameter. The catalyst was designed to be in the middle of the reactor. The thermocouple for measuring the catalyst temperature

was design to be in the middle of the catalyst bed. The thermocable outer diameter was 0.3 cm. One ml of the catalyst was found to have 1.36 cm bed. The reactor was filled as shown in Figure 3.4. The lower part was filled with quartz wool for 0.25 cm then calcium carbide for 0.5 cm. The catalyst sample was filled in the medial of the reactor. About 0.5 cm of quartz wool was filled above the catalyst. Again, calcium carbide was used to fill the upper part of the reactor. After the calcium carbide, 0.25 cm of quartz wool was added in the remaining volume of the reactor. All packings were performed nicely in order not to block the reactor or create back pressure. After packing, the reactor was fixed in the system. Before running the experiment, a leak test was performed using N_2 gas before starting the reaction. The exhaust of the reaction was connected to the hood since CO is highly poisonous and H_2 is highly filmable. A CO detector was used during the experiment to detect any CO in the laboratory.

The gas mixture and air were set to the exact volumetric flow rate, then a sample of final mixture of the gases (feed) was collected and analyzed by two GCs with FID and TCD detectors to conform the final concentration of H_2, CO_2, CO, O_2, and N_2. The results of the sample analysis were compared with the results from calculation of mass balance.

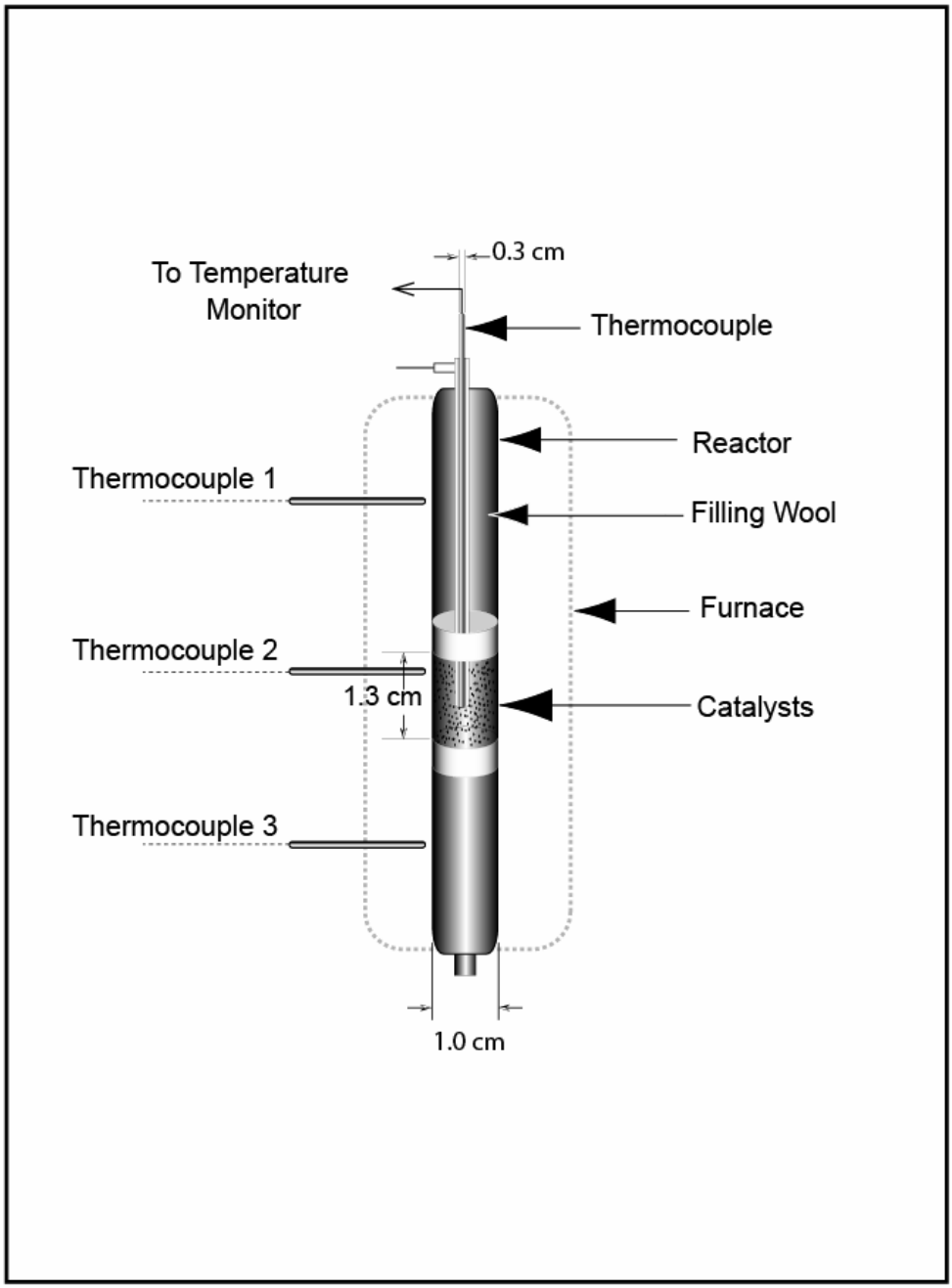

Figure 3.4 The Reactor used for PROX reaction

The reaction was started by feed gas to the reactor. The temperature of the reaction was increased using three temperature controls. As is it clear from the reactor diagram the reactor furnace is divided to three equal zones. Each of these controls is connected to one of these zones. First the temperature was setto 50ºC in all controllers. The temperature was fluctuated before reaching to the set point temperature. The catalyst-bed temperature was monitored. After catalyst temperature stabilized for 15 minuets, a sample was collected in special plastic bag then was analyzed by GC. The temperature was raised to 50, 75, 100, 120, 130, 140, 145,150,160, 170 and 180ºC. The same procedure using temperature 50ºC was applied for each of these set points temperatures with following reaction conditions:

Catalyst volume: 1 ml.

Space velocity: 9000h^{-1}.

Pressure: 1 atm

3.4.2 Testing Catalyst Activity with Steam in the Feed

To test the effect of water vapor on the activity of the catalyst for CO oxidation, water pump, steam unit, and water trap was added to the reaction system as shown in Figure 3.5. The steam unit consists of 1.5 m tube in a coil shape wrapped with heating tape. A Thermocouple was placed at the tube to measure the temperature. The thermocouple was connected to a heating control device to control the temperature of the coil. The steaming unit was connected to

the feed gas tube in order to have good mixing between the gas mixture feed and the water vapor. The tube between steam unit and the reactor was wrapped by heating tape and insulated in order to prevent water vapor to condense before the reactor. A water pump (has four digits ml/minute) was connected to the tube of steaming unit. The water bump was connected to steam unit. A water trap was added to the system after reactor to collect water vapor before is reaching sample collector.

The temperature of the steam unit coil and the tube to the reactor were set at 120ºC one hour before starting ware pump. The reactor temperature was set to 100ºC to prevent water steam to condense in the reactor. After calibration of water pump, the water was sent though the steam unit to the reactor.

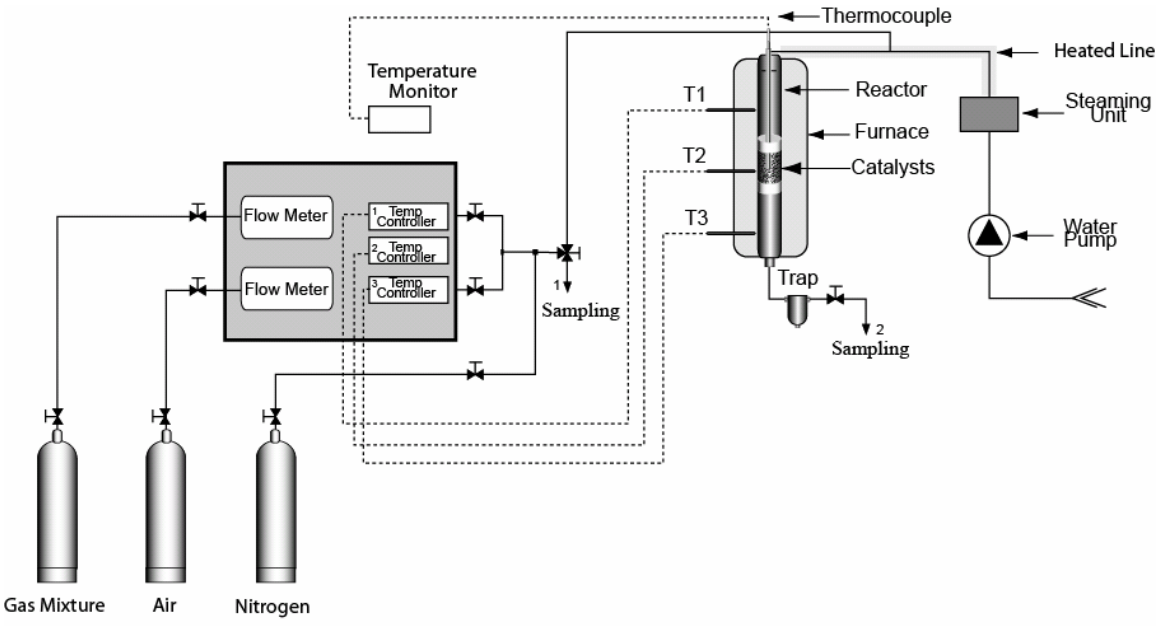

Figure 3.5 Reaction system used for PROX reaction with additional part fore steam

CHAPTER 4

RESULTS AND DISCUSSTION

4.1 Characterization

4.1.1 Results of Gas Sorption Analyzer

The surface area, pore volume, average pore radius, and pore volume distribution were evaluated for the prepared catalysts. The data is presented in Table4.1 and in Figures 4.1-4.4. The total surface area is summation of the out side area of the catalyst and internal surface area. The outside area is the area of out side surfaces of the catalyst. The internal surface area is the area of the wall of the pores. This area usually is 90% of the total area. The internal surface area increases with increases of the pore wall. Small pore size material has larger area than the material with large pore with the same total pore volume. The surface area was decreased with the increasing of metal loading as illustrated in Figure 4.1. For example, the surface area of the support was143.4 m^2/g whereas the surface area of Cat-6 104.7m^2/g. The surface area of the support was reduced by 27.7 % with loading 6 wt% of Cu with respected amount of other three metals. The Figure 4.1 clearly shows that up to 5 wt% Cu loading, the SA was not much decrease. However, a substantial decrease of SA was at 6 wt% of Cu. Also, the pore volume was decreased with increased of metal loading as shown in Figure 4.2. The pore volume of the support was reduced from 0.71

to 0.59 cm^3/g with loading with loading 6 wt% of Cu with respected amount of other three metals. This reduction of surface area and pore volume is related to blockage of the pores.

The average pores reduce was increased with the increased of metal loading as illustrated in Figure 4.3. Total pore volumes of the catalysts tested were reduced slightly since that the only small pore was blocked. The reduction related to loading 2, 4, and 6 % of Cu with respective other metal were 7, 11, and 17% only respectively.

TABLE 4.1 Summary of gas sorption analysis result

Catalyst name Cu %	Specific Surface Area (m^2/g)	Total Pore Volume (cm^2/g)	Average Pore Radius (A)
Support	143	0.71	90
Cat-2	134	0.66	98
Cat-3	133	0.63	96
Cat-4	130	0.63	97
Cat-5	128	0.64	99
Cat-6	104	0.59	115

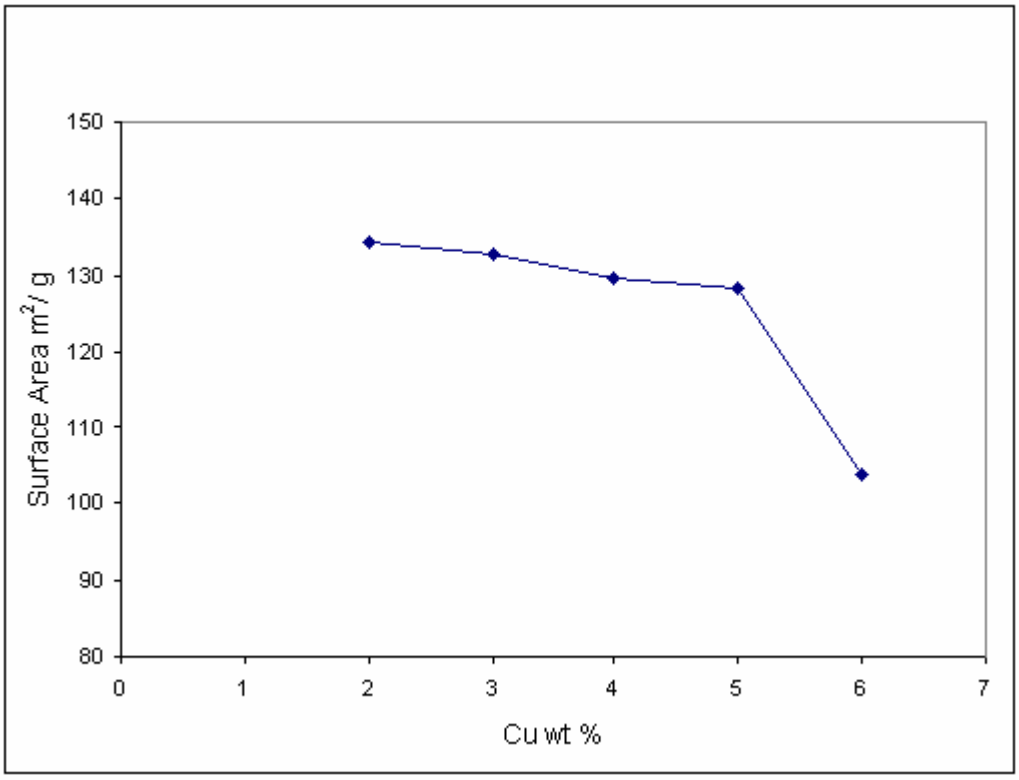

Figure 4.1 Effect of amount of metal loading on surface area

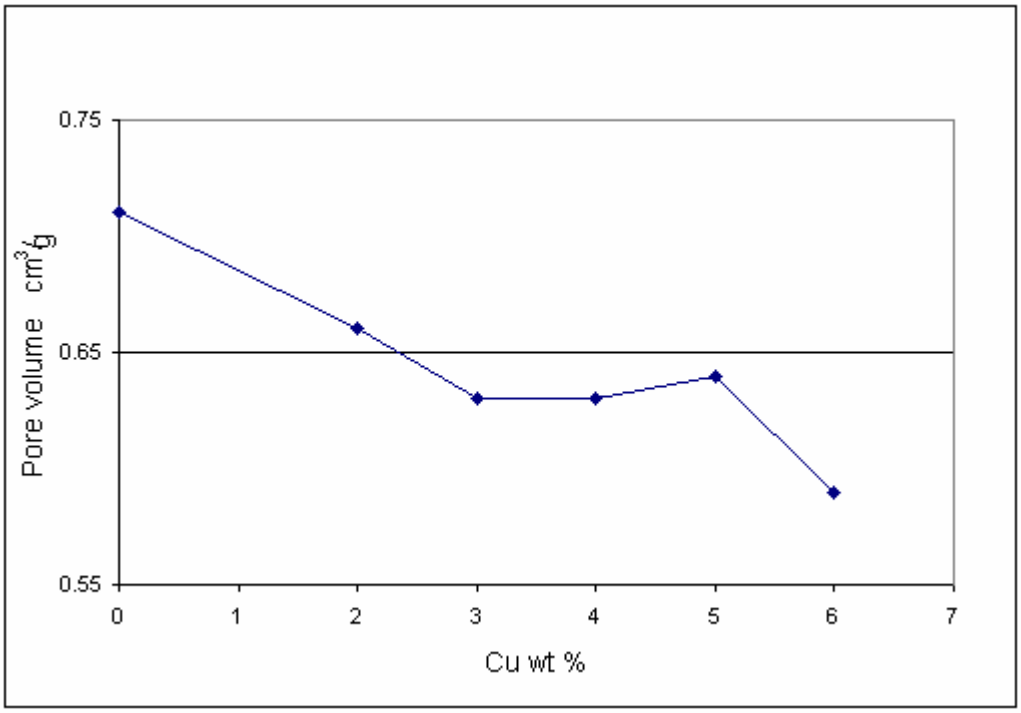

Figure 4.2 Effect of amount of metal loading on pore volume

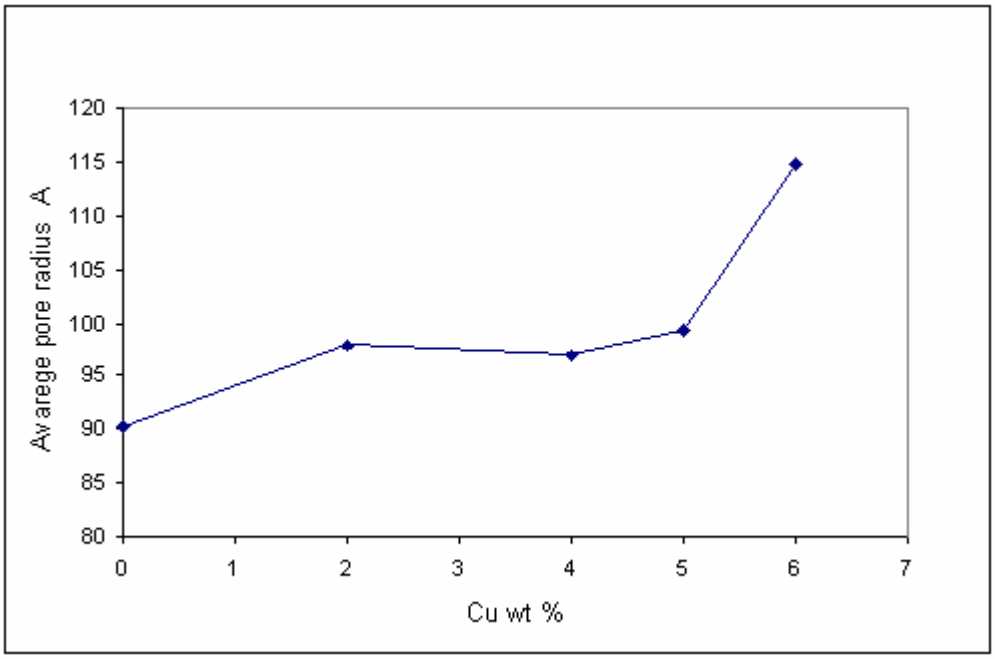

Figure 4.3 Effect of amount of metal loading on average pore radius

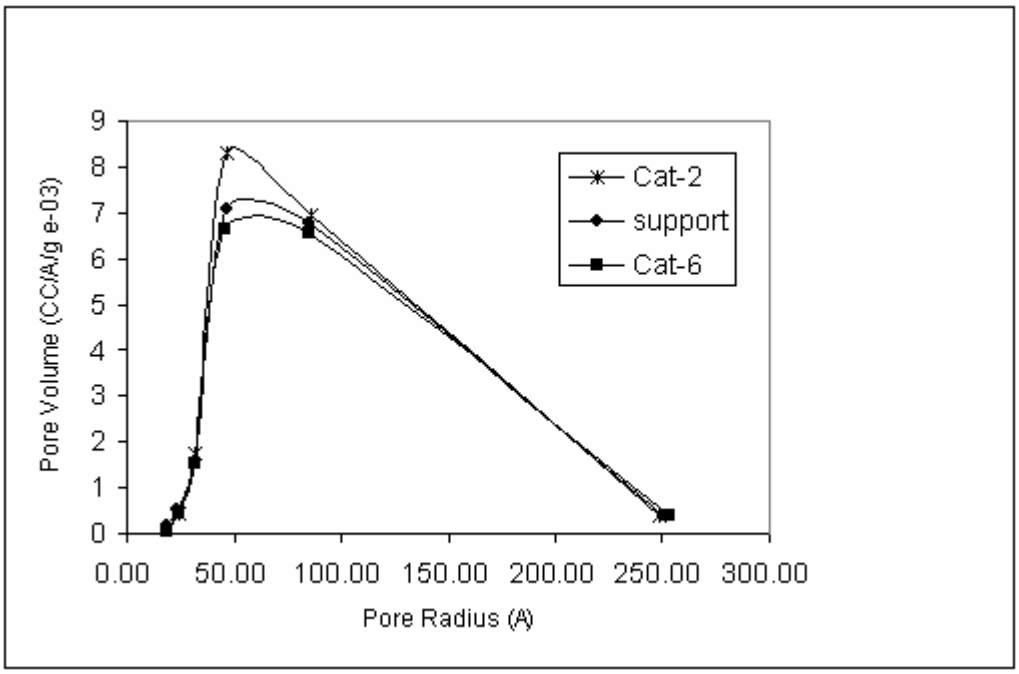

Figure 4.4 Pore volume distribution

Adsorption-desorption Isotherm

Adsorption-desorption isotherm of a material is one of the most characteristic of the porosity of that material which play very important role in catalyst activity and selectivity. The reaction takes place mostly on the internal surface area where the active site is placed. The reactant diffuses through the pore to contact active site on internal surfaces. The diffusion process depends of the kind of porosity as will as the size of defuses material. The isotherm profile can reveal the kind of porosity of the material. Figures 4.5, 4.6, and, 4.7 show adsorption-desertion isotherms of support, Cat-2, and Cat-8 respectively. These isotherm results are identical of mesoporose material isotherm. The PROX of CO catalyst support is selected usually from mesoporouse support. The adsorption-desertion isotherms of Cat-2 and Cat-6 show that loading 2 and 6 wt% with respective other three metals did not change the type of porosity of the support.

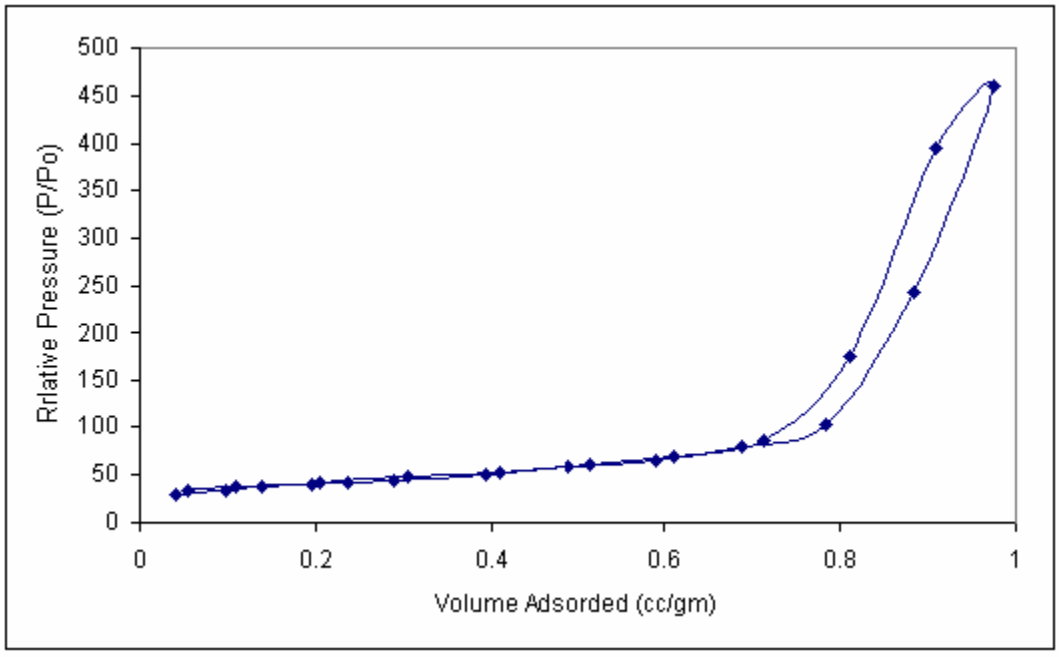

Figure 4.5 Adsorption-desorption isotherm of the support

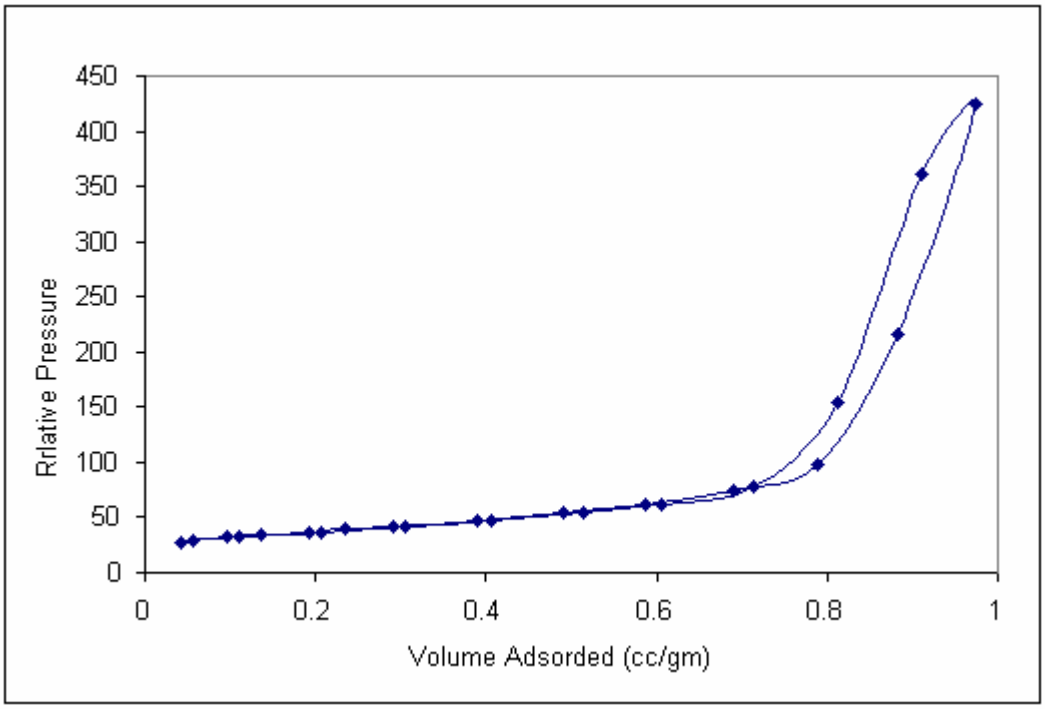

Figure 4.6 Adsorpion-desorptiom isotherms of Cat-2

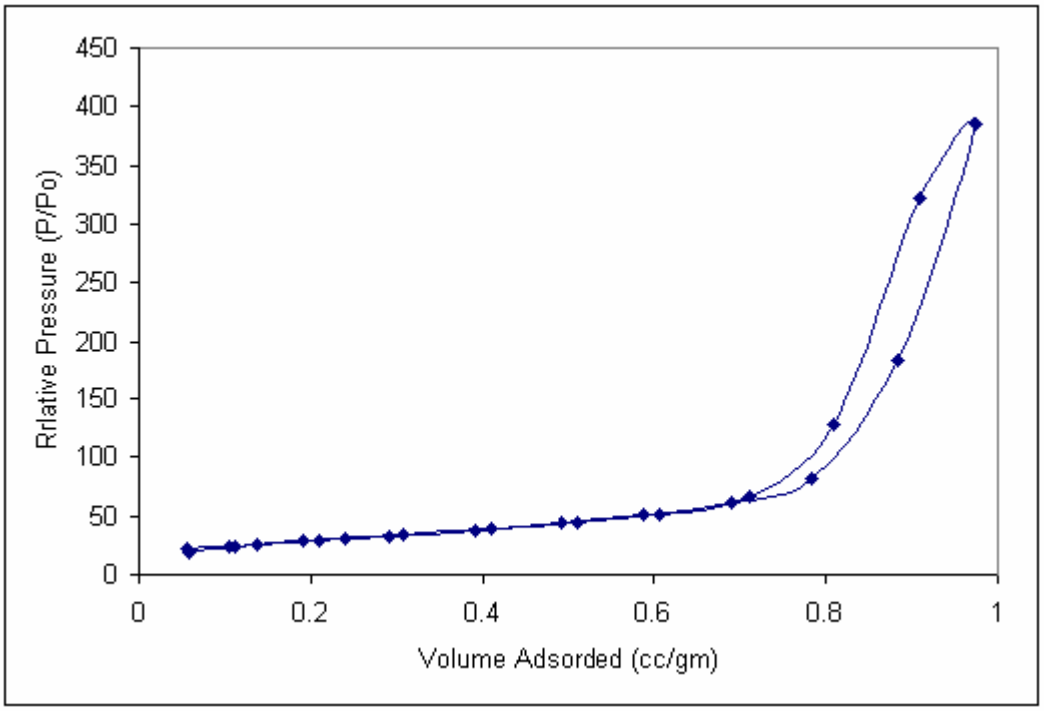

Figure 4.7 Adsorpion-desorptiom isotherm of Cat-6

4.1.2 Temperature Programmed Reduction Analysis (TPR)

The TPR profiles of catalysts prepared using γ-alumina as support with Cu, Ce2O3, Pt, and Rh metals are depicted in Figures 4.8 to 4.12. The consumption of H2 proportionally increased with active metal content. At Cu content 1 %, the H2 consumption peak was small while at 6% of Cu content gave very high H2 consumption peak. Cat-1, Cat-2, and Cat-3 catalysts showed three α, β, and γ peaks of H2 consumption as shown in Figure 4.8.

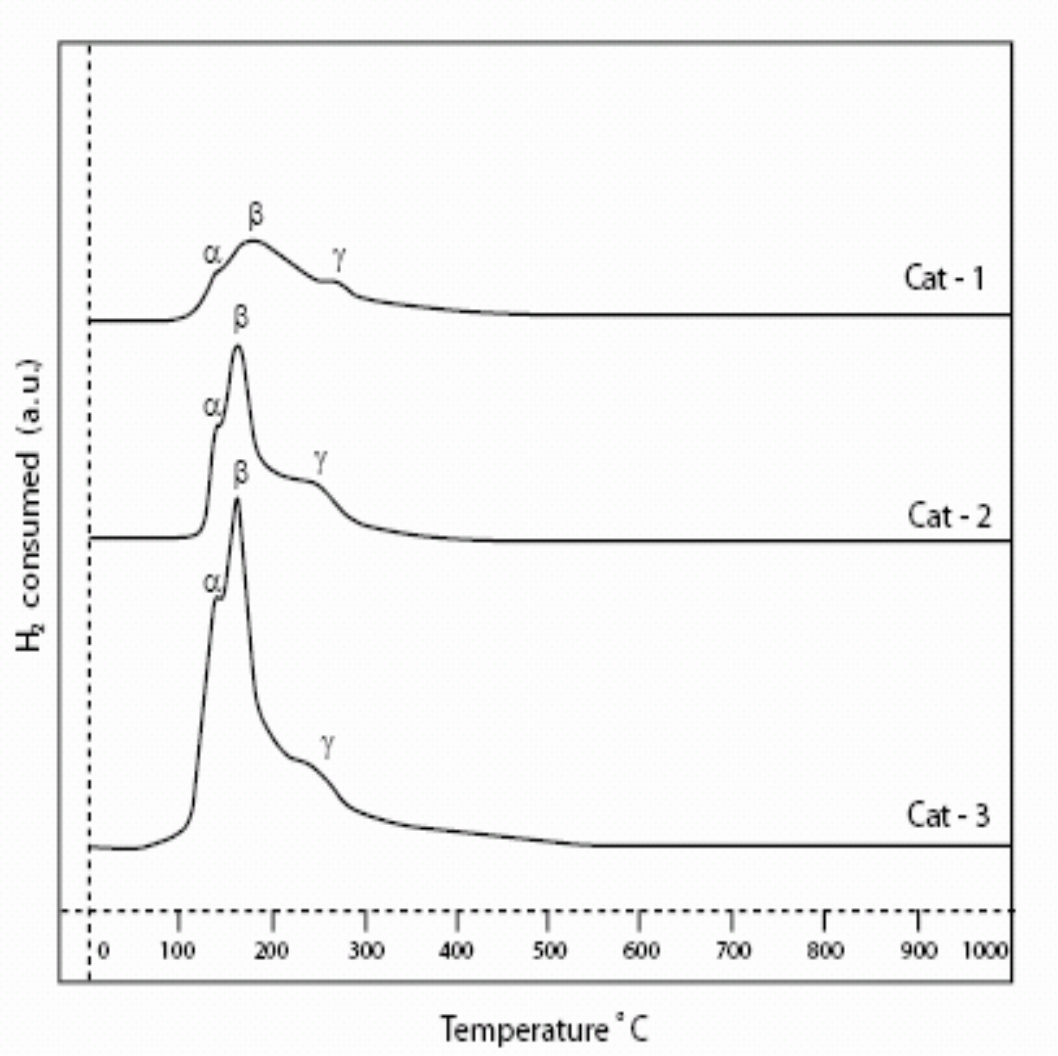

Figure 4.8 TPR profiles for Cat-1, Cat-2, and Cat-3

The temperatures of α, β, and γ peaks have no significant difference. Cat-1 catalyst showed three α, β, and γ peaks with small H2 consumption that has maxima at 136, 162 and 244 ºC, respectively. There was no H2 consumption at less than 120ºC. This gives evidence that no oxidation reaction for H2 in PROX of CO reaction system can occur below this temperate in selective CO oxidation reaction. All metals oxides in Cat-1 catalyst were reduced at less than 320ºC. Cat-2 and Cat-3 catalysts showed also α, β, and γ peaks at temperatures about 136, 160, and 245ºC but the H2 consumption over Cat-3 was higher than the H2 consumption over Cat-2. The reduction of these metals oxides in Cat-2 and Cat-3 started at 125ºC and completed 320ºC as no peak appeared at higher than that temperature.

Cat-4, Cat-5, and Cat-6 showed similar reduction behavior but the H_2 consumption amount was increased with increasing of metal loadings as illustrated in Figure 4.9.

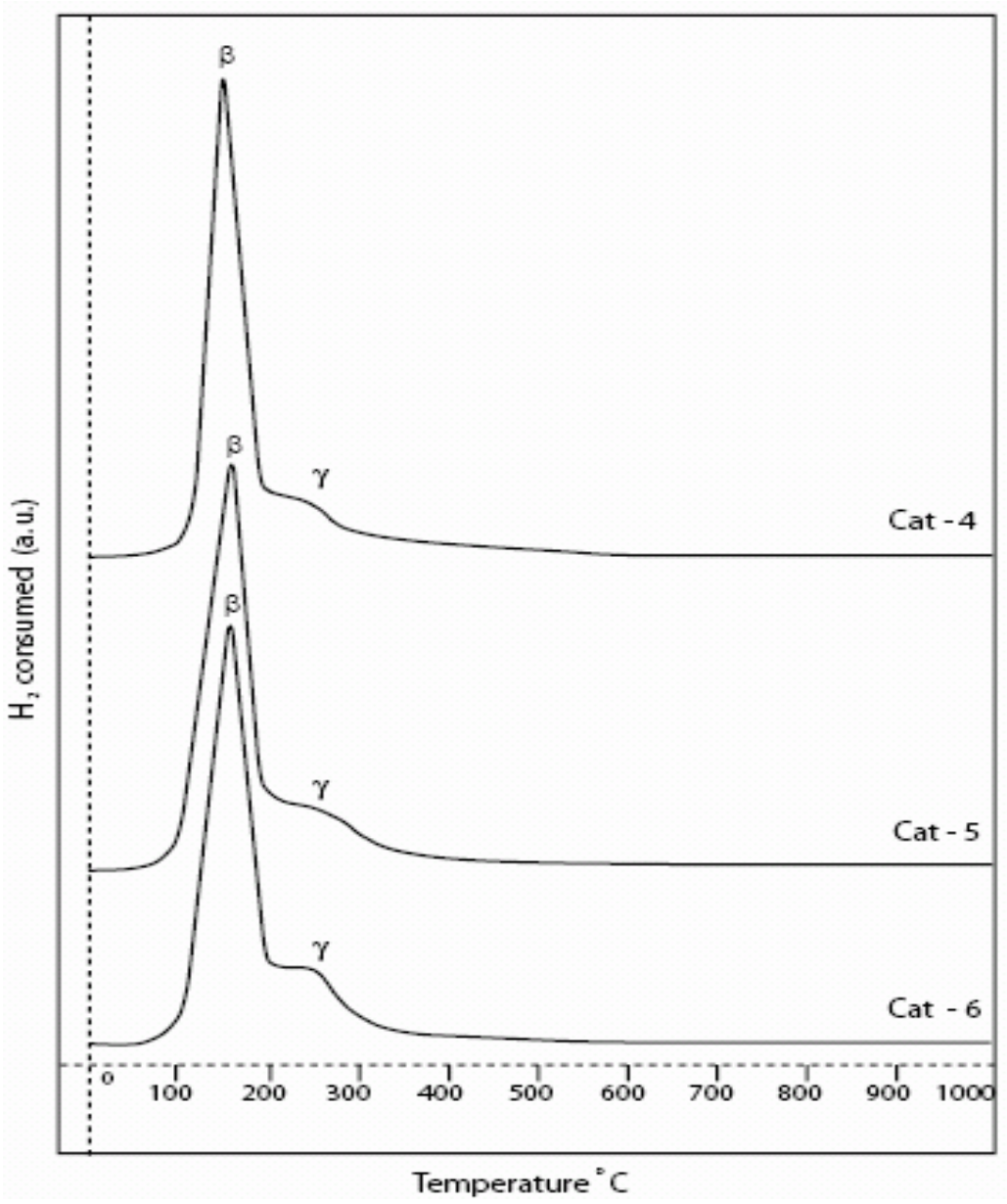

Figure 4.9 TPR profiles for Cat-4, Cat-5, and Cat-6

For all three catalysts, no reduction peak was observed lower than 100ºC or above 300ºC. The reduction reactions of the catalysts show two overlapping beaks as illustrated in Figure 4.9. The β peak is the main peak that is the result of α and β peaks appeared at low metal concentration catalyst. The β peaks has a maxim at 144, 151, and 154ºC for Cat-4, Cat-5, and cat-6 respectively while the y beaks has a maxim at 244, 251, and 246ºC for the same catalyst respectively.

The deference in reduction behavior is related to metal-metal interactions. Each catalyst prepared showed more than one interaction. Reduction peaks of Pt- and Rh- oxides themselves are expected to be negligible due to their very low loadings on the catalyst, however change the reduction behavior of Ce- and Cu-oxides was observed. Cerium oxide on γ-alumina is not easy to be reduced. It is reduced at very high temperature [71]. The H2 reduction peaks of Cu, Ce, Pt, and Rh oxides separately loaded on γ-alumina have a maxima temperature 210, 700, 260, and 138ºC, respectively. Adding Cu and Ce together on γ-alumina shifted the H2 reduction temperature of both metal oxides to the range of 178 - 270ºC with two deferent interactions between Cu and Ce in alloy and Cu-Ce alloy and the support.

Park [72] investigated H2-TPR measurements for the Cu–Ce/ γ-alumina catalyst. In ceria, no peak was observed below 500◦C. The reduction of CuO started at 170◦C and a single peak occurred at 210◦C. In the CuCe/A catalyst, the reduction started at 150◦C and showed two (α and β) overlapping reduction peaks which occurred at 178◦C and 198◦C, respectively. It was suggested that the α peak formation and β peak was caused by the existence of metal oxide–

metal oxide interaction induced by the establishment of intimate contact between the two components.

The result of TPR of catalyst prepared showed that the H2 reduction temperature shifts to higher side by adding very small amount of Pt and Rh. Figure 4.10 shows the deference of TPR profiles of Cat-2, Cat-2A, Cat-2B, and Cat-2C. Cat-2A contains Cu and Ce loaded on γ-alumina. The H2 reduction of Cat-2A had two beaks α at 150 and β at 170ºC. The α peak decreased and β peak increased when 0.032 % of Rh was added to Cat-2A (Cat-2C). When 0.18% of Pt was added to Cat-2A, part of α beak shifted to β peak and formed two identical peaks have maximum at 150 and 170ºC, respectively. Also, γ peak was appeared at 260ºC. It is clear from the Figure 4.10 that the amount shifted from α to β peak caused by addition of Pt is more than the amount caused by Rh addition since the percentage amount of Pt was added is 5.6 times the amount of Rh that added. When 0.032 % of Rh and 0.18 % of Pt where added together to Cat-2A, most of α peak was shifted to β peak. Also, γ peak was increased.

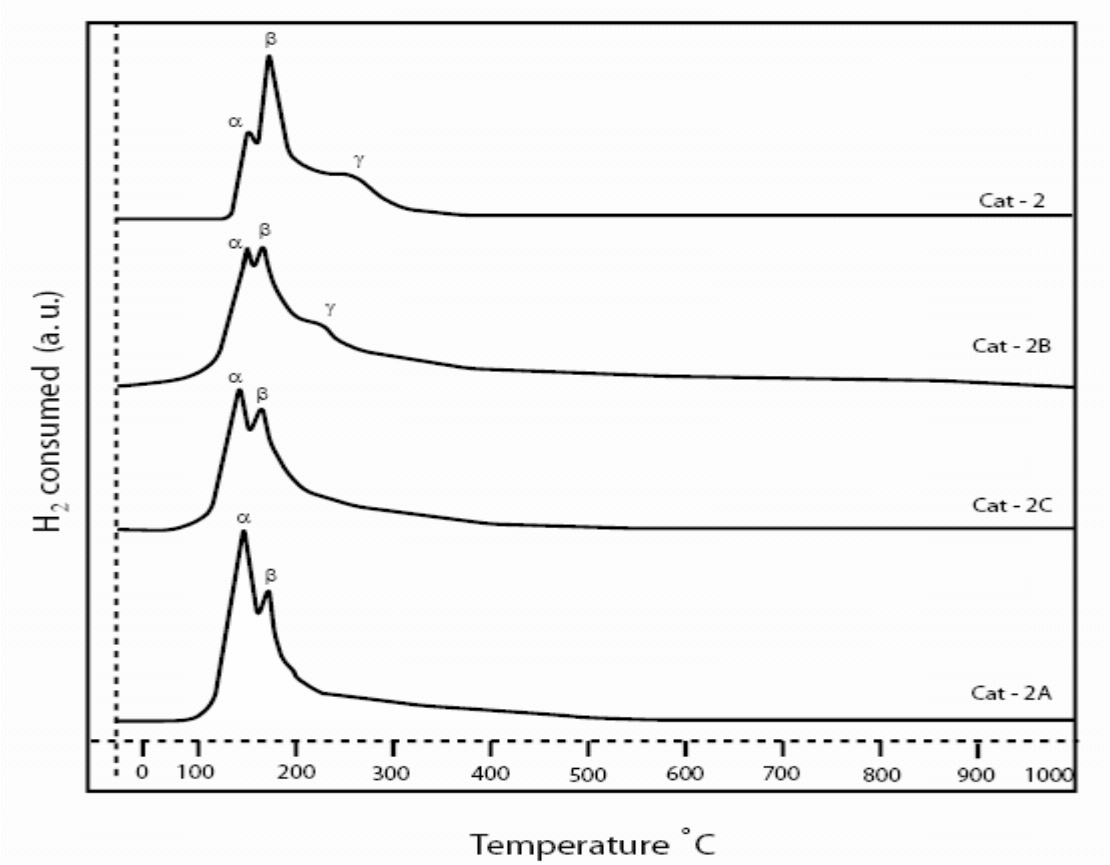

Figure 4.10 H2-TPR profiles for deferent metal composition of Cat-2 catalyst

It is obvious that the α shift to β peak is related to formation of metal–metal interaction between CuCe-oxide and the support induced by the establishment of intimate contact between the Pt and γ-alumina. Addition of Pt and Rh on γ-alumina modified the alumina surface and increased the interaction between CuCe-oxide and the active site on the surface of γ-alumina. This also was observed at high metal loading such as in Cat-5. Cu-Ce/γ-alumina gave one β reduction peak as illustrated in Figure 4.11. When Pt and Rh were added to the base catalyst, γ peak was observed. That interaction explains the difference in reduction temperature of CuCePtRh/ γ-alumina catalyst. The α peak is related to bulk CuCe-oxide over the surface of γ-alumina that have weak interaction with

the support while β peak is related to CuCe-oxide has moderate interaction with the support. The γ peak is related CuCe-oxide has strong interaction with the support.

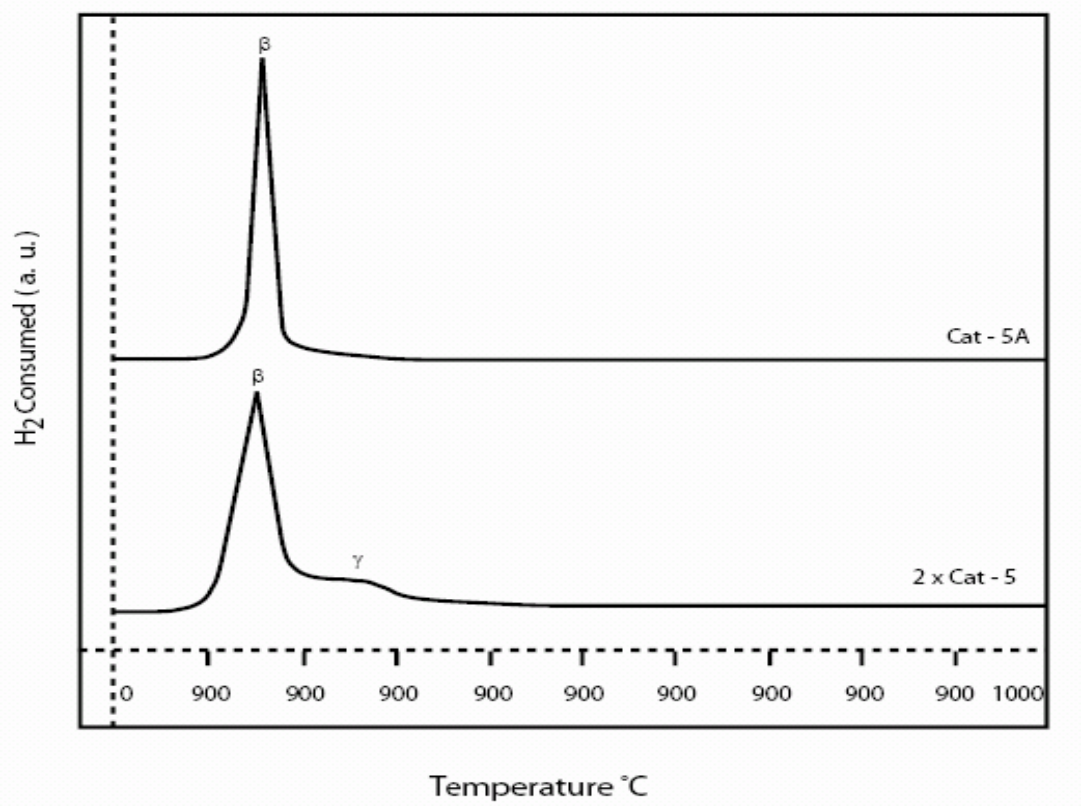

Figure 4.11 H2-TPR profiles for deferent metal composition Cat-5 catalyst

TABLE 4.2 Temperatures of H_2-TPR profiles peak

Catalyst Name	T_α	T_β	T_γ
Cat-1	137	174	260
Cat-2	136	162	244
Cat-3	136	159	148
Cat-4	-	144	244
Cat-5	-	151	251
Cat-6	-	154	246
Cat-2A	129	152	-
Cat-2B	134	152	210
Cat-2C	132	152	-
Cat-5A	-	160	-

4.1.3 Chemical Analysis

Results of chemical analysis of catalysts are shown in Table 4.3. The calculated amounts of metal loadings for four metal are presented in Table 4.4.The analyzed four metals percentage were less than the required percentage quantity since some of the metals solution were absorbed by filter paper during impregnation steps when the excess water on the catalyst was swiped by filter paper. The differences between analytical results and prescribed metal loading percentage for Cat-5 and Cat-6 catalysts are related to analysis procedure error and excess solution swiped.

TABLE 4.3 Calculated metal wt % in the catalyst

Catalyst Name	Cu wt %	Ce wt %	Pt wt %	Rh wt %
Cat-0.5	0.5000	0.1642	0.0461	0.0081
Cat-1	1.0000	0.3285	0.0921	0.0162
Cat-2	2.0000	0.6570	0.1842	0.0324
Cat-3	3.0000	0.9854	0.2763	0.0486
Cat-4	4.0000	1.3139	0.3684	0.0648
Cat-5	5.0000	1.6424	0.4605	0.0810
Cat-6	6.0000	1.9709	0.5526	0.0972

TABLE 4.4 Result of Chemical Analysis for metal wt% in the catalyst

Catalyst Name	Cu wt%	Ce wt%	Pt wt%	Rh wt%
Cat-0.5	0.4940	0.1600	0.0459	0.0079
Cat-1	0.9985	0.3128	0.0911	0.0168
Cat-2	1.9488	0.6460	0.1822	0.0321
Cat-3	2.9534	0.9786	0.2700	0.0481
Cat-4	3.7864	1.2880	0.3524	0.0604
Cat-5	4.5179	1.5458	0.4361	0.0618
Cat-6	5.4493	1.4443	0.4949	0.0795

4.2 Performance of Catalysts -

In this study, the effect of very small amount of addition of Pt and Rh on Cu–Ce/γ-Al_2O_3 base catalyst was investigated. The results obtained were compared with the previous studies. The atomic ratio of Cu, Ce_2O_3, Pt, and Rh catalysts were kept constant at 100, 20, 3, and 1 respectively. The catalysts were prepared by pore volume impregnation method. The activity tests were carried out in a conventional flow, fixed bed reactor to find the optimum loading of Cu-Ce-Pt-Rh metals and O_2 needed to achieve less than 10 ppm of CO on the product to meet the requirement of EFC application. The effect of water in the feed on CO selective oxidation was investigated. The following expressions were used to calculate H_2 conversion and selectivity at maximum conversion of CO. The results were tabulated in Tables 4.5 to 4.8. Equation 4.1 define the CO conversion which equal the CO converted ($[CO]_{in}$-$[CO]_{out}$) over the total CO fed to the system. The H_2 conversion was calculated in a similar way of CO conversion calculation using equation 4.2. Equation 4.3 defines the selectivity of CO reaction that based on the amount of CO reacted over the amount of O_2 that is fed to the system [72, 73].

$$\text{Xco}\ (\%) = \frac{[\text{CO}]\text{in} - [\text{CO}]\text{out}}{[\text{CO}]\text{in}} X\ 100 \qquad 4.1$$

$$\text{X}_{\text{H2}}\ (\%) = \frac{[\text{H2}]\text{in} - [\text{H2}]\text{out}}{[\text{H2}]\text{in}} X\ 100 \qquad 4.2$$

$$\text{Sco}(\%) = \frac{0.5([\text{CO}]\text{in} - [\text{CO}]\text{out})}{[\text{O2}]\text{in} - [\text{O2}]\text{out}} X\ 100 \qquad 4.3$$

4.2.1 Effect of Reaction Temperature

Catalysts prepared were evaluated at temperature range from 25 to 300°C. The results of the catalysts were presented in Figures 4.12 to 4.18. For all catalysts, no reaction was observed at less than 50°C since the activation energy of the reaction was not achieved. The CO conversion over all catalyst tested did not increase significantly with the increased in temperature up to about 70°C. Below that temperature, the energy given to the reaction system was not enough to activate all molecules so the reaction was not achieved completely. After 70°C, the CO conversion was increased sharply up to 150°C since the energy was given to the reaction system was enough for all molecules to have the activation energy to start reaction. Above 160°C, the conversion of CO started to decrease for all O_2/CO ratios. This decrease of CO conversion is caused by increase of O_2 consumption by H_2 oxidation reaction. The H_2-TPR profiles result of all catalyst showed that the metal reduction reaction started at about 100°C and has maximal at about 150°C for all catalysts. Therefore, the H_2 oxidation would start at this range of temperature.

The results showed that the temperature of a given CO conversion was increased with decreased of metal loading. For example, At 50 % CO conversion, the corresponding reaction temperature of Cat-0.5 (Cu 0.5%) and Cat-1 (Cu 1.0%), and Cat-2 (Cu 2.0%) were 145, 130, and 115°C respectively.

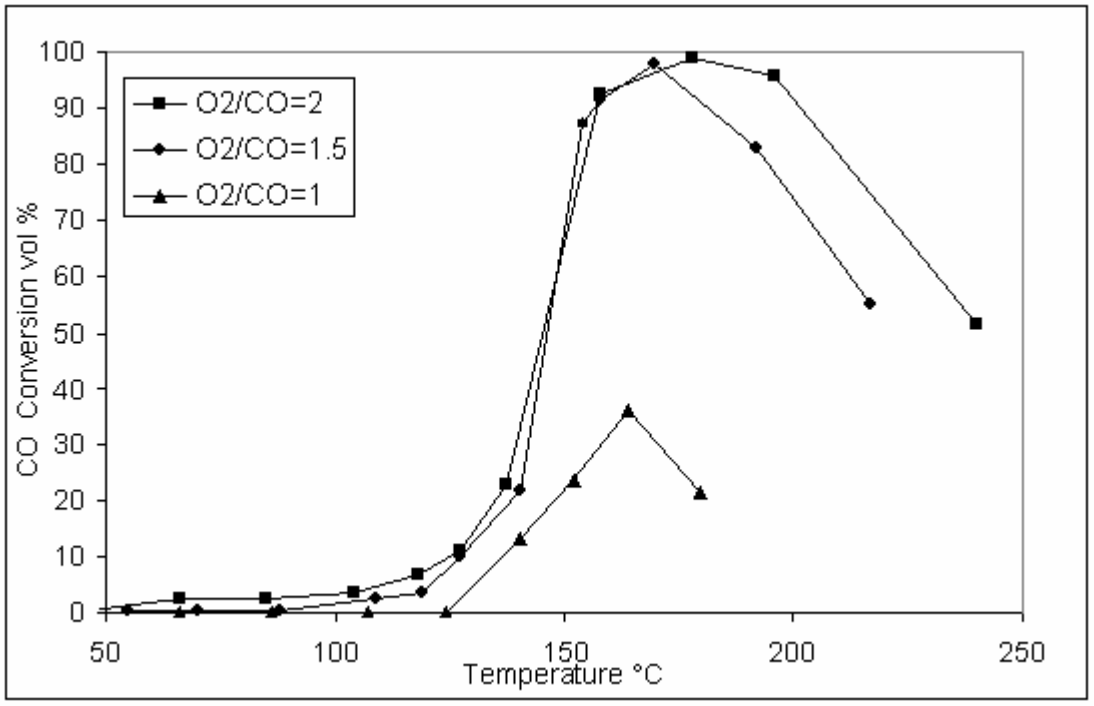

Figure 4.12 Effect of O_2/CO ratio on Cat-0.5 catalyst activity

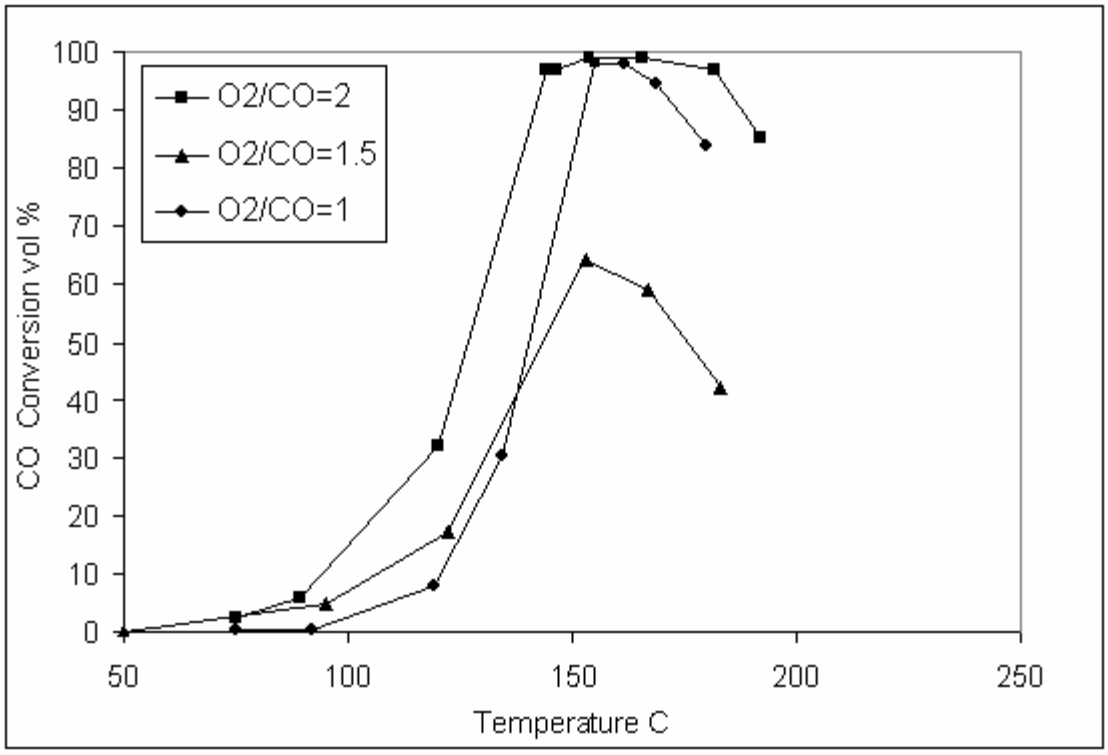

Figure 4.13 Effect of O_2/CO ratio on Cat-1 catalyst activity

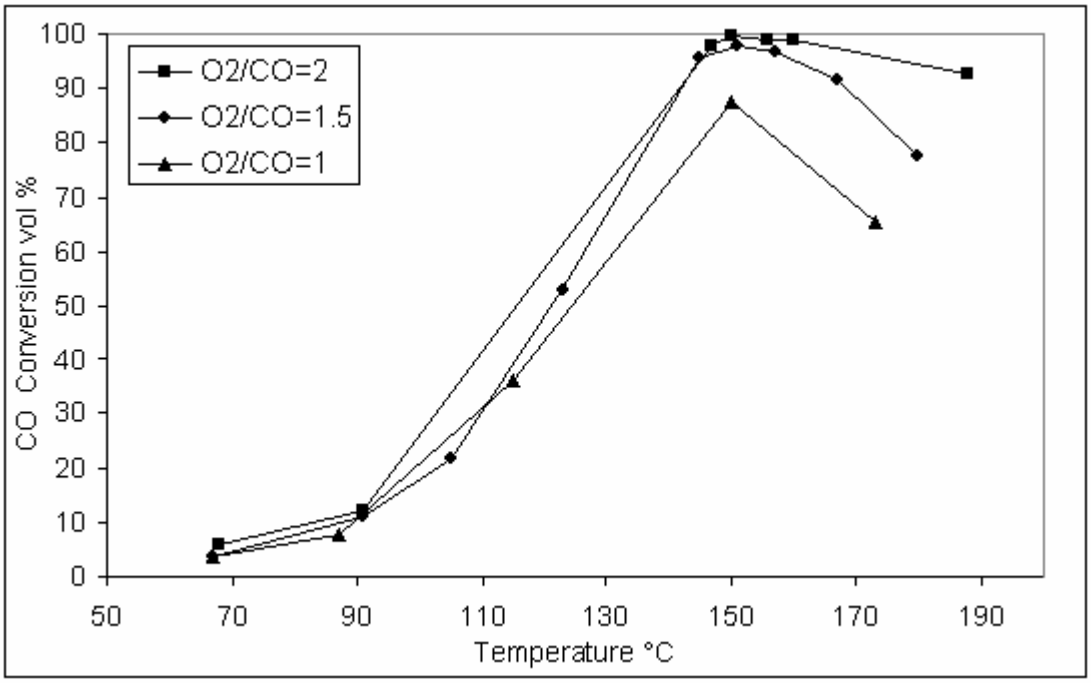

Figure 4.14 Effect of O_2/CO ratio on Cat-2 catalyst activity

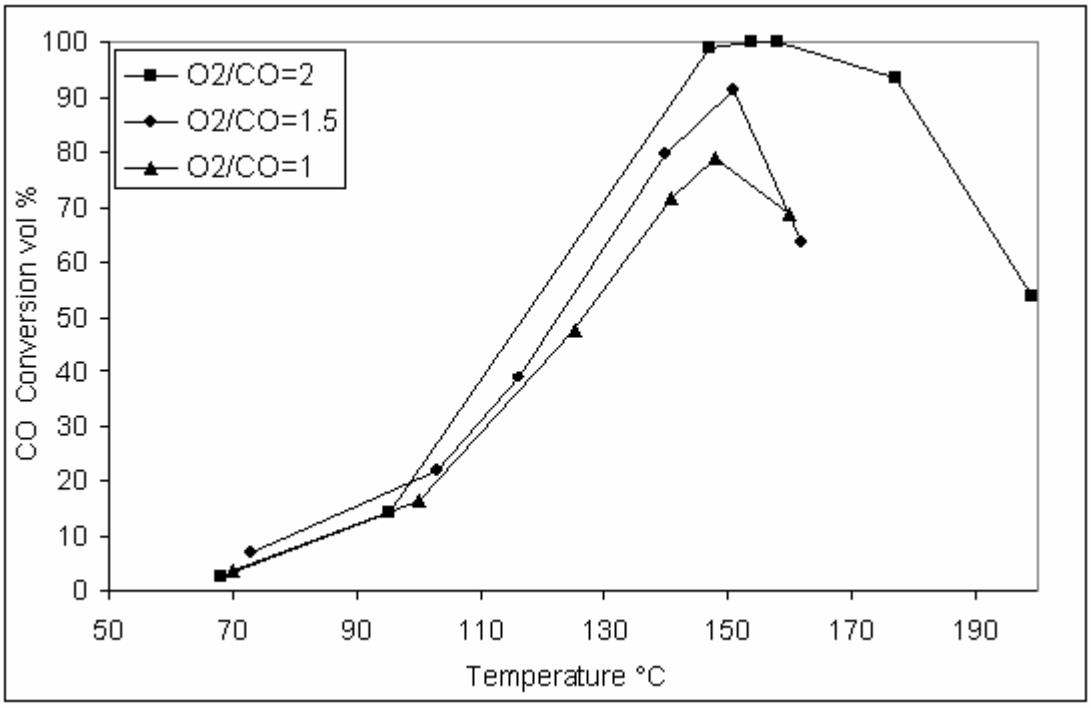

Figure 4.15 Effect of O_2/CO ratio on Cat-3 catalyst activity

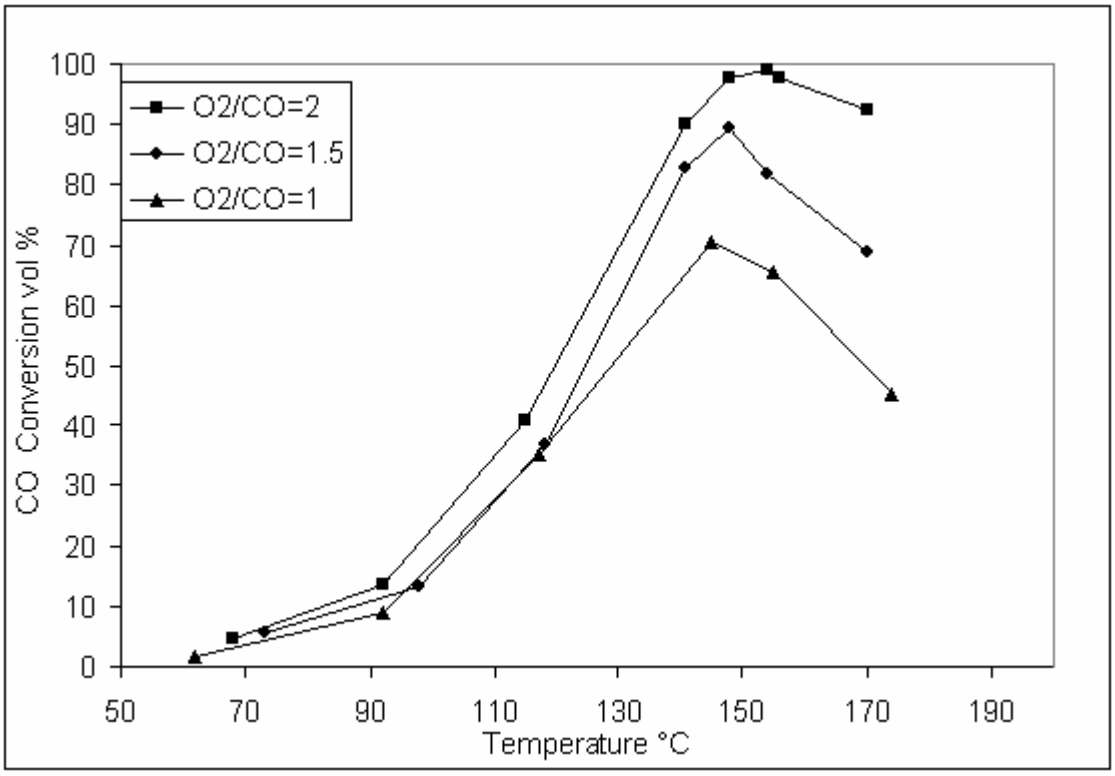

Figure 4.16 Effect of O_2/CO ratio in PROX Cat-4 catalyst activity

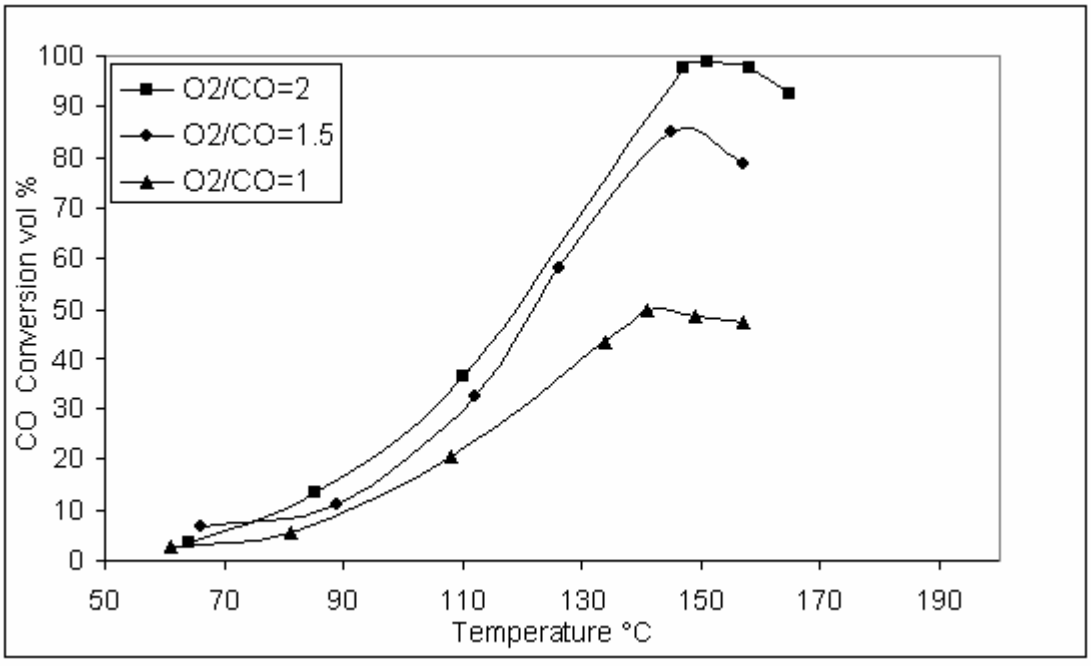

Figure 4.17 Effect of O_2/CO ratio in PROX Cat-5 catalyst activity

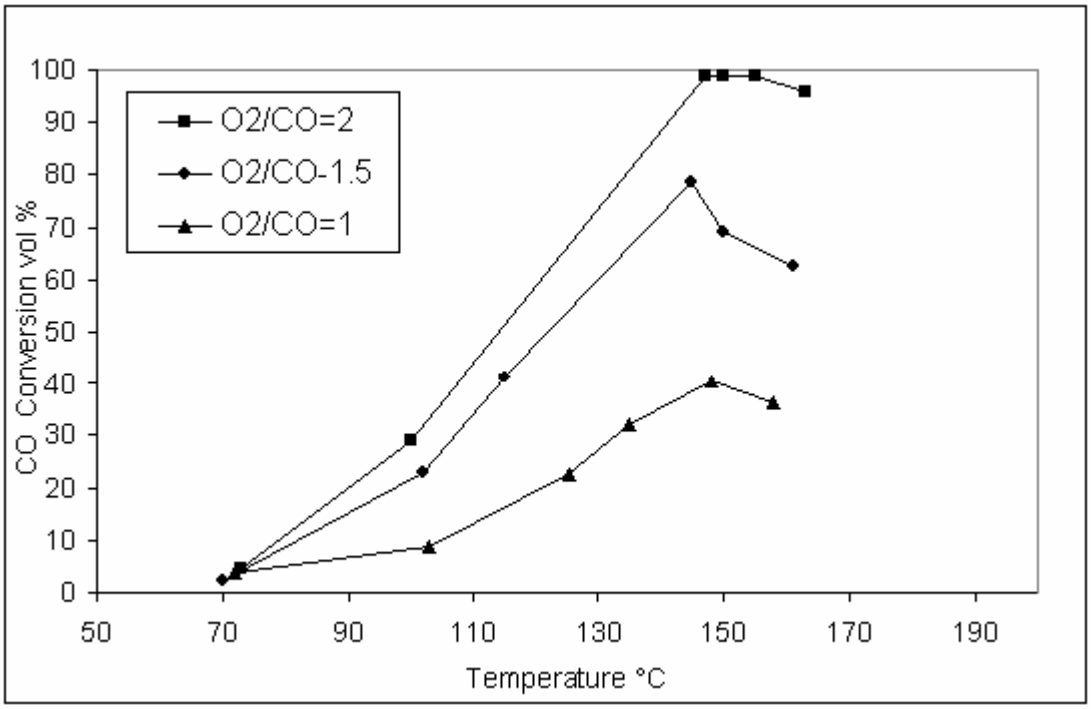

Figure 4.18 Effect of O_2/CO ratio in PROX Cat-6 catalyst activity

TABLE 4.5 Maximum conversion of CO and H_2 at O_2/CO = 1

Catalyst Name	CO In product (%)	CO conversion (%)	H_2 In product (%)	H_2 conversion (%)	Selectivity (%)	Temperate ºC
Cat-0.5	0.61	36.1	79.83	1.65	25.53	152
Cat-1	0.34	64.21	79.86	1.61	27.11	151
Cat-2	0.12	87.37	80.08	1.33	38.68	148
Cat-3	0.20	78.95	80.00	1.43	34.47	145
Cat-4	0.28	70.53	79.92	1.53	30.26	145
Cat-5	0.48	49.47	79.72	1.78	19.74	148
Cat-6	0.57	40.00	79.63	1.90	15.00	148

TABLE 4.6 Maximum conversion of CO and H_2 at O_2/CO = 1.5

Catalyst Name	CO in product (%)	CO conversion (%)	H_2 in product (%)	H_2 conversion (%)	Selectivity (%)	Temperature ºC
Cat-0.5	0.02	97.85	77.91	2.41	32.50	170
Cat-1	0.02	97.85	77.91	2.41	32.50	155
Cat-2	0.02	97.85	77.91	2.41	32.50	150
Cat-3	0.08	91.40	77.85	2.49	30.36	145
Cat-4	0.13	86.02	77.80	2.55	28.57	148
Cat-5	0.14	84.95	77.79	2.56	28.21	148
Cat-6	0.20	78.49	77.73	2.64	26.07	148

TABLE 4.7 Maximum conversion of CO and H_2 at O_2/CO = 2.0

Catalyst Name	CO in product (%)	CO conversion (%)	H_2 in product (%)	H_2 conversion (%)	Selectivity (%)	Temperature ºC
Cat-0.5	0.01	98.92	75.80	3.52	25.08	178
Cat-1	0.01	98.92	75.80	3.52	25.08	160
Cat-2	0.00	100.00	75.81	3.50	25.36	150
Cat-3	0.00	100.00	75.81	3.50	25.36	150
Cat-4	0.01	98.92	75.80	3.52	25.08	148
Cat-5	0.01	98.92	75.80	3.52	25.08	148
Cat-6	0.01	98.92	75.80	3.52	25.08	148

TABLE 4.8 The effect of O_2/CO ratio on temperature at maximum conversion

Catalyst	Temperature of maximum conversion for (C)		
	O_2/CO=1	O_2/CO=1.5	O_2/CO=2.0
Cat-0.5	152	170	178
Cat-1	153	155	160
Cat-2	151	150	150
Cat-3	148	145	150
Cat4	145	148	148
Cat-5	145	148	148
Cat-6	148	148	148

For Cat-0.5 and Cat-1, the CO oxidation reaction shifted to higher temperate rang than the other catalysts as it is shown in Figures 4.12 and 4.13. For Cat-1, the CO oxidation started significantly at about 10°C higher than Cat-2, but the maximum conversion on the catalyst was at about 150°C as Cat-2. When the Cu content was reduced to 0.5% with respected amount of other three metals (Cat-0.5), the CO oxidation started significantly at 50°C higher than Cat-1 as shown in Figure 4.13. This relates to oxidation metal complex of loaded metal behavior. The metal complex is oxidized at room temperature so for low concentrations (Cat-1 and Cat-0.5) the major part of the metal on the catalyst is oxide form. The oxide form of the metal is not active as reduced metal form. After the reaction was started, the oxide form is converted to metal form first so the activity of the catalyst is enhanced. This caused the reaction to proceeds but at higher temperature. For the catalyst have high metal concentration, the reduced part of the metal on the support is sufficient to start the reaction at lower temperature. Also, this phenomenon explains the deference in catalysts activity behavior in the temperature range of 100 to 150°C. It was found that the slope of the reaction line between mentioned above temperature ranges was decreasing with increasing of metal content as it is clear from Figure 4.12 to 4.18. Cat-6 had the minimum slope where Cat-0.5 had the maximum slope.

Also, it was found that the temperature range of the maximum conversion is increasing with decreasing of metal loading. At O_2/CO = 2 as an example, the maximum conversion ranges of CO oxidation obtained over Cat-1, Cat-3 (Cu

3.0%), and Cat-6 (Cu 6.0%) were 40, 30, and 10°C respectively. The maximum conversion reaction temperature ranges of CO were shifted to lower temperature as metal loadings were decreased. The temperature range of maximum CO conversion over Cat-1 was between 140 to 180ºC. Cat-0.5 gave the same temperature range as Cat-1 but at higher temperature. The reason for this reactivity is that the catalyst activity for H_2 oxidation increased with increased of metal content. At high metal loading (for example Cat-6 and Cat-4), when the temperature reached 140°C the O_2 available in the reaction system was consumed by the H_2 oxidation so the CO oxidation was decreased as temperature increased beyond this temperature. At low metal loading (for example Cat-0.5 and Cat-1), the catalyst had lower activity for H_2 oxidation reaction than CO oxidation so the O_2 was not consumed by H_2 oxidation reaction in the same range of temperature. Thus the CO oxidation proceeded up to 180°C.

From the above observation, it can be concluded that the reaction system has two contradictory reactivates. The first is high H_2 oxidation reactivity with high metal loading. The second is less CO oxidation reactivity with low metal loading. So is necessarily to optimize the metal loading to maximize the CO oxidation reaction and minimize H_2 oxidation.

4.2.2 Effect of O_2/CO Ratio of the Feed

The activities of all prepared catalysts were evaluated at 1, 1.5, and 2 O_2/CO ratios. For all catalysts, the conversion of CO increased with an increase of

O_2/CO ratio. As it is known from stoichiometric reaction of CO oxidation, one mole of CO needs half mole of O_2 for complete combustion but usually combustion reaction needs excess O_2. In the system of preferential oxidation of CO in presence of high H_2 concentration, two competing reactions are taking place in the system.

$$CO + 1/2O_2 \rightarrow CO_2 \qquad \Delta H^o_{298} = -283.6 \text{ kJ/mol} \qquad (1)$$

$$H_2 + 1/2O_2 \rightarrow H_2O \qquad \Delta H^o_{298} = -243.5 \text{ kJ/mol} \qquad (2)$$

The first reaction is oxidation of CO that is desired reaction, and the second is oxidation of H_2 that is undesired reaction. The O_2 that is fed to the system reacts with both CO and H_2 in deferent amount. The CO/H_2 ratio in the feed was 1/84 so the probability of O_2 molecules to contact H_2 is much higher than the probability of O_2 molecules to contact CO molecules since H_2 concentration is much higher than CO concentration. The catalyst function required is to accelerate CO oxidation and inhabit H_2 oxidation. The total O_2 consume is oxygen reacted with CO and H_2. The conversion of H_2 is calculated based on O_2 consumed by H_2 assuming that all O_2 consumed completely at the maximum conversion since O_2 is limiting reagent as clear from concentrations of the CO and H_2 components in the feed. This is also in lines with published literature for PROX of CO reaction [71, 72].

Figure 4.12 shows the conversion of CO verses temperature for Cat-0.5 (Cu 5.0%) at all O_2/CO ratios. The CO conversion was 38.0% at O_2/CO = 1 of the feed. It increased to 97.9 % at O_2/CO=1.5. When the O_2/CO was increased to 2, the CO conversion further increased to 98.9%. The CO conversion over Cat-1 (Cu 1.0%) at O_2/CO = 1 was higher than Cat-0.5. At O_2/CO ratio equal 1.5 and 2.0, The CO conversion over Cat-1 was the same conversion over Cat-0.5 but at lower temperature. The activity of Cat-2 (Cu 2.0%) catalyst for selective oxidation is presented in Figure 4.14. At O_2/CO = 1, the maximum conversion of CO was 87% while the conversion of H_2 was about 1.33%. The CO conversion increased by 10% (CO conversion was 98%) by increasing O_2/ CO ratio to 1.5. On the other hand, the H_2 conversion increased to 2.41%. The CO conversion increased to 99.96% when the O_2/CO ratio was increased to 2. The CO concentration in the product was 4 ppm only. This CO conversion is meeting the requirement of fuel cell application for CO cleanup of hydrogen fuel. The hydrogen conversion at this O_2/CO ratio was only 3.5%. Cat-3 (Cu 3.0%) showed less CO oxidation activity than cat-2. At O_2/CO = 1, the maximum conversion of CO was 78.95% while the H_2 conversion was 1.43%. The CO and H_2 conversion was increased to 91.4 % and 2.5 % respectively with increased O_2/CO ratio to 1.5. The maximum conversion of CO and H_2 was 99.88 % and 3.5% respectively at O_2/CO = 2. The concentration of CO in the product gas was 11 ppm at this maximum. At O_2/CO = 1, the maximum CO conversions over Cat-4 (Cu 4.0%), Cat-5 (Cu 5.0%), and Cat-6 (Cu 6.0%)were 70.53, 49.47, and 40 whereas the H_2 conversions were 1.35, 1.8, and 1.9 % respectively. When the O_2/CO was increased to 1.5, the

maximum conversion increased to 86.0, 85, and 78.5 for CO and 2.6, 2.6, and 2.6 for H_2 respectively. At O_2/CO = 2, the maximum conversions of CO and H_2 were 98.92 and 3.5% respectively for all three catalyst.

4.2.3 Effect of Metal Composition

To study the effect of CuCe, Pt, and Rh in the catalyst activity, four catalysts were prepared. Cat-2A (Cu 2.0%) and Cat-5A (Cu 5.0%) have the same composition of Cat-2 and Cat-5, respectively but without Pt and Rh. Cat-2B and Cat-2C had the same metal composition of Cat-2 but Cat-2B without Rh and Cat-2C without Pt. These catalysts were tested for CO selective oxidation with ratio of O_2/CO=2 in the feed.

Cat-2A and Cat-5A showed very low activity as illustrated in Figures 4.19 and 4.20 and summarized in Table 9. The maximum CO conversion over catalysts Cat-2A and Cat-5A was only 23.1% at 238ºC and 11.3% at 200ºC, respectively. The CO conversion increased drastically and temperature of maximum CO conversion decreased with adding very small mount of Pt and Rh to the catalyst. The maximum CO conversions over Cat-2 and Cat-5 were 99.96 at 150ºC and 98.9% at 151ºC, respectively.

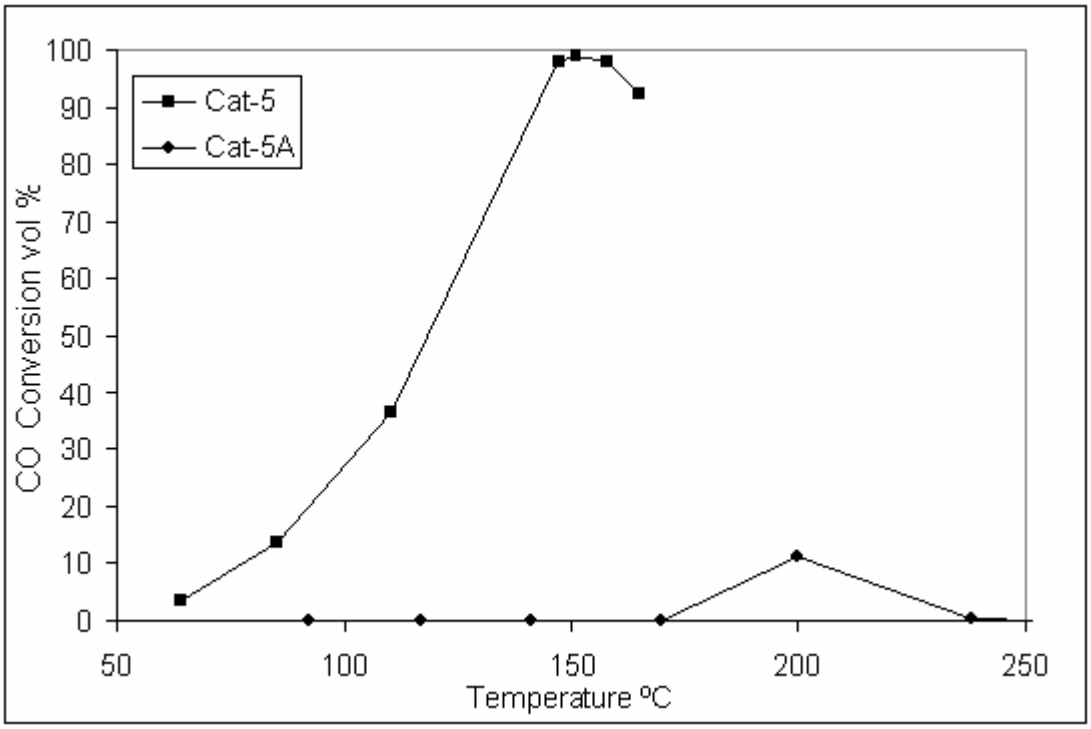

Figure 4.19 Cat-5 and Cat-5A activity for selective oxidation of CO

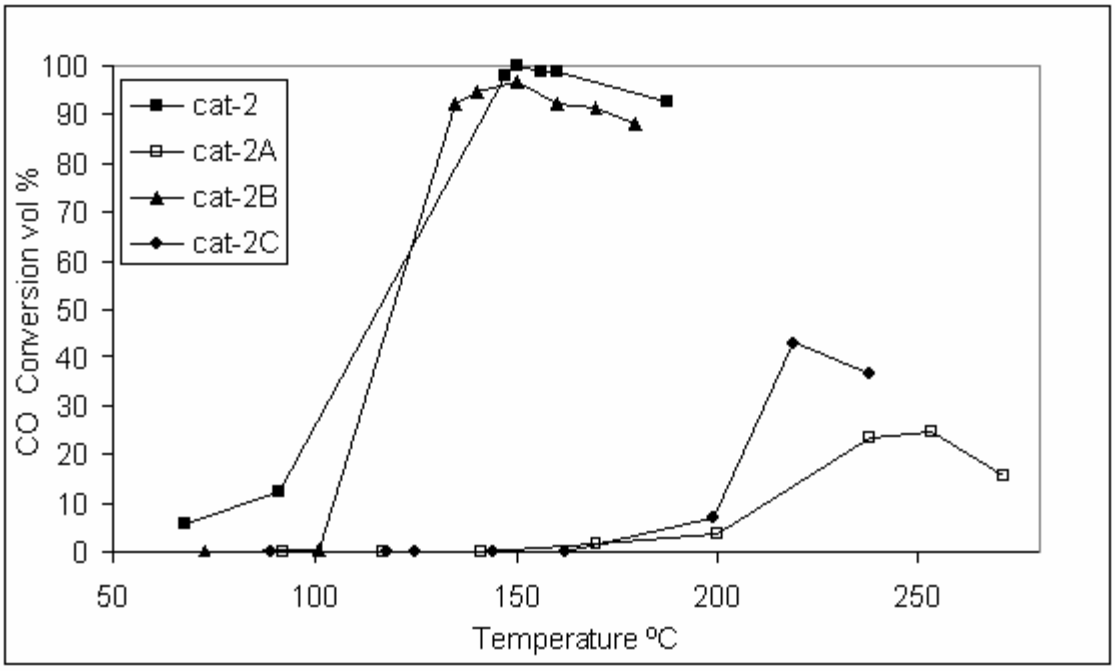

Figure 4.20 Cat-2, Cat-2A, Cat-2B, and Cat-2C activity for selective oxidation of CO

TABLE 4.9 Maximum conversion of CO and H_2 at O_2/CO = 2.0

Catalyst Name	CO in product (%)	CO conversion (%)	H_2 in product (%)	H_2 conversion (%)	Selectivity (%)	Temperature of max. conv. ºC
Cat-2	0.00	99.95	75.81	3.50	25.35	150
Cat-2A	0.70	24.73	75.11	4.42	5.92	238
Cat-2B	0.03	96.77	75.78	3.54	24.53	219
Cat-2C	0.52	44.09	75.29	4.18	10.92	238
Cat-5	0.01	98.92	75.80	3.52	25.08	238
Cat-5A	0.81	12.90	75.00	4.56	2.86	151

Comparing CO oxidation activity of Cat-2, Cat-2A, Cat-2B, and Cat-2C with the catalyst prepared by Park et al [72] for selective oxidation of CO in presence of high H_2 concentration shows that the Cat-2 give the highest CO conversion. The results of study done by Park showed upon different Cu loading in the selective CO oxidation using synthetic reformate gas (1% CO, 1% O_2, 60% H_2 and N_2 as balance) while maintaining total metal content of 10 wt%. For a metal loading of Cu–Ce (1:9 wt%)/γ-Al_2O_3, the maximum CO conversion obtained was 93.5% at 250ºC and for a metal loading of Cu –Ce (2:8 wt%) / γ -Al_2O_3, it was 94.6% at 200ºC . Further increase in Cu content above 2 wt% showed a decreasing trend in catalytic activity indicating that the maximum activity was obtained with Cu:Ce weight ratio of 2:8. This result is much higher than the result obtained in this study with catalyst Cat-5A and Cat-2A because of two reasons. First, the catalyst preparation method in the two studies is different. Second, the H_2 concentration in feed used this study is much higher than Park's study. Also, CO_2 concentration in the feed used in this study is 14 vol% while the feed used in Park's study did

not has C O_2. Both H_2 and CO_2 presence in the feed reduce the CO conversion as will as selectivity.

Addition of small amount of Co to Cu-Ce/ γ-Al_2O_3 catalyst prepared by Park [72] increased CO conversion to 99%. On the other hand, addition of small amount of Pt and Rh to Cat-2A base catalyst increased conversion from 43.1 at 219ºC to 99.96 at 150ºC. That reveals the Pt and Rh enhance the CO oxidation more than Co. Figure 4.20 shows the CO conversion activity of Cat-2, Cat-2A, Cat-2B, and Cat-2. The maximum CO conversion over Cat-2A was increased from 23.3 at 238ºC to 43.1 at 219ºC by addition of small amount of Rh (atomic ratio Rh/Cu = 0.01) to Cat-2A catalyst. The maximum CO conversion over Cat-2A was increased from 23.3 at 238ºC to 96.5 at 150ºC by addition of small amount of Pt (atomic ratio Pt/Cu = 0.03) to Cat-2A catalyst. This shows the Pt has more effect in increasing activity of CuCe/γ-alumina for CO selective activity. This drastic increase of CO selective oxidation is attributed to hydrogen spillover effect.

At low temperatures such as below 200°C, Cu changes to copper carbonate in existence of H_2O and CO_2 so the Cu catalyst is deactivated fast and change to irreversible deterioration. The key to keep Cu catalyst active is to protect it from carbonate transformation by hydrogen spillover. The hydrogen spillover enhances the catalyst activity by keeping metal catalyst in reduced form. Hydrogen usually dissociates into H atom on noble metals such as Pt and Rh [51 - 53]. The reactive atomic H spreads on the surface of the catalyst (this kwon as hydrogen spillover) and keeps the base metal catalyst in partially reduced form.

Optimum metal loading for maximum conversion

The activity of the catalysts for CO oxidation was compared at all three O_2/CO ratios as shown in Figures 21, 22, and 23. At O_2/CO=2, the activity difference between the prepared catalysts was not substantial since the CO conversion approach 100 % as shown in Figure 4.21. However when O_2/CO ratio was reduce to 1.5, the activity differences between the catalysts increased as shown in Figure 4.22. At ratio of O_2/CO=1, all catalyst showed varied amount of conversion and therefore it was clear to differentiate the performance of all the catalyst as shown in Figure 4.23.

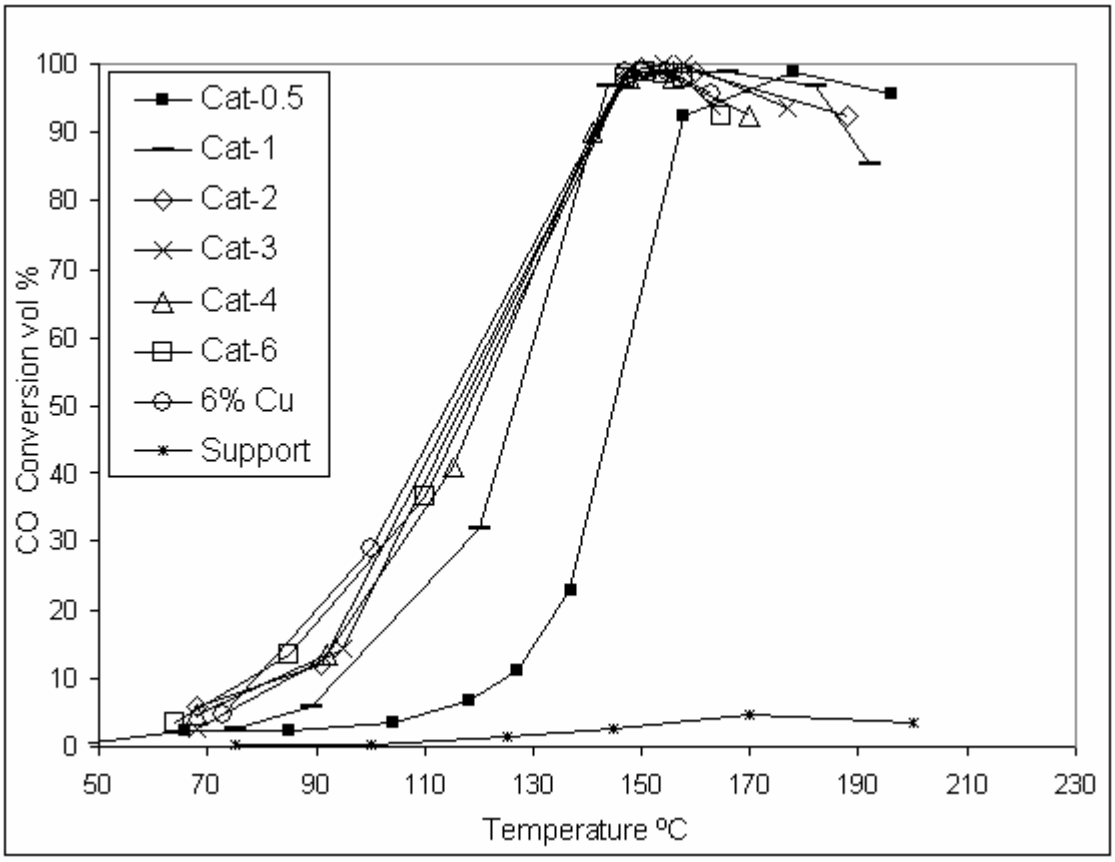

Figure 4.21 Effect of metal loading on PROX activity under the condition of large excess of O_2-ratio of O_2/CO = 2)

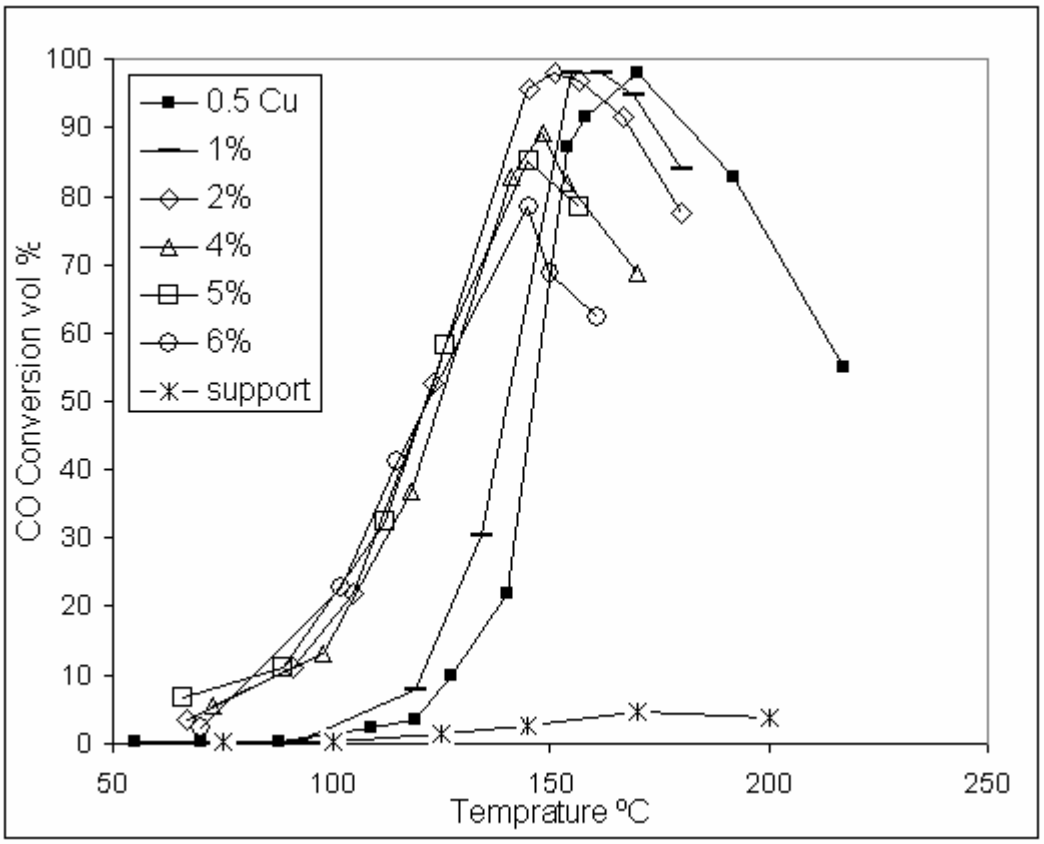

Figure 4.22 Effect of metal loading on PROX activity under the condition of stoichiometric of O_2/CO = 1.5 (for support O_2/CO = 2.0)

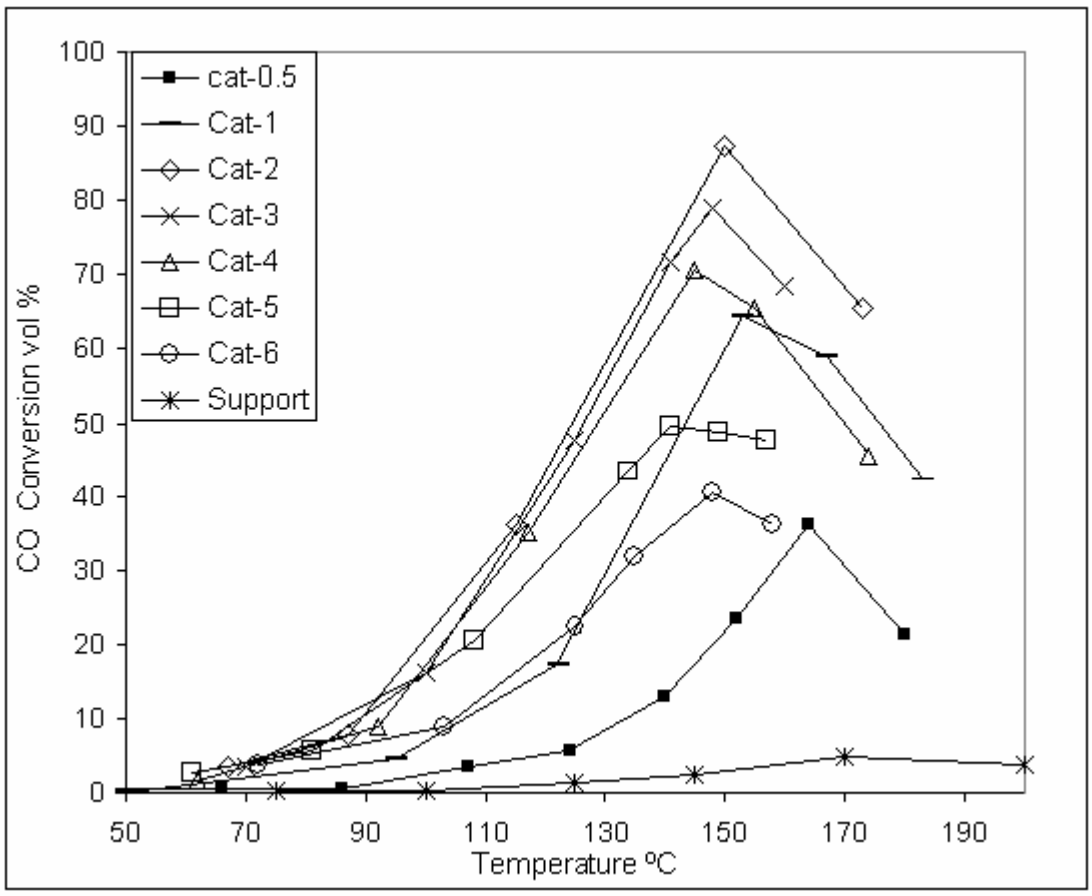

Figure 4.23 Effect of Metal loading in PROX catalyst activity under the condition of stoichiometric ratio of O_2/CO = 1 (for support O_2/CO = 2.0)

To find the optimum loading for maximum conversion, the maximum conversions over Cat-0.5 to Cat-6 at O_2/CO=1 were plotted verses Cu wt% loading as shown in Figure 4.24.

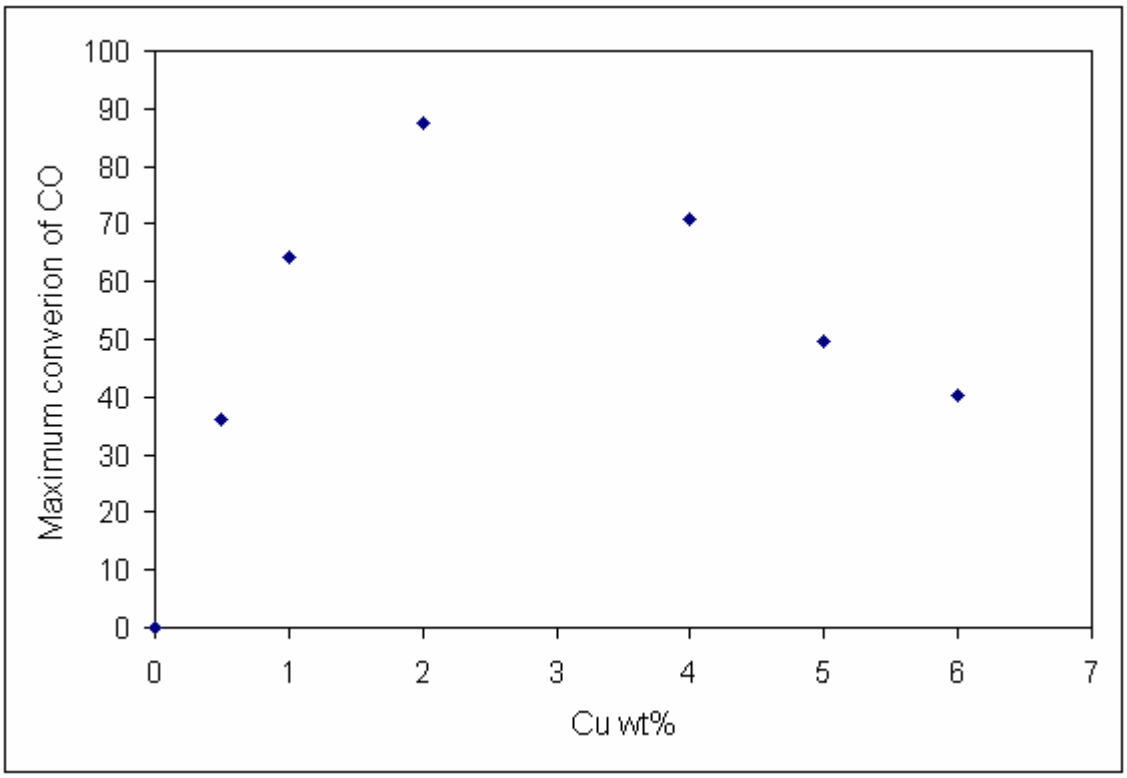

Figure 4.24 Optimum metals loading for maximum CO conversion

The CO oxidation activity was increased drastically with increasing Cu with respected amount of other metal. At 2% of Cu with respective other three metals, the highest of maximum conversions was achieved. The CO conversion decreased when Cu was increased more than 2% with respective amount of other three metals. Parka [72] investigated Cu-Ce catalyst promoted with Co. He

found that increasing Cu content above 2 wt% decreases the catalytic activity of Cu-Ce/γ-alumina at shown in table 4.10. This result agreed with the result was obtained with this study even though the Cu/Ce ratio was deferent in the two studies.

In earlier works on Cu based catalysts were done by Kim et al, it was shown that Cu/(Cu+Ce) atomic ratio of 2:8 [74] or 1.5:8.5 [75], prepared by the coprecipitation gave the best results for selective CO oxidation. But in actual application, selective oxidation catalyst are normally prepared by impregnating the active component on to a porous support such as γ-Al_2O_3, and thus it is necessary to determine the optimum metal content and weight ratio experimentally when these active metals are deposited on γ -Al_2O_3.

TABLE 4.10 Maximum conversion of CO for deferent Cu-Ce combination

Catalyst	Max. CO conversion (%)	Window for T (◦C)
Cu–Ce [1 : 9 wt%]=γ-Al_2O_3	93.5 (at 250◦C)	220–260
Cu–Ce [2 : 8 wt%]=γ-Al_2O_3	94.6 (at 200◦C)	185–230
Cu–Ce [4 : 6 wt%]=γ-Al_2O_3	92.8 (at 200◦C)	190–210
Cu–Ce [8 : 2 wt%]=γ-Al_2O_3	53.5 (at 200◦C)	----

Tong Won Park, and other" Selective oxidation of CO in hydrogen-rich stream overCu–Ce catalyst promoted with transition metals" international Journal of Hydrogen Energy 30(2005) 209-220 [72]

The dispersion of the metals on the support plays major role in catalyst activity. At low concentration loading metals (0.5 or 1.0 Cu wt% with respective other three metals), metals were dispersed nicely on the support. When the Cu was increased to 2wt%, the sites on the support were increased with high dispersion of metal so the maximum CO was achieved. More addition of metals reduced the surface area as it was shown in the surface area measurement

result that reduced the active sits in the catalyst. In addition, increasing metal loading reduced the dispersion and increasing the alloy metal crystal size on the surface of the catalyst which decreased CO oxidation and enhanced H_2 oxidation.

4.2.4 Effect of H_2O Vapor on the CO Oxidation

In this study where catalyst was prepared by pore volume impregnation Cat-1 (Cu 1.0%) and Cat-2 (Cu 2.0%) were selected to study the effect of water vapor addition in the feed on catalyst activity. For each catalyst, the reaction was carried out with a feed contained 10 and 20 vol% of steam. The O_2/CO and space velocity ratio were fixed to 2 and 9,000 h-1, respectively. Figures 4.25 and 4.26 show the results obtained for the selective CO oxidation over Cat-1 and Cat-2 catalysts without H_2O, with 10 and 20 vol% of H_2O in the reactant feed. The results were summarized in Tables 4.11 and 4.12. Addition of 10 and 20 vol% of H_2O vapor to the H_2-rich feed stream reduced the temperature of maximum conversion of CO over Cat-1 and Cat-2. For Cat-1, the peak of CO conversion verses temperature shifted down by 15ºC when 10 vol% of H_2O was added. When water vapor in the feed was increased to 20 vol%, the CO conversation further decreased 10ºC. The same behavior was obtained with Cat-2. The CO conversion peak shifted about 30ºC down by adding 10 vol% H_2O. The peak further decreased with an increase of H_2O to 20 vol% as shown in Figure 4.26.

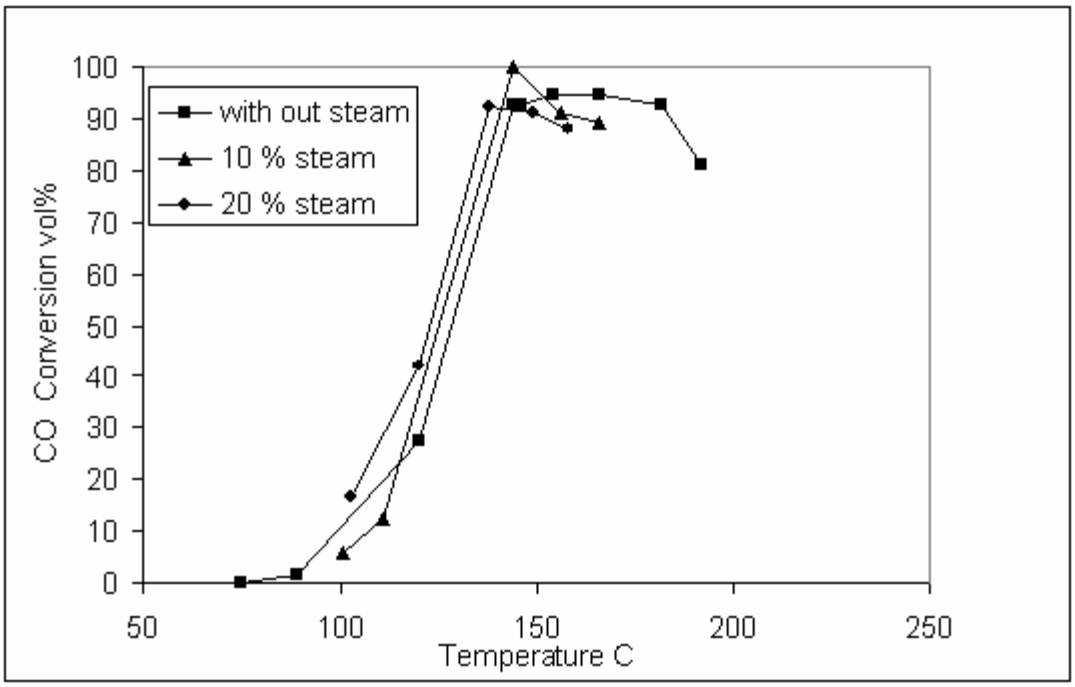

Figure 4.25 Effect of steam on Cat-1 catalyst activity for CO selective oxidation

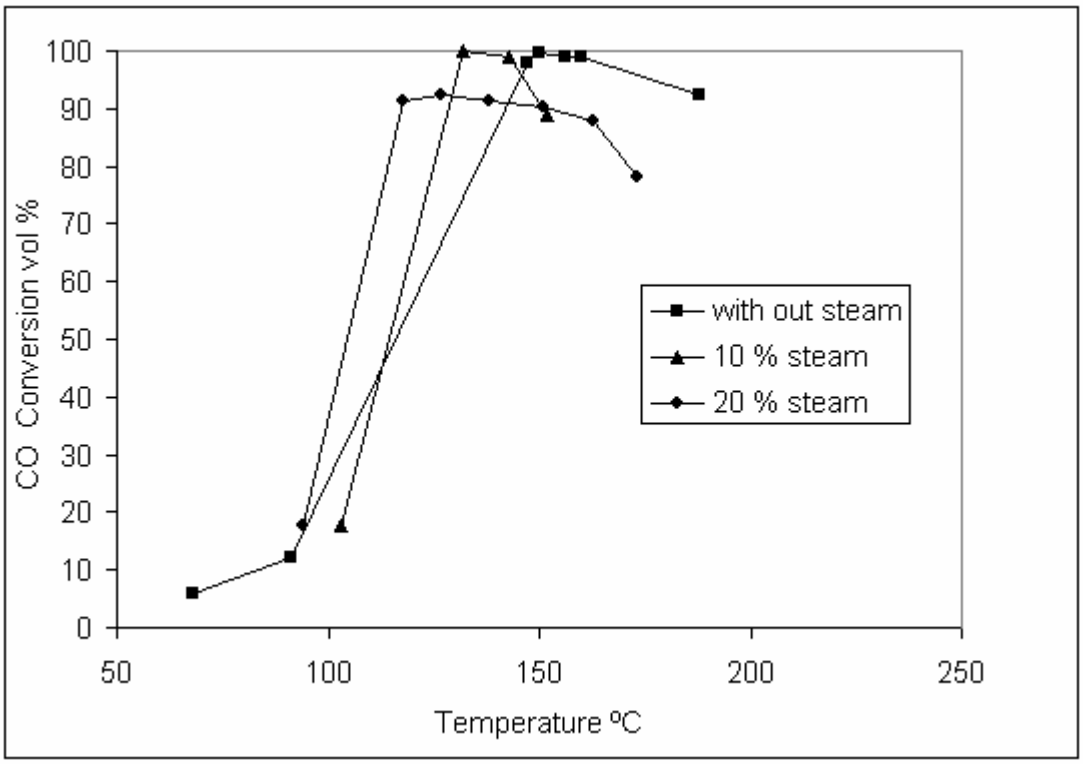

Figure 4.26 Effect of steaming on Cat-2 catalyst activity for CO selective oxidation

TABLE 4.11 Maximum conversion of CO at O_2/CO = 2.0 and 10 vol% steam in the feed

Catalyst Name	CO In product (%)	CO conversion (%)	H_2 In product (%)	H_2 conversion (%)	Selectivity (%)	Temperature ºC
Cat-1	0.00	100.00	75.81	3.5	25.36	144
Cat-2	0.00	100.00	75.81	3.5	25.36	132

TABLE 4.12 Maximum conversion of CO at O_2/CO = 2.0 and 20 vol% steam in the feed

Catalyst Name	CO in product (%)	CO conversion (%)	H_2 In product (%)	H_2 conversion (%)	Selectivity (%)	Temperature ºC
Cat-1	0.07	92.47	75.74	3.6	23.42	138
Cat-2	0.07	92.47	75.74	3.6	23.42	127

The activity of both Cat-1 and Cat-2 catalysts increased with addition 10 vol% of H_2O the H_2-rich feed stream and reduced with an increase of H_2O up to 20 vol%. The maximum conversion of CO over Cat-1 and Cat-2 increased slightly with addition of 10 vol% of H_2O. When water vapor was increased to 20 vol%, the CO conversion decreased over both Cat-1 and Cat-2 catalysts as shown in Table 4.12 and 4.13.

Parka [72] showed that the H_2O addition to the H_2-rich feed stream reduced the activity of CuCe/A and CuCeCo0.2/A catalysts prepared by coprecipitation method. The CO conversion temperature shifted about 50ºC higher .The blockage of the active sits was suggested to be the reason for reduction of catalyst activity. The effect of water addition in the feed on CO conversion in this study is different than study mentioned above because two reasons. The

preparation method of the catalysts and metal composition were different in both studies.

The increase of CO conversion of selective oxidation at 10 vol% H_2O addition to the feed was not attributed to a consumption of CO by water gas shift, since water gas shift is negligible at temperature low than 145ºC [76, 77]. It was related to addition of Pt and Rh to the feed. It. Addition of Pt and Rh to the base catalyst inhabited Cu to form Cu carbonate which is not active in presence of H_2O as discussed before. Therefore the catalyst did not lose it's activity. This result is agreed with study was don by Avgouropoulos [73]. He found that the CO conversion achieved on Pt/ γ-alumina at a given temperature is significantly higher in the presence of water vapor than in the absence of water vapor. This conclusion is in agreement with by also other investigations of water vapor effect on the CO oxidation over Pt/alumina catalyst [78,79].

The decrease of CO conversion at selective oxidation of CO over the Cat-1 and Cat-2 catalysts in the presence of 20 vol% H_2O vapor may be attributed to the blockage of catalytic active sites in high water vapor concentration by adsorbed water as well as to the formation of CO-H_2O surface complexes which are less active than adsorbed CO since the Pt weight % in the Cat-1 and Cat-2 are very small.

4.2.5 Reproducibility

To test reproducibility, Cat-2 was prepared three times and tested for selective oxidation of CO. The result is presented in Figure 4.27 and Table 4.13. The activities of the three catalysts were closed. The error obtained was within 3%. The maximum conversion temperatures of the three catalysts were almost the same.

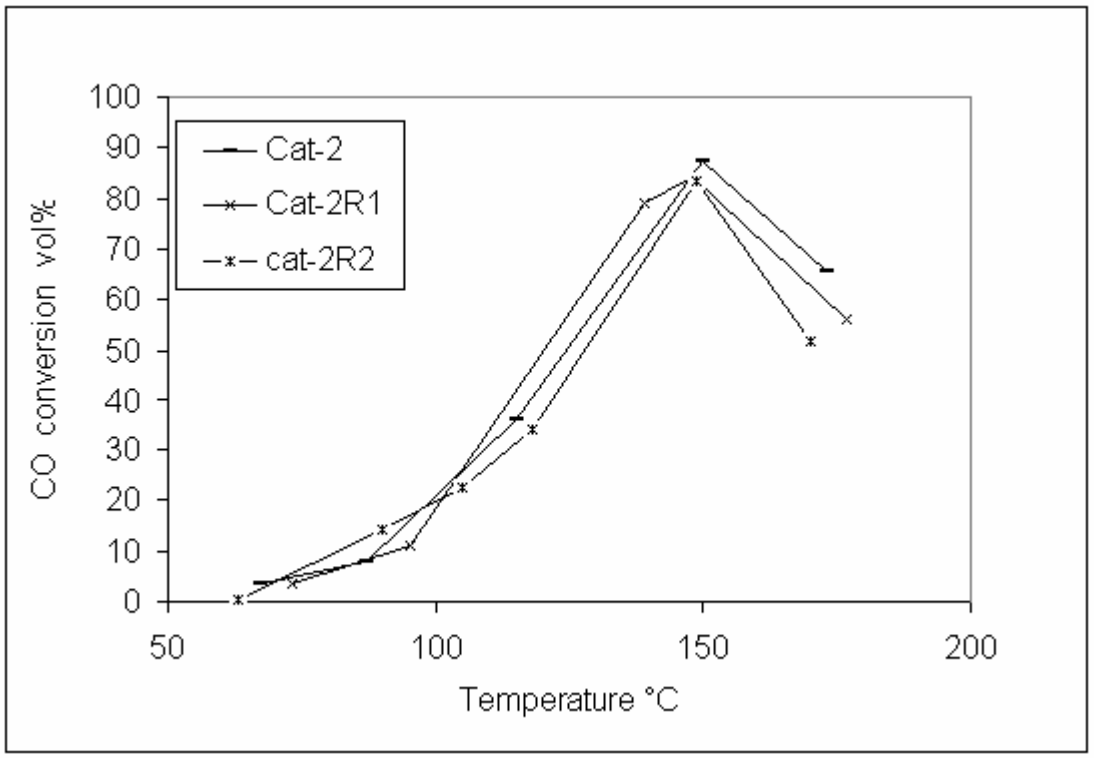

Figure 4.27 Conversion of CO over Cat-2, Cat-2R1, and Cat-2R1

TABLE 4.13 Maximum CO conversion over Cat-2, Cat-2R1, and Cat-2R1

Catalyst Name	Maximum Conversion of CO	Temperature Of max. Conversion	Error in Conversion (%)	Error in T of max. Conversion (%)
Cat-2	87.4	150	2.9	0.6
Cat-2R1	84.3	148	-0.8	-0.6
Cat-2R2	83.2	149	-2.1	0

CHPTER 5

CONCLUSION AND RECOMMENDATIONS

5.1 Conclusion

This work can be concluded with follows:

1. Surface area and pore volume were decreased with increased of metal content in the catalyst whereas the average pore reduce was increased.
2. The interactions between the metals loaded and the support were increased by addition very small amount of Pt and Rh.
3. The CO conversion and selectivity was increased with increased of reduction temperature peak of catalyst metal oxide.
4. The catalyst activity test for selective CO oxidation showed that the optimum loading of Cu, Ce, Pt, Rh were 2.0, 0.657, 0.183, 0.0324 wt% respectively. The CO concentration in the product was 4ppm only which meet the requirement of PEMFC.
5. The addition of 0.183 wt% of Pt to the base catalyst cat-2A increased the CO conversion from 24.7 to 96.77%. Whereas
6. The addition of 0.0324 wt% of Rh to the base catalyst cat-2A increased the CO conversion from 24.7 to 44.1%.
7. The addition of 0.183 wt% of Pt and 0.0324 wt% of Rh to the base catalyst cat-2A increased the CO conversion from 24.7 to 99.96 %.

8. The CO conversion was increased when 10 vol% of water vapor was added to the feed whereas the temperature of maximum conversion was decreased.
9. When water vapor content in the vapor was increased to 20 vol% CO conversion and temperature of maximum conversion were decreased.

5.2 Recommendations

1- Improve CuCe/γ-alumina activity by trying deferent preparation methods. It was found that CuCe/γ-alumina catalyst prepared by co-precipitation give higher activity than the same catalyst prepared by pore volume impregnation

2- Zeolite is promising support, so it can be also investigated with the same metal composition.

3- Dilute catalyst with inert material to avoid overheating.

APPENDICES

Appendix [A]

TPR Measurement

<< P A R A M E T E R >>

(1) DATA NAME ..... =		251003
(2) INITIAL TEMP(℃) ..... =		30
(3) INITIAL TEMP HOLDING TIME (min) =		1
(4) TIME BY TARGET TEMP (min) ..... =		100
(5) FINAL TEMP(℃) ..... =		1030
(6) FINAL TEMP HOLDING TIME (min) . =		10
(7) CALIBRATION = (μmol) ..... =		1
(COUNT) ..... =		1
(8) SAMPLE WEIGHT (g) ..... =		1
(9) MEMO ..... =		cat-M5
(10) X-AXIS(TIME:'0' / TEMP:'1') . =		1

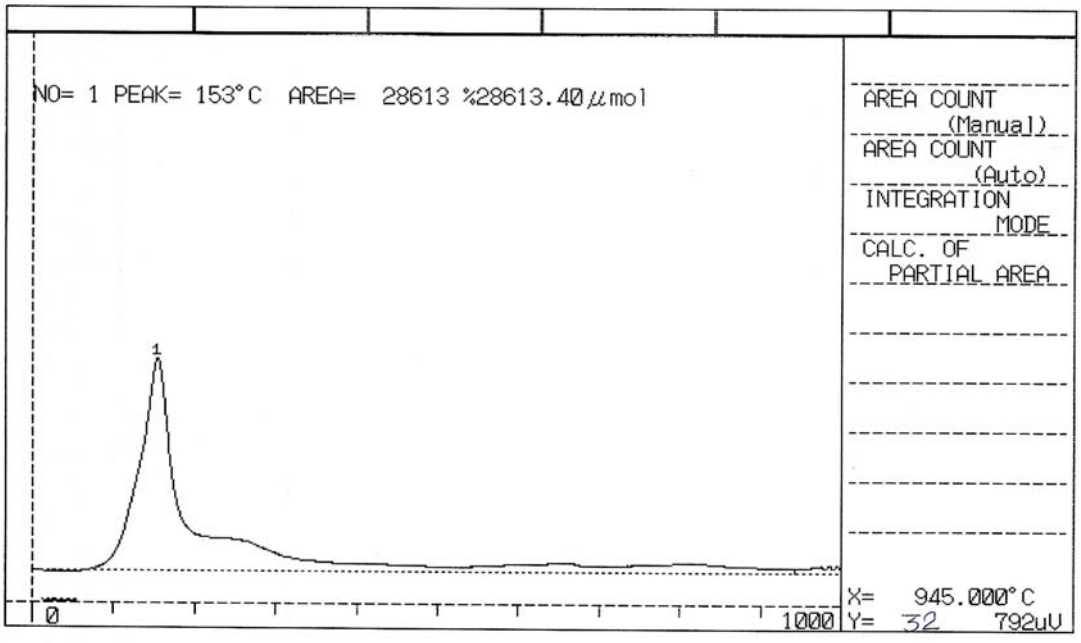

Appendix [B]

Calculation of Feed Composition

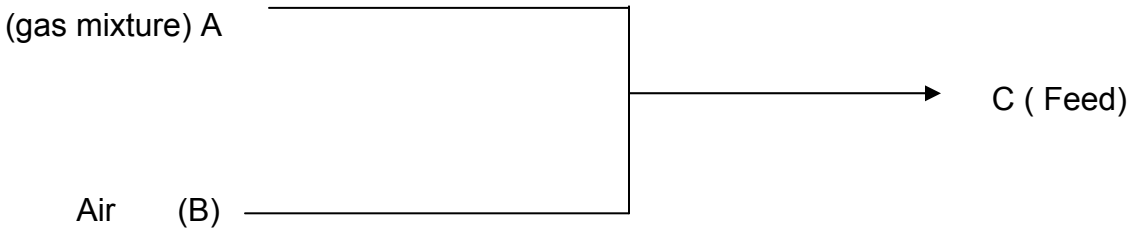

$A \times y_{H2(A)} + B \times y_{H2(B)} = C \times y_{H2(C)}$ ……(1)

$A \times y_{N2(A)} + B \times y_{N2(B)} = C \times y_{N2(C)}$ ……..(2)

$A \times y_{CO2(A)} + B \times y_{CO2(B)} = C \times y_{CO2(C)}$ ……..(3)

$A \times y_{CO(A)} + B \times y_{CO(B)} = C \times y_{CO(C)}$ ……..(4)

$A \times y_{O2(A)} + B \times y_{O2(B)} = C \times y_{O2(C)}$ ……..(5)

$A + B = C$ ……..…….(6)

At space velocity 9,000 s^{-1} and catalyst volume = 1 ml

Space velocity = Feed volume/ Catalyst volume

9,000 s^{-1} = C/ 1ml

C= 9,000 ml/ s

C = 150 ml/ min

$y_{H2(A)}$ = 0.84	y_{H2}(B) = 0	y_{H2}(C) = ?
y_{N2}(A)= 0.0	y_{N2}(B) = 0.79	y_{N2}(C)= ?
$y_{CO2(A)}$ = 0.15	$y_{CO2(B)}$ = 0.0	$y_{CO2(C)}$ = ?
$y_{CO(A)}$ = 0.01	$y_{CO(B)}$ = 0.0	$y_{CO(C)}$= ?
$y_{O2(A)}$ = 0.0	$y_{O2(B)}$ = 0.21	$y_{O2(C)}$ =?

Solving for CO and O_2 first using equations (4), (5),(6), and (7)

For $\frac{O_2}{CO} = 1.0$ ……(7)

From equation (4) $0.01B=150\ y_{CO(C)}$……..…..……(8)
From equations (5) and (7) $0.21B=75\ y_{CO2(C)}$……..……..(9)

Solving equations (8), (9), (6)
A= 143.2 ml/min
B= 6.8 ml/min
$y_{CO2(C)}$= 0.00954
$y_{CO(C)}$= 0.00954

Solving the other equation leads to complete feed composition. The same procedure was applied for the other two ratio of O_2/CO by same way

TABLE 3.2 Feed compositions with out steam

O_2/CO Ratio	A mi/min	B mi/min	C mi/min	Feed Composition				
				$y_{H2(C)}$	$y_{CO2(C)}$	$y_{CO(C)}$	$y_{O2(C)}$	$y_{N2(C)}$
1.0	143.2	6.8	150	0.802	0.143	0.00954	0.00954	0.0359
1.5	140	10	150	0.784	0.14	0.00933	0.014	0.0527
2	137	13	150	0.767	0.137	0.00913	0.0182	0.0685

With steam

For 10 vol % of steam

Total flow rate is 150ml/min

Flow of steam is 15ml/ min

Flow of gas mixture is 135

For 20 vol % of steam

Total flow rate is 150ml/min

Flow of steam is 30ml/ min

Flow of gas mixture is 120 ml/min

Appendix [C]

Calculation for Metal Loading

Sample calculation of chemical analysis result

For Cu 3% with bases 10 g of the catalyst

Element	Cu	Ce2O3	Pt	Rh
Ratio	100	20	3	1
Mw	63.546	328.24	195.09	102.9055

Metal Salt	Purity (%)	Mw ((g/mole)
Copper(II)nitrate (Fluka AG, CH-9470 Buchs)	98	241.6
Cerium(III)nitrate (Aldrich)	99.99	434.23
PtCl (Aldrich)	98	336.9
RhCl (Aldrich)	98	209.26

The weight of metal salt needed to prepare 10 g of catalyst

For example Cu wt% =3

W_{Cu} = 0.03 X 10g= 0.3 g

$$W_{Cu(NO_3)_2} = \frac{Mw_{Cu(NO_3)_2}}{Mw_{Cu}} \times 0.3 = \frac{241.6}{63.546} \times 0.3 = 1.1406 \ g$$

$$W_{Ce(NO_3)_3} = \frac{Mw_{Ce(NO_3)_3}}{Mw_{Cu}} \times 0.3 \times \frac{20}{100} = \frac{434.23}{63.546} \times 0.3 \times \frac{20}{100} = 0.4100 \ g$$

$$W_{PtCl_4} = \frac{Mw_{PtCl_4}}{Mw_{Cu}} \times 0.3 \times \frac{3}{100} = \frac{336.9}{63.546} \times 0.3 \times \frac{3}{100} = 0.0487 \ g$$

$$W_{RhCl_3} = \frac{Mw_{RhCl_3}}{Mw_{Cu}} \times 0.3 \times \frac{1}{100} = \frac{209.26}{63.546} \times 0.3 \times \frac{20}{100} = 0.0101 \ g$$

The result for other concentration is presented in Table C1

TABLE C1 The weight required to prepare 10 g of catalyst

Cu	0.0050	0.0100	0.0200	0.0300	0.0400	0.0500	0.0600
Cuber(II) nitrate	0.1901	0.3802	0.7604	1.1406	1.5208	1.9010	2.2812
Cerium(III) nitrate	0.0683	0.1367	0.2733	0.4100	0.5467	0.6833	0.8200
Platinum(IV) Cloride	0.0081	0.0162	0.0325	0.0487	0.0649	0.0811	0.0974
Rhodium(III) Chloride	0.0017	0.0034	0.0067	0.0101	0.0134	0.0168	0.0202

Appendix [D]

Calculation for CO and H_2 Conversion

The result of GS analysis is in volume (mole) percent since the calibration was used based on volume percent. The following equation were used to calculate CO and H_2 conversion as well as selectivity.

$$\text{Xco}\ (\%) = \frac{[\text{CO}]\text{in} - [\text{CO}]\text{out}}{[\text{CO}]\text{in}} X\ 100$$

$$\text{XH2}(\%) = \frac{[\text{H2}]\text{in} - [\text{H2}]\text{out}}{[\text{H2}]\text{in}} X\ 100$$

$$\text{Sco}(\%) = \frac{0.5([\text{CO}]\text{in} - [\text{CO}]\text{out})}{[\text{O2}]\text{in} - [\text{O2}]\text{out}} X\ 100$$

For example, the CO concentration in product with O_2/CO=1.5 in the feed was 0.14 % for cat-5 .The GC result is shown in Figure D1

The $[CO]_{in}$=0.933 vol%

$[O_2]_{in}$= 1.400 vol %

$[H_2\}_{in}$=0.784 vol%

With the assumption at maximum CO conversion $[O_2]_{out}$=0

$$\text{Xco}\ (\%) = \frac{0.93 - 0.14}{0.93} X\ 100 = 85.5$$

$$XH2(\%) = \frac{[H2]in - [H2]out}{[H2]in} X\ 100$$

H_2 reacted with O_2 = 2x[O_{2feed}-0.5$CO_{reacted}$]

= 2.0x(0.014-0.5x(0.0093-0.0014)=2.01%

So $[H_2\}_{out}$=0.784-0.0201=0.764

$$XH2(\%) = \frac{0.784 - 0.764}{[0.784} X\ 100 = 2.56\ \%$$

$$Sco(\%) = \frac{0.5(0.0077\ )}{0.014} X\ 100 = 28.3$$

Figure D1 The GC result of PROX of CO reaction for Cat-6 at 148ºC

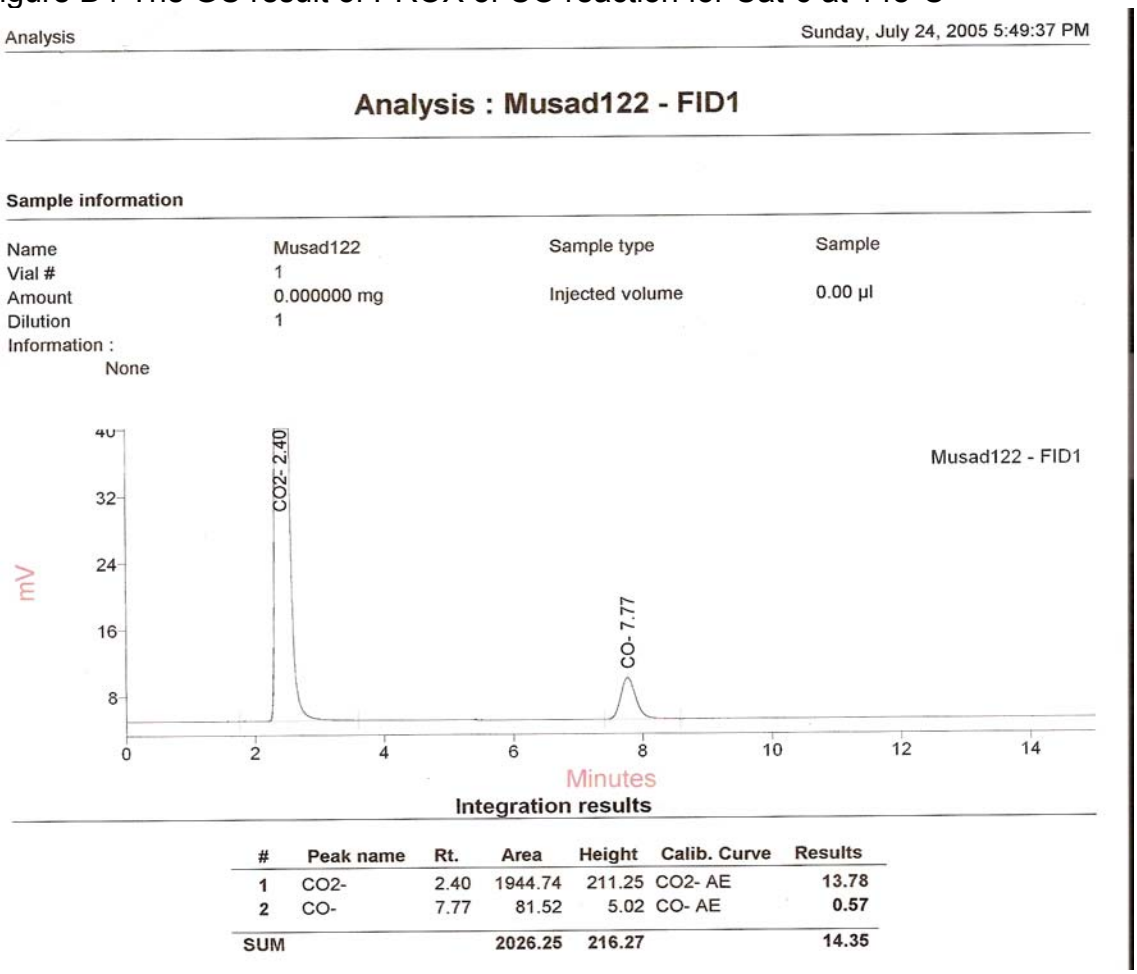

#	Peak name	Rt.	Area	Height	Calib. Curve	Results
1	CO2-	2.40	1944.74	211.25	CO2- AE	13.78
2	CO-	7.77	81.52	5.02	CO- AE	0.57
SUM			2026.25	216.27		14.35

REFERENCES

1. Rajesh K. Ahluwaliaa Rajesh K. Ahluwalia, Qizhi Zhanga, Donald J. Chmielewski,Kevin C. Lauzze, Michael A. Inbody, Catalysis Today,2004
2. Springer T.E., T. Rockward, T.A. Zawodzinski, S. Gottesfeld, J. Electrochem. Soc. 148,2001, 11.
3. Ahluwalia R.K., E.D. Doss, R. Kumar, J. Power Sources 117 (2003) 45.
4. Cohn J.G.E., US patent 3 216 783 (1963), to Engelhard Industries.
5. Cohn J.G.E., US Patent No. 3,216,783 (1965).
6. Bonacci J.C., US Patent No. 4,238,468 (1980).
7. Vanderborgh N.E., C.A. Spirio, J.R. Huff, Extended Abstract of the International Seminar on Fuel Cell Technology and Applications, Hague, Netherlands, 1987, p. 253.
8. Oh Se H., R.M. Sinkevitch, J. Catal. 142 (1993) 254.
9. Kahlich M.J., H.A. Gasteiger, R.J. Behm, J. Catal. 171 (1997) 93.
10. Schubert M.M., H.A. Gasteiger, R.J. Behm, J. Catal. 172 (1997) 256.
11. Chan Kwak, Tae-Jin Park, Dong Jin Suh, Applied Catalysis A: General 278 (2005) 181–186.
12. Chan Kwak, Tae-Jin Park, Dong Jin Suh Journal of Power Sources, Volume 142, Issues 1-2, 24 March 2005, Pages 70-74.

13. Cécile Rossignol, and Other Journal of Catalysis, Volume 230, Issue 2, 10 March 2005, Pages 476-483.

14. Arrii S., F. Morfin, A.J. Renouprez, J.L. Rousset, J. Am. Chem. Soc. 126 (2004) 1199.

15. Dong Jin Suh□, Chan Kwak, Jin-Hong Kim, Se Mann Kwon, Tae-Jin Park, Scincedirect, 27 September 2004.

16. Haruta M., S. Tsubota, T. Kobayashi, H. Kageyama, M.J. Genet, B. Delmon, J. Catal. 144 (1993) 175.

17. Okamura M., S. Nakamura, S. Tsubota, T. Nakamura, M. Azuma, M. Haruta, Catal. Lett. 51 (1998) 53.

18. Valden M., X. Lai, D.W. Goodman, Science 281 (1998) 1647.

19. Okumura M., K. Tanaka, A. Ueda, M. Haruta, Solid State Ionics 95 (1997) 143.

20. Haruta M., N. Yamada, T. Kobayashi, S. Iijima, J. Catal. 115 (1989) 301.

21. Yuan Y., A.P. Kozlova, K. Akasura, H. Wan, K. Tsai, Y. Iwasawa, J. Catal. 170 (1997) 191.

22. Bollinger M.A., M.A. Vannice, Appl. Catal. B 8 (1996) 417.

23. Ruth K., M. Hayes, R. Burch, S. Tsubota, M. Haruta, Appl. Catal. B Environ. 24 (2000) L133.

24. Bethke G.K., H.H. Kung, 194 (2000) 43.

25. Griesel R.J.H., B.E. Nieuwenhuys, J. Catal. 199 (2001) 48.

26. Kahlich M.J., H.A. Gasteiger, R.J. Behm, J. Catal. 182

27. Valden M., S. Pak, X. Lai, D.W. Goodman, Catal. Lett. 56 (1998) 7.

28. Bond G.C., D.T. Thompson, Catal. Rev.-Sci. Eng. 41 (1999) 319.

29. Choudhary T.V., D.W. Goodman, Top. Catal. 21 (2002) 25.

30. Choudhary T.V., D.W. Goodman, Catalysis Today 77 (2002) 65–78

31. Igarashi H., H. Uchida, M. Suzuki, Y. Sasaki, M. Watanabe, Appl. Catal. A 159 (1997) 159.

32. Masahiro Watanabe, Hiroyuki Uchida, Kyoko Ohkubo, Hiroshi Igarashi, Applied Catalysis B: Environmental 46 (2003) 595–600.

33. Ilaria Rosso□, Camilla Galletti, Guido Saracco, Edoardo Garrone, Vito, Applied Catalysis B: Environmental 48 (2004) 195–203

34. Igarashi H., H. Uchida, M. Watanabe, Chem. Lett. (2000) 1262.

35. Igarashi H., H. Uchida, M. Watanabe, Stud. Surf. Catal. 132 (2001) 953.

36. Fernando Marin˜oa,b, Claude Descormea, Daniel Dupreza , Applied Catalysis B: Environmental 58 (2005) 175–183.

37. Shan W., W. Shen, C. Li, Chem. Mater. 15 (2003) 4761.

38. Madier Y., C. Descorme, A.M. Le Govic, D. Duprez, J. Phys. Chem. B103 (1999) 10999.

39. Liu W., M. Flytzani-Stephanopoulos, J. Catal. 153 (1995) 304.

40. Liu W., M. Flytzani-Stephanopoulos, J. Catal. 153 (1995) 317.

41. Liu Y., Q. Fu, M.F. Stephanopoulos, Catal. Today 93–95 (2004) 246.

42. Fernando Mario, Claude Descorme, Daniel Duprez ,Applied Catalysis B: Environmental 54 (2004) 59–66.

43. Teng Y., H. Sakurai, A. Ueda, T. Kobayashi, Int. J. Hydrogen Energy 24 (1999) 355.

44. Schubert M.M., M.J. Kahlich, G. Feldmeyer, M. Huttner, S. Hackenberg, H.A. Gasteiger, R.J. Behm, Phys. Chem. Chem. Phys. 3 (2001) 1123.

45. Schubert Markus M., Vojtech Plzak, Jürgen Garche, R. Jürgen Behm. Specchia, Applied Catalysis B: Environmental 48 (2004) 195–203.

46. Inui Tomoyuki, Takashi Ueda, and Masatoshi Suehiro, J. Chem. Soc. Japan, Chem. Ind. Chem., No.7, pp.934-940 (1977).

47. Inui Tomoyuki, Takashi Ueda, Masatoshi Suehiro, and Haruo Shingu, J. Chem. Soc., Faraday Trans. I, 75, pp.2490-2500 (1978).

48. Inui Tomoyuki,Stud. Surf. Sci. Catal., 77, pp.17-26 (1993).

49. Inui Tomoyuki, Yukiyoshi Ono, Yoichi Takagi, and Jin-Bae Kim, Appl. Catal. A: General, 202, pp.215-222(2000).

50. Inui Tomoyuki, Masatoshi Suehiro, Yuji Saita, Takanori Miyake, and Yoshinobu Takegami,Appl. Catal., 2, pp.389-398 (1982).

51. Inui Tomoyuki., “Reforming of CH_4 by CO_2, O_2 and/or H_2O”, Catalysis, 16, pp.133-154 (2002).

52. Inui Tomouki, ACS Fuel Chem. Div. Preprints, 48(1), pp.370-371(2003).

53. Inui Tomoyuki, 14th Annual Saudi-Japanese Symposium on Catalysts in Petroleum Refining & Petrochemicals, KFUPM, December 5-6, 2004, Proceedings, pp. 11-23.

54. Delsmana E.R., M.H.J.M. De Croona,A. Pierika, G.J. Kramera, P.D. Cobdenb, Ch. Hofmannc, V. Cominosc, J.C. Schoutena, Chemical Engineering Science 59 (2004) 4795 – 4802.

55. Sujit Srinivas, Amit Dhingra, Hong Im, Erdogan Gulari, Applied Catalysis A: General 274 (2004) 285–293.

56. Ouyang, R.S. Besser , Journal of Power Sources 141 (2005) 39–46

57. Han Y.-F., M. J. Kahlich†, M. Kinne, and R. J. Behm, Phys. Chem. Chem. Phys., subm.

58. Kahlich M.J., H.A. Gasteiger, R.J. Behm, "J. Catal. 182 (1999) 430-440

59. Schubert M.M., H.A. Gasteiger, and R.J. Behm, J. Catal. 172 (1997) 256-258

60. Markus M. Schubert, Vojtech Plzak, Jürgen Garche, R. Jürgen Behm Activity, Selectivity, and Long-Term Stability of Different Metal Oxide Supported Gold Catalysts for the Preferential CO Oxidation.

61. Meng M., P. Lin, Y. Fu, Catal. Lett. 48 (1997) 213.

62. Lee C.-H., Y.-W. Chen, Ind. Eng. Chem. Res. 36 (1997) 1498.

63. Sanchez R.M.T., A. Ueda, K. Tanaka, M. Haruta, J. Catal. 168 (1997) 125. (1999) 430.

64. Sirijaruphan A., J.G. Goodwin Jr., R.W. Rice, D. Wei, K.R. Butcher, G.W. Roberts, J.J. Spivey, Metal foam supported Pt catalysts for the selective oxidation of CO in hydrogen, Appl. Catal. A: Gen. 281 (2005) 1–9.

65. Sirijaruphan A., J.G. Goodwin Jr., R.W. Rice, J. Catal. 224 (2004) 304.

66. Kenneth R. Butcher, George W. Roberts, James J, Applied Catalysis A: General 281 (2005) 11–18.

67. Manuel Ojeda a, Manuel L´pez Granados a, Sergio Rojas a, Pilar Terreros a, F. Javier Garc´ıa-Garc´ıa b, José Luis G. Fierro a, Applied Catalysis A: General 261 (2004) 47–55.

68. R. Burch, P.K. Loader, N.A. Cruise, Appl. Catal. A 147 (1996) 375.

69. H.J. Borg, L.C.A. van den Oetelaar, J.W. Niemantsverdriet, Catal. Lett. 17 (1993) 81.

70. Carvalho L.S. a, C.L. Pieck b, M.C. Rangel a, N.S. F´ıgoli b, J.M. Grau b, P. Reyesc, J.M. Parera b, Applied Catalysis A: General 269 (2004) 91–103.

71. I-Pin Chena,□, Shiow-Shyung Lin a, Ching-Huei Wang b, Lizone Changc, Jing-Song Changa, Applied Catalysis B: Environmental 50 (2004) 49–58.

72. Jong Won Parka, Jin Hyeok Jeongb, Wang Lai Yoonc;, Chang Soo Kimc, Deuk Ki Leed,Yong-Ki Parke, Young Woo Rheea, International Journal of Hydrogen Energy 30 (2005) 209 – 220.

73. G. Avgouropoulos a,d, T. Ioannides a, Ch. Papadopoulou b, J. Batista c, S. Hocevar c, H.K. Matralis a,b,, Catalysis Today 75 (2002) 157–167.

74. Kim DH, Cha JE. A CuO–CeO2 mixed oxide catalyst for CO clean-up by selective oxidation in hydrogen-rich mixtures. 9th APCChE Congress, 2002. p. 619.

75. Avgouropoulos G, Ioannides T, Matralis HK, Batista J,Hocevar S. Catal Lett2001;73:33–40.

76. Kim G., Ind. Eng. Chem. Prod. Res. Dev. 21 (1982) 267.

77. Whittington B.I., C.J. Jiang, D.L. Trimm, Catal. Today 26 (1995) 41.

78. Nibbelke R.H., M.A.J. Campman, J.H.B.J. Hoebink, G.B.Marin, J. Catal. 171 (1997) 358.

79. Muraki H., S.I. Matunaga, H. Shinjoh, M.S. Wainwright, D.L. Trimm, J.Chem. Technol. Biotechnol. 52 (1991) 415.

VITA

Name	Musaed Salem Al-Ghamidi
Date & Place of Birth	July 1, 1969, Al-Baha
Nationality	Saudi
Religion	Islam
Marital Status	Married
Educational qualifications	Bachelor of Science in Chemical Engineering from KFUPM University, Dhahran, KSA (February. 3003). M. Sc. in Chemical Engineering from King Fahd University of Petroleum & Minerals, Dhahran, Saudi Arabia (2006-todate).